Journal of
Food and Packaging
Science, Technique and Technologies

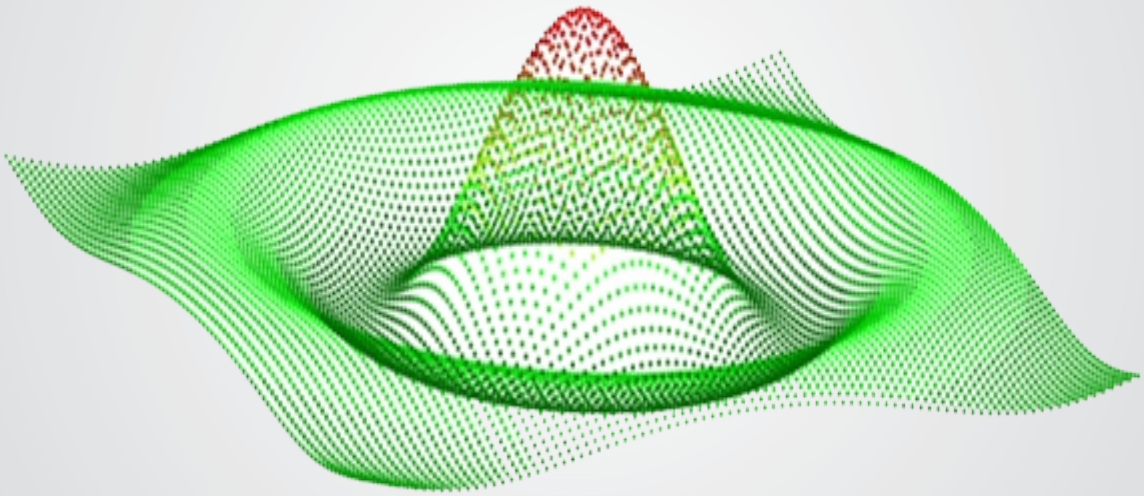

7

ISSN 1314-7773

ISSN 1314-7773

7

Journal of **FOOD** and **PACKAGING** Science, Technique and Technologies

Year IV, №7, 2015

National Academy of Packaging - Bulgaria

Web-site: http://mahvp.uft-plovdiv.bg/

Address: 26, Maritza Blvd., 4002, Plovdiv, BULGARIA

Phone: +359 32 603 814
+359 32 603 805

E-mail: mahvp@mail.bg
mahvpuht@gmail.com
jfpstt@gmail.com

CONTENTS

THE SELECTION OF THE PACKAGING FOR FOODSTUFF AND FORECASTING ITS SHELF LIFE

V. V. Ananyev – *PhD, Prof., Head of the laboratory of the Centre of research activities of Moscow State University of Printing Arts of Ivan Fedorov;*
M. E. Chernov – *DSc. Eng., Prof., Head of the Department of Design and Packaging Production Organization of Moscow State University of Technologies and Management named after G. K. Razumovskiy*

Abstract: *Computer program is made for determining the permeability of packaging material by storing foodstuff in the noble, modified or controlled atmospheres. This program allows to select the packaging type out of variant offered of its geometrical sizes. It works in the operational environment MS Windows. The example of its using for packing and storing of flour products and pastry in the modified atmosphere is shown here.*

Key words: permeability, program, noble, modified and controlled atmospheres, interface, foodstuff storing.

The modern market of consumer goods is making rigid requirements for packaging. One of the main functions of packaging is supplying packed product with protection from the deleterious effect of the environment and prolonged conservation of its consumer's characteristics for as long as it is possible.

There are chemical and microbiological changes by the storing of the majority of foodstuff. By these changes oxygen and light, which can initiate these changes, and temperature, which determines their kinetics, play the main role.

Different ways are used to prevent deleterious effect of oxygen on foodstuff. They include following methods: oxygen removal, creating of protective atmosphere in the packaging, freezing procedure.

The most accessible method is oxygen removal by vacuumization. Monolayer, multi-layer and combined films with high barrier properties are used for this purpose.

It is possible to prolong shelf life of some products by creating a special atmosphere in the packaging, which leads to the abrupt slowing-down of the process of their "breathing" (gaseous exchange with the environment), the slowing down growing of microorganisms and functioning. Thus the increase of product's shell life will follow.

Following ways of packaging are distinguished in the gas atmosphere:

- in the noble atmosphere (N_2, CO_2, Ar);
- in the modified atmosphere (MA), when the atmosphere of a special composition is created depending on the character of products store;
- in the controlled atmosphere (AC), when the composition of a gaseous mixture must be changed only within the prescribed methods as the result of product's "breathing" and certain permeability of packaging.

The permeability of the packaging must be minimal in the first two cases. By storing in the AC it is necessary to provide level and selectivity of permeability of packaging concerning basic atmospheric gases (N_2, O_2, CO_2).

It is obvious that for the right selection of packaging we should know how to rate its permeability with split-hair accuracy not only concerning gases, but also moisture. Diffusion characteristics of many polymeric materials, which are used for the production of packaging, are listed in many publications. However, these characteristics published in different sources sometimes differ more than in decimal exponent. Besides, various authors use different systems of units that makes difficulties for estimating and comparing these characteristics. But the chief thing is that overwhelming majority of researches are made for the membranous materials in standard or steady-state conditions, when the constant differential of concentrations or partial gas pressures is maintained astride the material. Constant temperature, which differs depending on country's standards, where the researches have been performed, is also maintained

It is obvious that it is difficult to use such data for estimating packaging characteristics. Particularly when it is made of different elements (e.g. thermoformed body with a cover cloth welded to it). Every element can include at the same time several layers of various thickness, which are made of different materials. Storing of products is realized in ambient temperature (that can be different in various regions of the country) or in cold storage. It is necessary to take into consideration not only the permeability of packaging, but also the permeability

of potting components (adhesive or more often field welds). As it has been found out, field welds in some packaging types can be determinal factor for barrier properties.

The scheme, which is illustrating the impact of different factors on storing of the packed product, is in the Fig. 1.

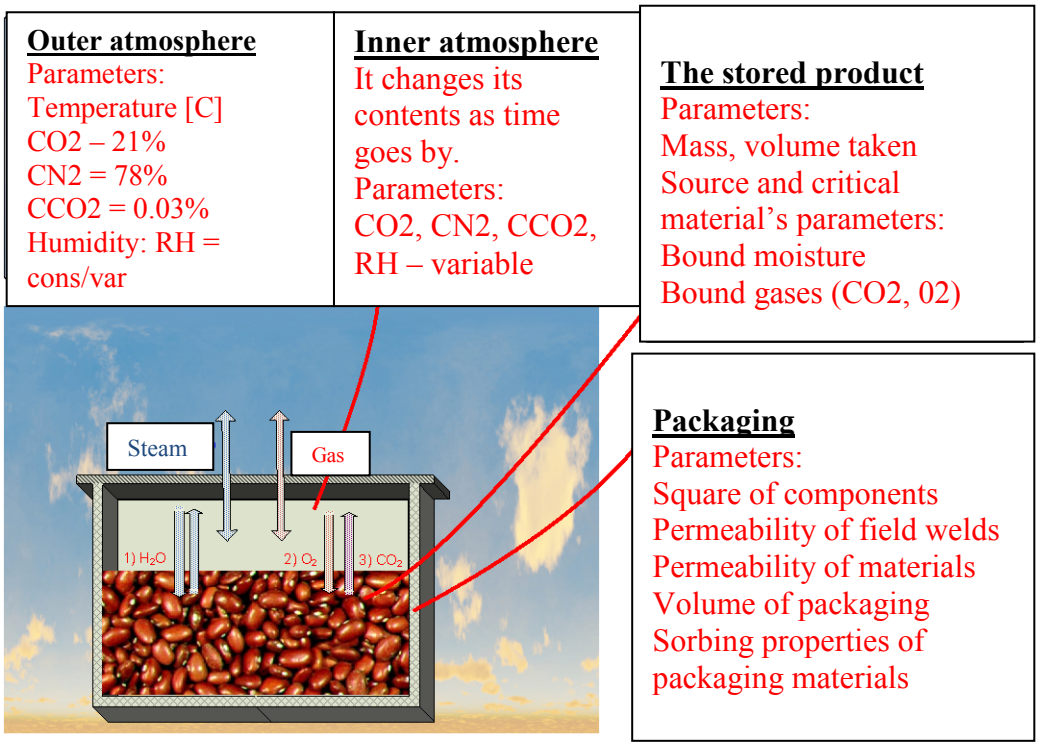

Fig. 1. *The scheme of processes occurred by the storing of products in packaging and the factors, which determine these processes.*

As it is possible to see in the scheme, it is necessary to take into consideration a lot of factors by selecting the packaging, which provides optimum properties by storing meat ware. It is clear that if there are difficulties even by estimating the barrier properties of monolayer material, it is impossible to rate the permeability of complex packaging using ordinary calculus.

That is why a computer program was created, which allows to accomplish a similar task with sufficient split-hair accuracy. Its modular construction is shown in the Fig. 2.

Databases were made attached to the creating of the program by means of numerous measurements of permeability of packaging material and potting components. They include diffusion characteristic of almost all polymeric membranous materials that are used now for creating of the packaging and field welds, which are formed by various methods. The dependences of permeability of materials on temperature, humidity of gases (Fig. 3) and their capabilities of sorbing the diffusant (e.g. paper and cardboard sorb water, oxygen absorbents are sometimes brought in polyethylene terephthalate and so forth) have been obtained. The example of such a dependence is shown in the Fig. 3.

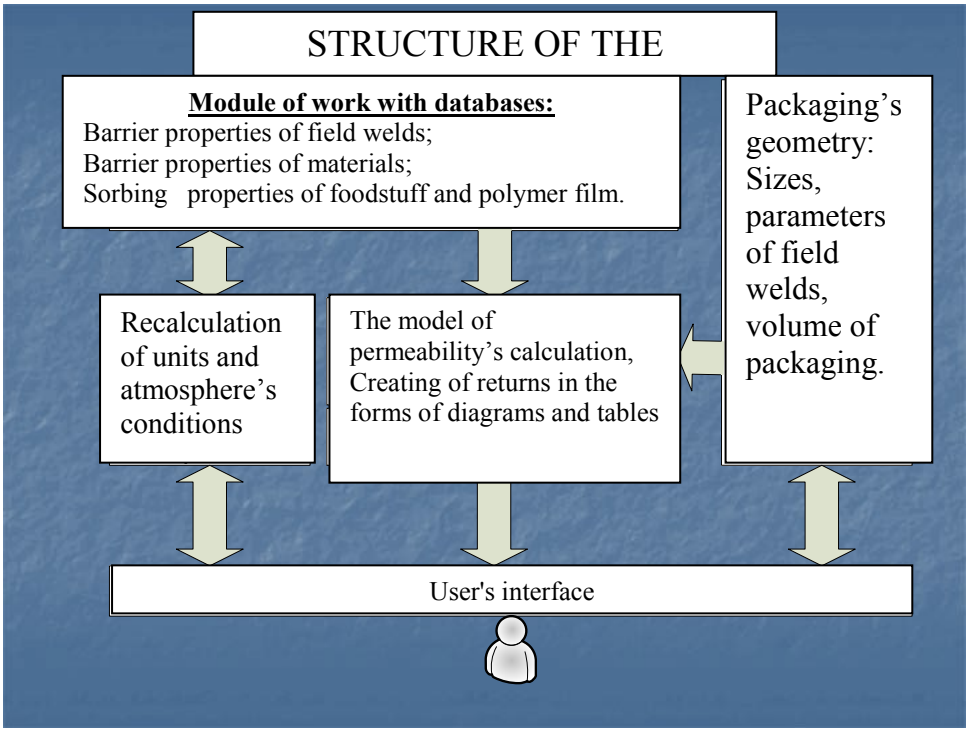

Fig. 2. *Program's structure for calculating permeability of packagings and forecasting foodstuff shelf life.*

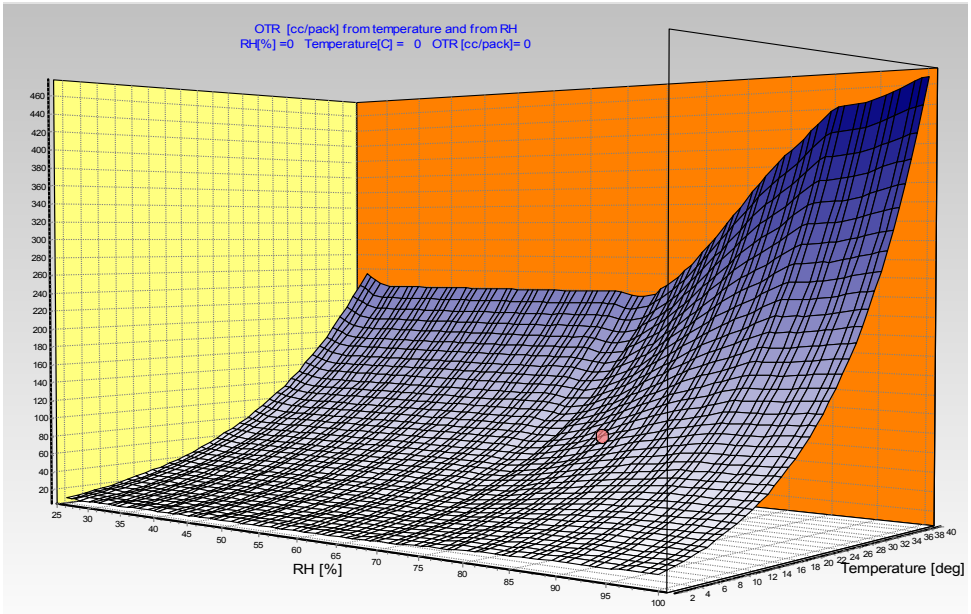

Fig. 3 *The dependence of oxygen material's permeability on relative humidity and temperature.*

The program works in the operational environment MS Windows.

The special operating module allows to input data and to output the results in any possible units, providing their recalculation.

The program allows to select packaging type out of the range offered and its geometrical sizes. The squares of its components and the extension of its potting welds are calculated automatically at the same time. It is also possible to select the type of weld (Fig. 4).

The calculation of permeability is made on the developed algorithm and the results given can be a module of return's output. The output is possible in the form of tables, which contain source data and the results of calculations (Fig. 5). There is also a diagrammatic formulation in the form of dependences of, for example, partial gas pressure or product's water content, if the parameters of its water sorption are known (Fig. 6). It is possible to import the results into one of MS Windows program applications (e.g. Microsoft Excel).

The program possesses easy-to-use interface.

It is possible to see the dependence of product's water content on its shelf life in the Fig. 6. The red horizontal line shows maximum water content. So that is possible to determine the limiting shelf life of this product in this very packaging. This time is 95 days in the given example.

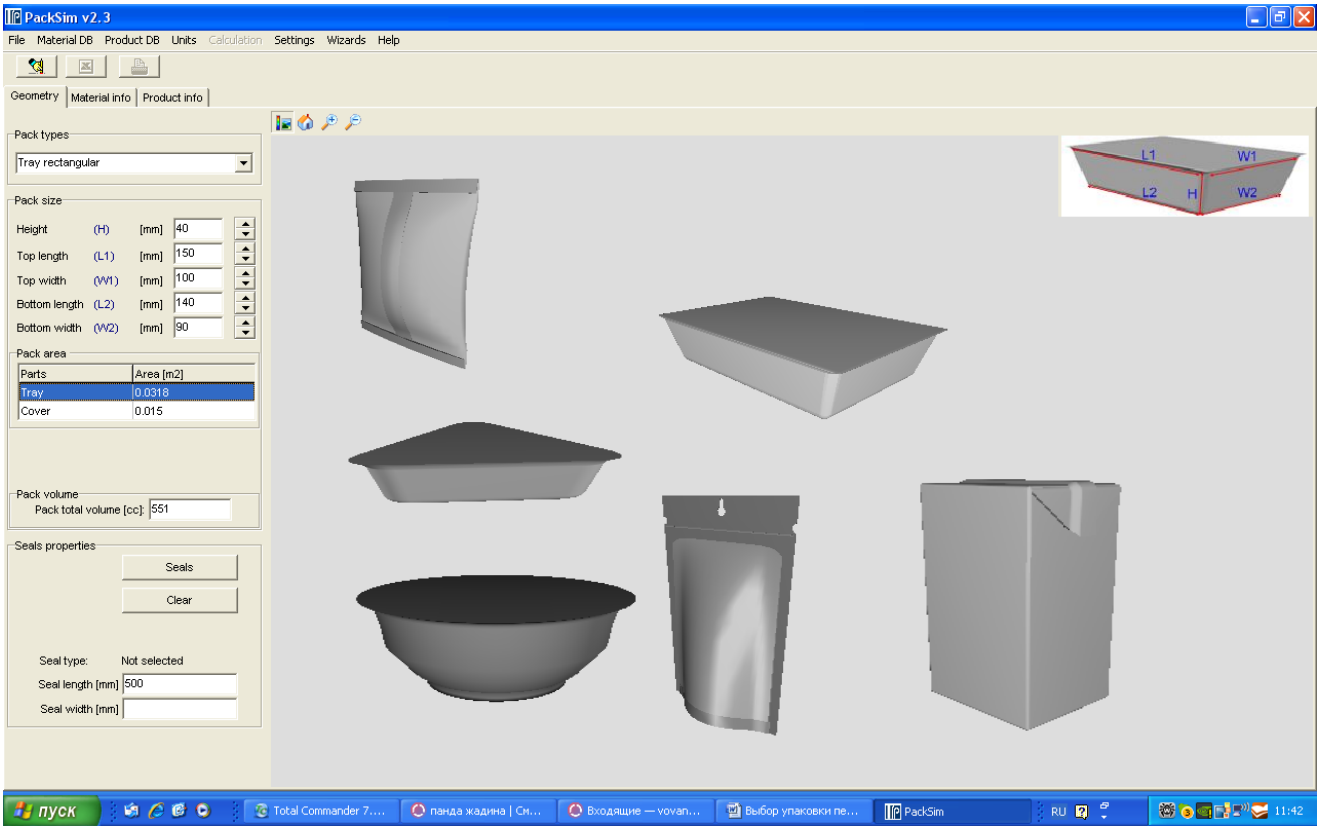

Fig. 4. *Selection of the packaging type and size and its field welds.*

INPUT DATA			RESULT		
Packaging			**Tray rectangular Permeability**		
Pack Type	Tray rectangular		Used Model of Calulation	Closed model	
Pack Material, Thickness [mm]	PVC [unplasticised]	0,2	Pack Permeability [cc/pack]	WVTR	0,00026
Cover Material, Thickness [mm]	PET	0,05		OTR	12,82
Seal Type	Thermoseal (PE)			NTR	-0,326
Pack Area [m2]	0,02340			CDTR	-14,15
Cover Area [m2]	0,02228		Cover Permeability [cc/cover]	WVTR	0,000702
Seal Length [mm]	600			OTR	10,99
Seal Width [mm]	10			NTR	-0,174
Headspace [cc]	233			CDTR	-29,94
Conditions			Seal Permeability [cc/seal]	WVTR	0,0000007
Temperature [oC]	23			OTR	0,0277
External RH [%]	50			NTR	-0,000828
Internal RH [%]	30			CDTR	-0,0166
External atmosphere [%]	Oxygen	20,9	Total Pack Permeability [cc/total pack]	WVTR	0,000963
	Nitrogen	78,8		OTR	23,83
	Carbon Dioxide	0,3		NTR	-0,501
Internal atmosphere [%]	Oxygen	0		CDTR	-44,11
	Nitrogen	80			
	Carbon Dioxide	20			
Exposure Time [days]	144				

Fig. 5. *The output of entry parameters and results of calculation in the table.*

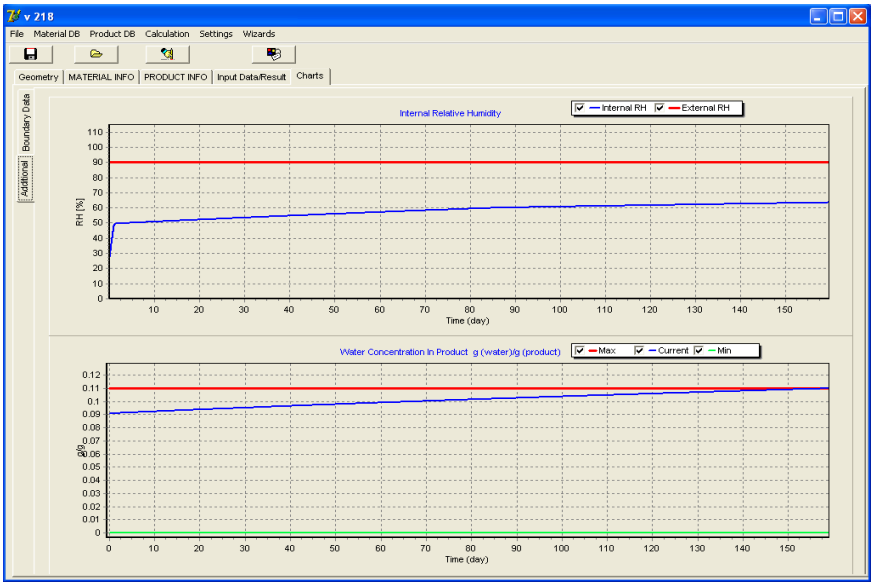

Fig. 6. *The output of the results of calculation in the form of diagrammatic dependences.*

The determination of limiting product's shelf life can be the main purpose of the calculations made by the program.

The experiments on controlling changes in the inner atmosphere in different packagings and shelf lives of the products in them have been carried out together with the enterprises that produce foodstuff. They have shown high-scale reliability of calculations made. In none of these experiments the difference between experimental and design value exceeded 30%.

Thus created program allows to rate the possibilities on packaging offered and to select the most appropriate and economically sound variant without long and expensive full-scale experiments.

It is necessary to have the information about product's behavior in the atmosphere of different contents or the kinetics of its interaction with, for example, oxygen, which can be of different concentration, to get accurate and reliable estimation of foodstuff shelf life.

As the example of using the program offered the researches and experimental-industrial approbation of storing the cake "Charodeika" have been carried out. This cake possesses a packaging of devised three-layer polymeric material: PP+ЭVOH+PP with thickness of 400 mcm and high protective properties packed in MA N2/CO2=80/20 at JSC CRC "Cheremushki" in Moscow.

In the course of researches the positive technological effect of impacts of cake's storing conditions in MA-1 has been determined. It is ascertained that carbon dioxide in the gaseous mixture possesses bacteriostatic properties and slows down the growth of aerobic bacteria and mold, which can cause product's spoiling. This effect increases by low temperature. Rise of storing's temperature till (20±2) ºC decreases packaging's protective properties for gas and steam permeability in 2,5 and 3,2 times accordingly. It creates the conditions, in which oxygen and moisture can appear and cause complex fermentative and hydrolytic oxidizing processes of carbohydrates. That can lead to microbiological foodstuff spoiling in relatively short period of time after 10 days of storing.

The economic benefit of introduction of technology of prolonged storing of cake "Charodeika" in the new packaging in MA made 3, 72 million of rubles. Using of "the program for calculating packaging's permeability and forecasting foodstuff shelf life" in the storing technology of cakes and biscuits in the packed form and in MA will allow to increase the production volume of cakes owing to widening trade limits and their consumption.

References:

[1] A. Y. Malkin, A. E. Chalykh Diffusion and tenacity of polymeric materials. Measuring methods. M., Chemistry, 1979, p. 304 .

[2] V. V. Ananyev, O. V. Videnin The permeability of polymeric packaging and shelf lives of dairy products. The magazine "Molochnaya promyshlennost", 2009. *Ананьев*

[3] A. D. Magomedova Working out technological ways of biscuits prolonged storage/Dissertation materials, Moscow, 2013.

[4] V. V. Ananyev, O. V. Videnin The magazine "Plastiks" Number 2007 №1-2/47-48 How to calculate protective properties of packaging.

COMPARATIVE QUANTITATIVE ANALYSIS OF THE USE OF PAPER AND COMPUTER

V.G. Lasheva [1], A.B. Blazheva, H.H. Lasheva

[1]*University of Chemical Technology and Metallurgy –Sofia, Bulgaria* veska_lasheva@abv.bg

Abstract. *The aim of the study was to undertake a survey of the Bulgarian undergraduate and graduate students about their reading and writing habits for the use of a computer or pen and paper when writing and reading in the learning process and leisure, what kind of digital devices they prefer to use for school work and for pleasure, how many hours they spend reading and writing each week. We investigate how the length of the text influences the preference for reading on a screen or in a hard copy, possibilities for reading and multitasking and at what kind of reading and writing the concentration is better. The study was conducted in Sofia, Bulgaria in the period December 2014-February 2015. It involved 220 undergraduate and graduate students from Sofia, Bulgaria, 160 of which were bachelors aged 19-25 years and 60 were Master's and Doctoral students aged 23 -26 years of different specialties: pulp, paper and packaging; printing, computer science, psychology, chemical engineering, marketing, industrial management, social psychology, accounting.*

In accordance with the requirements the questions to the students were given in Bulgarian, the answers were also in Bulgarian.

Key words: paper, computer, writing, reading, hard copy, digital screen, multitasking

I. Ownership and use of digital devices

We investigated what kind of digital devices Bulgarian students possess and what of them they use most often for school work and for leisure. After counting the answers of filled questionnaire we calculate that our undergraduate and graduate students use mainly laptop computers (75% of them) and mobile phones with and without internet. Some of them possess both laptop computer and desktop and 2 mobile phones each. When they read for school work student use most often laptop computers and Master's and Doctoral students use laptop computers and desktop. For reading for pleasure they use different digital devices: desktop, laptop computers (32%), mobile phones (50%), tablet computers, eReaders. For writing for school work bachelors prefer to use paper and pen (56%) and laptop (25%) and postgraduate students use paper and pen and laptop at equal amounts (50%). There is a big variety of used digital devices when students write for pleasure: mobile phones (50%), laptop computers (18%), desktop, tablet computers, paper and pen.

As a conclusion we can say that for writing for school work our students use preferable paper and pen and for writing for pleasure they use mainly mobile phone.

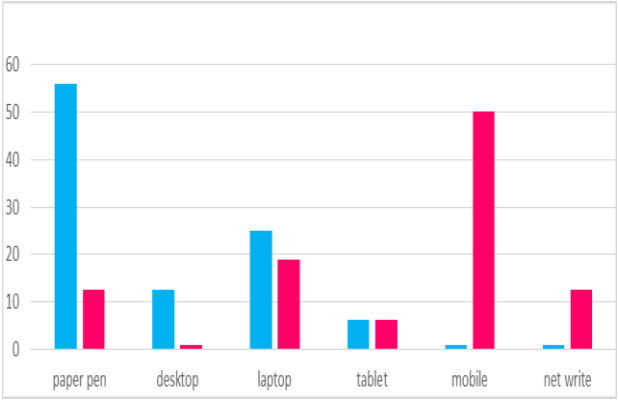

II. Amount of reading for school work and for pleasure

The next set of questions is connected with the time which students spend reading for school work and for pleasure each week. A big part of students read 5-6 hours/week (50% of answers) and 9-10 hours/week (25 % of answers) for school work. The quantity of students reading more than 10 hours/week and less than1 hour/week is only 6%. Doctoral students read more: 9-10 hours/week (50%) and more than 10 hours/week (33%). The time of reading for pleasure is different: 44% of bachelors spend 7-8 hours/week at reading for pleasure and 31% read 3-4 hours/week. Master's and Doctoral students read more for pleasure: more than 10 hours/week (33%) and 5-6 hours/week (33%).

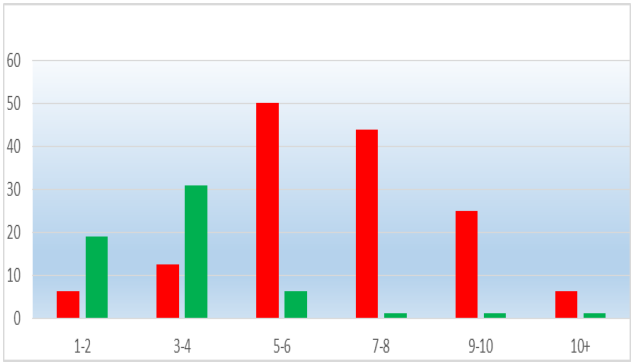

This results show that as a rule Bulgarian Master's and Doctoral students read more for school work and for pleasure in comparison with bachelor students. We have not data for comparison with students from other countries.

III. Reading in hard copy or digital screen

The next questions refer the student's habits for reading in hard copy (using a printed book, academic journal or paper copy printed out from online) or on a digital screen (desktop or laptop computer, mobile phone, a tablet computer or an eReader). Our research shows that around 44% from Bulgarian students have not preferences reading in hard copy or on a digital screen and 32% prefer to use a hard copy for their school work. When they read for pleasure they prefer to use digital screen (62, 5%). These results show that for reading for school work Bulgarian students use both hard copy and digital screen, but for reading for leisure they use mostly digital screen.

IV. Text length

The next questions are devoted to influence of the length of the text on the choice of used device for reading - in hard copy or on a digital screen. When the text for school work is short (up to 1 page) students rather use a digital screen for reading. Doctoral students noted that they have not preferences reading short text in hard copy or on a digital screen. For reading a long text (more than 1 page) for school work students use hard copy and digital screen at equal amounts (50%). Doctoral students prefer to use a hard copy (67% of them). From answers of these questions we could make a conclusion that for school work students prefer to use digital screen when the text is short and use more frequently a hard copy when the text is long. When students read for pleasure they prefer to use a digital screen and the size of text does not influence their choice.

V. Reading and multitasking

The next set of questions is connected with the possibility of reading in hard copy or on a digital screen and be engage in other activity at the same time. These activities may be different: doing something with mobile phone, doing something with computer, talking with someone face-to-face and other. Our study shows that when students read in hard copy they rarely do something else. When reading on digital screen they frequently multitask. Some students indicated such answer as "I am taking care for my child" or answer "I do not multitask when reading in hard copy". The most disseminated answer for bachelor students in time of reading in hard copy is "Doing something with my mobile phone". Doctoral students indicated the answer "Talk with someone face-to-face" as the most preferable kind of multitasking in time of reading in hard copy.

When students read on a digital screen the answers about multitasking were similar. A big part of bachelor students indicated the answer "Doing something with my mobile phone" as the main multitasking activity. The Master`s and Doctoral students gave different answers: "Doing something with my computer" and "Talking with someone face-to-face". These answers indicate that the reading in hard copy or on a digital screen do not influences the possibility of multitasking, but student multitask more frequently when read on a digital screen. Usually they read in hard copy or on a digital screen and speak at their mobile phones or talk with somebody at the same time.

VI. Reading and concentration

The next questions are connected with the possibility of concentration in time of reading in hard copy or on a digital screen. We investigated in which platform it is easier to concentrate on reading. 57% of bachelor students and all doctoral students indicated that they concentrate easier in time of reading in hard copy. They noted as a hardest concentration reading on mobile phone and desktop. Small part of them noted reading on hard copy as hardest for concentration. These answers correlate well with results of reading and multitasking. When students read in hard copy they are more concentrated and multitask less.

VII. Writing and concentration

Almost all investigated bachelor students (76%) indicated that for them it is easier to concentrate when they write on paper. For Master`s and Doctoral students this amount is 67%. Bachelor students noted

that they hard concentrate in writing on mobile phone and tablet computer. Doctoral students indicated that they concentrate hardest writing on mobile phone. These results show that for Bulgarian students it is easier to concentrate when they write on paper and it is hard to concentrate in writing on mobile phone.

VIII. Learning to read and write

Before students learn to read the members of their families read to them frequently (50%) and sometimes (50% from answers). Their parents were the people who learnt them to read (75% from answers of bachelors). The second place is for school and teachers. The contribution of parents and teachers for learning to read of Master`s and Doctoral students is equal. A big part of them learn to use a keyboard at their homes (69% from bachelors) and at school (67% from doctoral students). These results show that Bulgarian family participates actively in education of their children.

There was a question about habits of communication of students with their family members, their friends, their schoolmates and social media concerning reading books and stories for pleasure. Bulgarian students gave different answers of this question. More of them discuss about what they read mainly with their family members and their friends but they indicated that they do it sometimes. They rarely discuss with their schoolmates and never or rarely with social media. This shows the important roles of family and friends in life of students.

IX. Conclusion

At conclusion we may say that Bulgarian students possess and use different kinds of electronic devices, mainly laptops and mobile phones with or without Internet access. For their school work they use laptop and hard copy and for pleasure they prefer to use digital devices. Bulgarian students multitask more frequently when read on a digital screen but are more concentrated reading in hard copy. They prefer to write on paper because the concentration in this case is easier and better. Their families supported them in learning to read and use keyboard. They discuss books and stories they read mainly with their parents and friends.

References

[1] Zhelev,S.,"Marketing Research", UIS, Sofia, 2008.
[2] Gatev K. Gateva, N., "Statistics: Statistical methods in empirical research and business," Publishing "Paradigm" in 2008
[3] Taipale S. Telematics and Informatics, www.elsevier.com/locate/tele(2013)
[4] Baron, N., 2008. Always On: Language in an Online and Mobile World. Oxford University Press, New York.
[5] Baron, N., 2014. Does mobile matter?: the case of one-off reading. In: Goggin, G., Larissa, H. (Eds.), The Routledge Companion to Mobile Media. Routledge,London.
[6] Fortunati, L., Taipale, S., 2013. The advanced use of mobile phones in five European countries. Br. J. Sociol, accepted.
[7] Fortunati, L., Vincent, J., 2014. Sociological insights on the comparison of writing/reading on paper with writing/reading digitally. Telemat. Informat. (online).

STUDY QUESTIONS DIVISION AIR FUEL EXTENT OF ORGANIC ORIGIN

A.A. Osmak, A.A. Seregin, S.I. Blazhenko

National University of Food Technologies, Volodimirska 68, Kiev, Ukraine

Abstract: *The benefits of using biomass as a renewable energy source. The mechanism of the process thermal processing (gasification) biomass. The process of gasification plant waste gas generator as the most important factor for the stability of the process, in terms of physical characteristics of fuels, such as flow ability fuel and uniform permeability in the reservoir. Studied the movement of the gas flow through porous backfill - cooking fuel. The problem of air distribution in a layer of fine fuel plant with a certain factor of porosity.*

Keywords: plant biomass, gasification, fuel flow ability, gas permeability, renewable energy.

I. Introduction

Plant biomass is one of the most powerful and affordable renewable energy on earth. For centuries, including in Ukraine, it was the main source of energy. At the end of the 19th century, more than 60% of world energy balance fuel was wood. However, the situation has changed. Coal and later oil and gas extraction are much better exposed industrialization gradually replaced with wood fuel balance.

In the energy sector of any country provides for a gradual increase in the role of non-traditional sources and raw materials for the production of alternative fuels. Recently, there is a rapid transition to the use of biomass as fuel.

The advantages of biomass as an energy source specifies the environmentally friendly than traditional fossil fuels (biomass combustion leads to low emissions of carbon dioxide), and the ability of the fuel updated. Compared with coal burning plant biomass is characterized by a decrease in emissions of sulphur oxides (20 ÷ 30 times) and ash (3 ÷ 5 times).

One of the key technologies of thermal processing of biomass gasification is. The basis of the process is the chemical compound reducing agent (carbon and hydrogen) with an oxidant (oxygen). The process of gasification is a shortage of oxygen, and the complete oxidation of the fuel does not occur [1, 2]. In temperatures above 800 ° C in a shortage of oxygen at 80 ÷ 85% of the mass of organic material goes into a gaseous state. Support the temperature necessary to complete the process is due to the combustion of carbon residue. The main components of the combustible gas is formed H2 and CO.

Gasification of biomass allows use to generate electricity instead of steam power cycle more efficient in relation diesel thermodynamic cycle (for units with electric capacity below 1.5 MW) [2], combined-cycle gas turbine and combined cycle (for electric power plants more 1.5 MW). The main advantage of thermo chemical gasification fuel before combustion direct is the ability to use more efficient thermodynamic cycles of power generation and less stringent requirements for fuel preparation.

Investigation of gasification plant waste into gas generator shows that the most important factor in the stability of the process from the point of view of physical characteristics fuels are fuels flowability and his uniform permeability in the reservoir. The whole technological process of preparation of fuel for gasification plant (in addition to its previous drying) and is to provide the above two physical characteristics. These characteristics can be achieved in three ways: preparing press packets of a certain density, compaction layer of fuel in coal mine gas generator forced his promotion and crushing, grinding or machining fuel for a homogeneous grain mass [3].

II. Materials and methods

This work is devoted to aerodynamic fine layer of vegetable fuels and related design features calculation reactor chamber gas generator.

Study of driving the gas flow through porous backfill, which essentially is the small lump fuel plant origin, is the most important part of gas production caused by aerodynamic interaction laws air with a layer of fuel.

The gas stream entering a fuel layer, is divided into a large number of individual jets moving at a very complex trajectories in the space between the lump. Last channels are of irregular shape with a variable cross section, many interconnected. Therefore, physical, or other structural characteristics of the layer can be determined by the following factors: a) the average grain size in the layer; b) density layer; c) its roughness [4].

If the layer of fuel gas generator in the area of supply air has a different bulk density, the air rushes bulk of the path of least resistance, forming local branches of rapid oxidation of the fuel, while the distribution of air over the cross section layer of fuel is changing dramatically.

Due to the low thermal density layer of organic fuel or other vegetable saturation process air local burnout develops extremely rapidly, causing a sharp destabilization process gassing, which means eliminate outside interference is very difficult. So, to organize sustainable gasification process fine vegetable consumption priority which is to provide a higher level of homogeneity fractional layer of fuel to heat and density of such a maximum speed of air in between lumpy spaces in which the layer structure is not subject to sudden changes.

For fuel herbal most important quantity characterizing the hydrodynamics of the gas in the reservoir is the drag coefficient.

For gas filtration through a bed of granular backfill layer resistance Δp can be determined from the following equation:

$$\Delta_p = \frac{\lambda_ш \cdot l}{d} \cdot \frac{\gamma}{g \cdot \omega_\psi} \qquad (1)$$

where Δp - resistance layer height l mm of water. c. at ω filtration rate in m / s and typical particle size d in mm;

γ - gas weight in kg \ m3;

g - acceleration of gravity;

λш - coefficient of resistance layer, which is a function Reψ.

$$\mathrm{Re}_\psi = \frac{\omega_\psi \cdot d}{\upsilon}$$

where ν - kinematics viscosity.

Normal stationary filtering mode is set in the event that the filtration rate on conventional lump between channels is identical, uniform cross section and is responsible for the normal size of the system resistance layer Δ_p.

The increase in resistance layer is associated with a decrease in the diameter d lump between channels and increase filtration rate ωψ, resulting in increased oxygen zones, increase heat loss and deterioration of the gasification process.

III. Results and discussion

Thus, the normal conditions for gasification of fine fuels will be the structural layer requirements that ensure: a) the required amount of "grain" of fuel; b) the required rate of porosity layer of fuel that does not change the cross section and time of the layer.

Addressing structural requirements for fine-grained layer of vegetable fuel at its gasification is closely related to the method of supplying air to the fuel layer and its distribution.

Addressing the issue of air distribution in a layer of fine fuel plant with a certain ratio porosity should first stop on the range of flow air stream coming out of the lance, in determining the limits of the value of the cell area, which can be equipped with the necessary amount of air coming out of the lance. It should just point out that the layer of vegetable fuel, which is in the area of oxygen should be regarded as a layer of semi-stationary particles with different mobility.

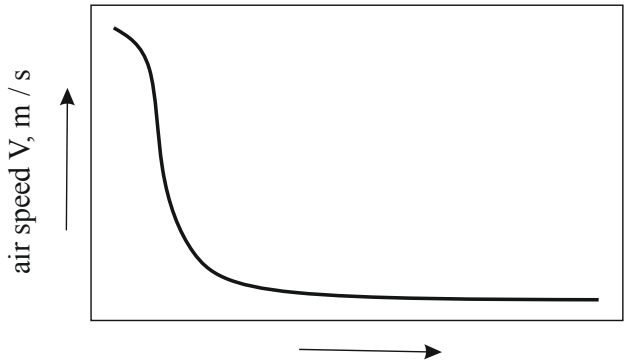

Figure 1. *Axial characteristic air lance*

The foregoing especially include the oral air-gas duct (active region oxidative process before the neck lance), where the action of the kinetic energy of the air coming from the lance fuel particles are in constant motion. In considering the range of flow air stream coming out of the lance in the gasifier fuel layer, and related designs, should focus on some characteristics of lances. Under the characteristic axial lance understood graphical representation speed air stream depending on the distance of the considered point of the neck lance toward its axis. From the graph (Figure 1) shows that the neck near the central part of the jet lance is not investigated in this region braking effect of the environment and has a constant speed, with constant velocity field width equal to the diameter of the hole lance (Fig. 2) and as the distance lance of the neck tends to zero.

The width of the jet axis, however, continuously expanded to capture still particle environment, and thus the flow rate decreases. As a result of jet fuel produced fine layer of air-gas duct from "hanging" in it fuel particles.

Within the area of air-gas duct (shown in Fig. 2 thick dashed line) on the gasification process consumes oxygen coming from the air through the lance. What with the length axis of action channel L,

a fast fading speed air stream as it is the distance from the lance?

In general, the speed reduction is expressed first derivative of the velocity v = f (x), and the damping rate is directly proportional to the square of the speed. The diameter of the lance is important in reducing the rate of speed as far as the distance from the lance at the same value of the initial speed.

Reducing speed directly proportional to the diameter reduction lance. The speed of the jet at a given point at a distance x from the mouth of the lance is equal to:

$$v = \frac{0,96v_0}{\frac{ax}{R_0} + 0,29}, \qquad (2)$$

This means that with decreasing diameter lance denominator of the right side of the equation increases and decreases speed (if this initial rate remains unchanged). So the range of flow jet at the same pressure of growing with increasing diameter of the lance, and the speed of the jet at a considerable distance from the lance is inversely proportional to the diameter of the lance.

Shown in Fig. 2 steps duct axis L defines essentially radial channel characterization data for its origin. By varying the diameter of the lance and its profile, and you can change the characteristics of radial duct (deflection angles and the length axis L), approaching the borders of such a construction area of the Strait, which provides the most complete saturation of oxygen consumption layer this area subject to appropriate its hydraulic characteristics.

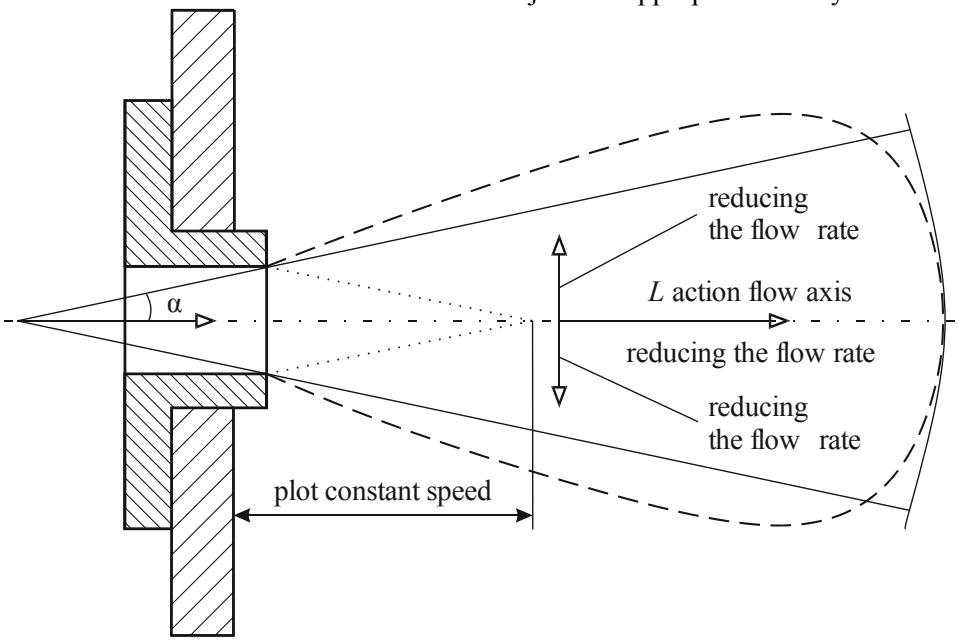

Figure 2. *Scheme of the air-gas flow*

Changing characteristics depending on the radial profile lance according to practical tests are shown in Fig. 3 for a distance L = 50 mm. It should draw attention to the characteristics of the lance IV, where there is no directional jets along the axis.

Air speed not exceeding 10 m / s and does not change to the deflection angle of 20 °.

If you know the initial velocity of the air at the mouth of the lance V_0, his flow is equal to:

$$V = afV_0 \text{ m / s} \qquad (3)$$

where *a* - compression ratio of the jet;

f - the minimum cross-sectional area of the lance.

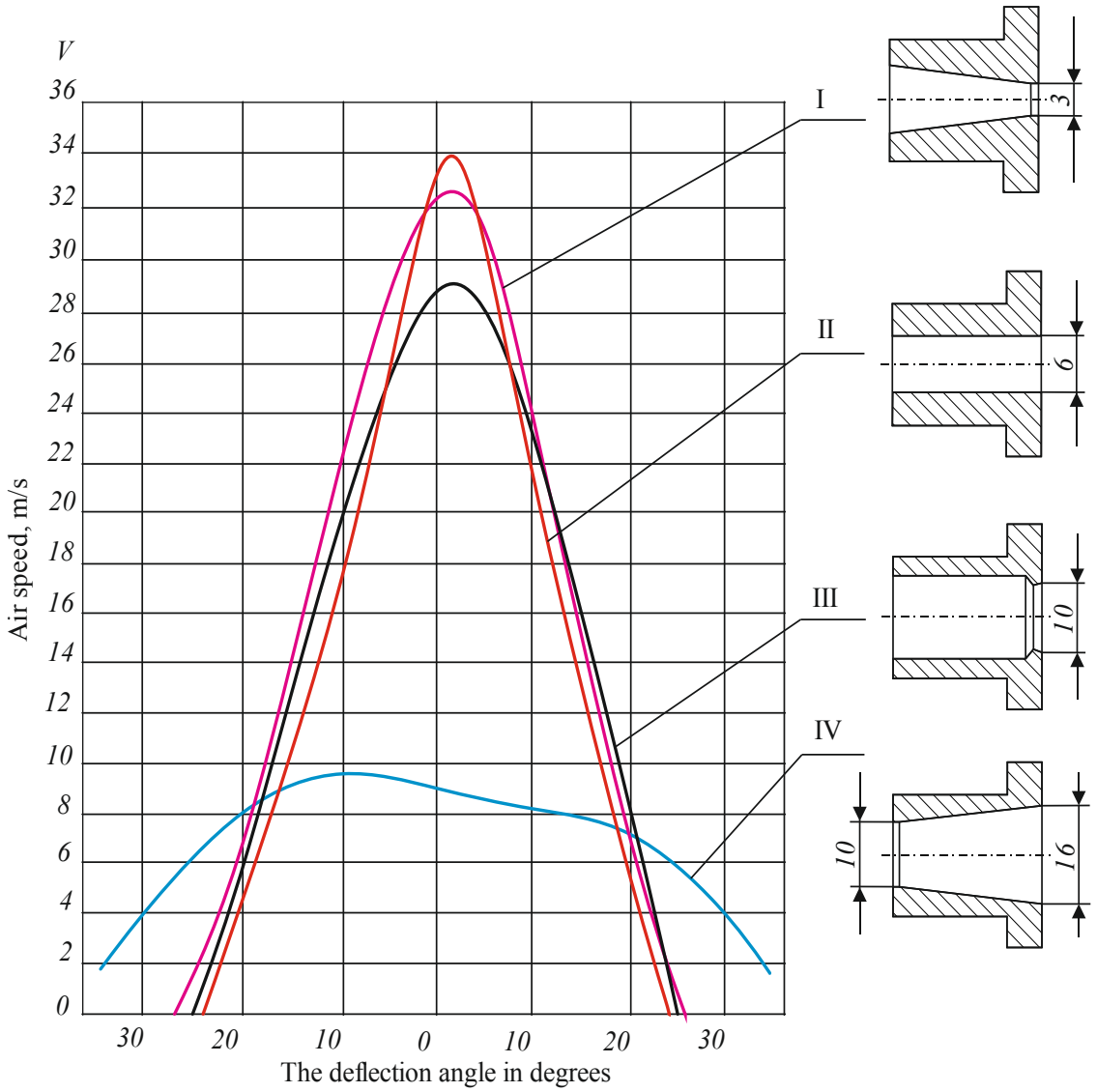

Figure 3. *Radial characteristics of different lances at hydrostatic pressure*

The size of the area saturation layer air-gas environment plays an important role in the reduction of low-flow gasification process and vegetable consumption is associated with the value of tar in the gas. In this regard, the construction of air distribution system in a layer of such fuel is highly responsible design stage gasifier for the gasification of the fuel to synthesis gas.

In the study of gasification process in the free layer of loose adopted a principle point of air distribution. The main element of building such a system is air-duct gas generated in the fuel layer embedded in his lance. The combination duct system made it possible to create a plane blowing filing a kind of "air-gas grid", which we take as a basis for building the oxygen reduction zone in the low-temperature gasification gas generator for a free loose layer.

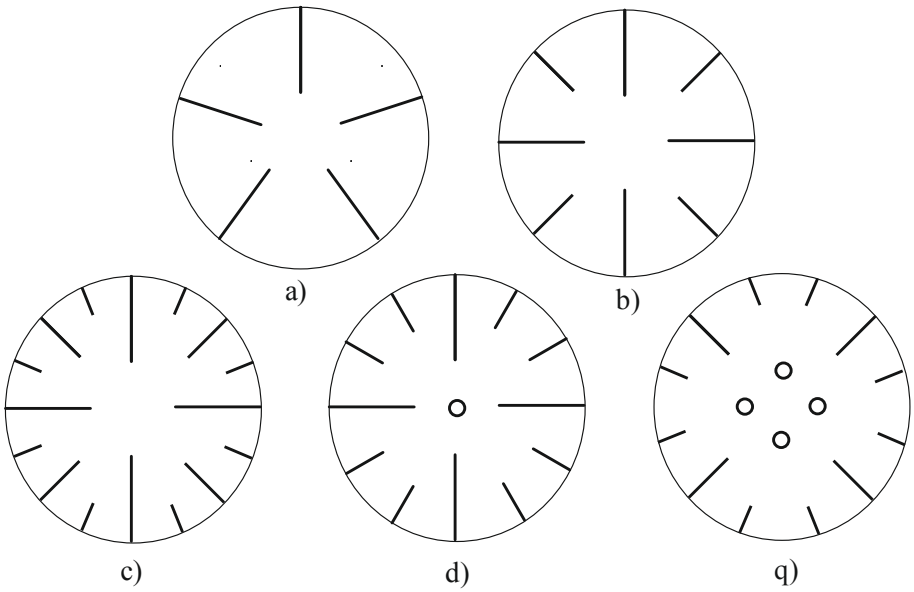

Figure 4. *The schematic diagram of the lances in the chamber of the gas generator for the gasification of fossil fuels in a freely poured layer*

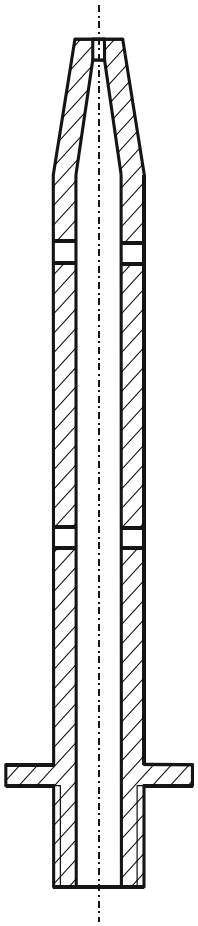

Figure 5. *Scheme lance*

Depending on the diameter of the gasification chamber air-gas grid can be constructed by combining various depth in layer lance.

Fig. 4 shows more of the following schematic. The basis for these schemes adopted the position that a given layer of fuel density coefficient length axis of the active part of the air-gas duct L does not exceed 30-35 mm with air velocity in the nozzle lance on cold blast of 10-12 m / s.

At this speed the air layer of coke is the scope of the duct has a relatively low mobility, easily observable by eye in which the resistance layer as a whole is not broken and does not lead to fluctuations in quantity and quality out of gas.

As seen from the FIG. 4 Diagram of air-gas lattice elements on which the camera is air (lance) immersed in the fuel layer at different depths and are depending on the location in the layer, one, two or more nozzles (Fig. 5).

Scheme a, b, c (Fig. 4) constructed by a combination of different lengths peripheral lance. If the diameter of the chamber is large enough and can not solve the construction of air-gas grilles on the above chart, you should go to the d and q schemes. These schemes are based on a combination of peripheral transverse and vertical lance that can be introduced into the bottom layer or dropped on top of mine. Constructive solutions adopted in each case depending on the specific type of fuel and its characteristics and purpose gasifier.

Practical experience shows that the transverse lances enable the most appropriate to allow the air in question layer chamber diameter of 500 mm. For the construction of air-gas lattice in the chambers of larger diameter should dwell on the combined systems consisting of transverse and vertical air distribution elements.

Fig. 6 is a diagram of building air-gas grid (1/4 of

the area) in the chamber gasification gasifier.

The air-conducting elements of the camera consists of three types of cylindrical cross lances of different lengths: short, medium and long.

Focusing on the hour air flow required for gasification of fuel, air speed and the estimated average area of saturation structure designed air-gas grid for this type camera.

The lattice consists of 16 cross-lance 4 long, 4 and 8 medium short. Each of these has one lance nozzle face and two to four sides. Axis ducts are constructed in such a way that within the settlement area of saturation of air-gas grid consists of 64 individual elements of saturation.

The value of the saturation element must be determined for each type of plant waste and its structural characteristics (grain size, bulk density ratio). The higher the ratio of bulk density, the higher should be the size and area element saturation and contrast, with the reduction rate should decrease bulk density and saturation area.

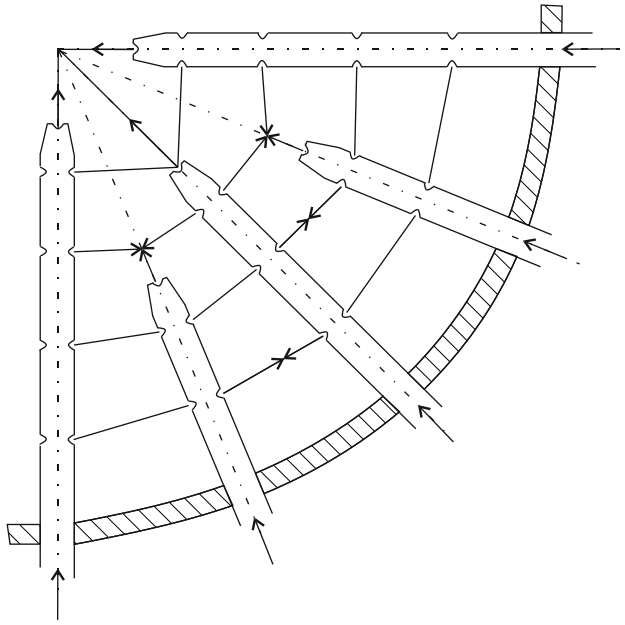

Figure 6. *The typical construction of air-gas grid (1/4 of the area of the camera) in the gasifier*

IV. Conclusions

Considered in this paper material associated with the gasification plant of fine fuels is attempt to summarize as experimental results and theoretical issues intensify search and controllability flatulence gas generator in reverse type. Further development work on fuel gasification plant is directly connected with finding ways and means of establishing continuity and stability of the process. The stability and relative ease of modeling air-gas flow gasifier chamber make such searches perspective. Testing of static and dynamic models can significantly accelerate the solution of theoretical and practical issues of gas generator technology.

Experience of practical tests show that cross-lance enable the most appropriate to resolve the issue in a layer of air supply to chamber diameter of 500 mm. To build air-lattice gas chambers in larger diameter should stop at the combined system consisting of transverse and vertical elements of the camera on which air is supplied.

References

[1] *Богданович В. П.* Перспективы использования альтернативного топлива в сельском хозяйстве [Текст] / В. П. Богданович, Н. В. Шевченко // Техника в сельском хозяйстве. – 2012. – № 5, pp. 38-40.

[2] *Сергеев В.В.* Научно-технические предпосылки для газификации растительной биомассы / В.В.Сергеев/ Научные исследования: материалы науч.-практ. конф. – СПб.: Изд-во Политехн. ун-та, 2007, pp. 148-153.

[3] *Сергеев В.В.* Проектирование и расчет газогенераторных установок при использовании биомассы.: Учеб. пособие / В.В.Сергеев, А.А.Калютик, В.Н.Моршин. – СПб.: Изд-во Политехн. ун-та, 2004, p.60.

[4] *Алешина А.С.* Моделирование процесса газификации растительной биомассы в газогенераторах кипящего слоя / С.А. Иванов, А.С. Алешина // Вестник ЗабГУ. 2013. - № 3, pp. 7

AROMATIC EMULSION BEVERAGE CATERING AND INDUSTRIAL PRODUCTION

O. Lugovska[1], V. Sidor[2]

[1]Faculty expertise and health food products, National University of Food Technologies, Volodimirska 68, Kiev, Ukraine, e-mail:oksana.lugovska320@gmail.com
[2] Faculty expertise and health food products, National University of Food Technologies, Volodimirska 68, Kiev, Ukraine

Abstract: *This article describes the use of emulsions for the production of beverages for for the restaurant business and industry. This paper describes the physico-chemical principles underlying the functional role of hydrocolloids in oil-in-water emulsions. The procedure of emulsion preparation with hydrocolloids which are stabilizer-emulsifiers, namely gum-arabic and starch, was updated by introducing new technological parameters. The food emulsion samples were investigated by their stability in beverages during their term storage. The optimum ratio between aqueous stabilizer and oil phase is characterized by maximum number of emulsion particles with the size under 1 micron.*

Keywords: emulsion, drink, stability, hydrocolloids, particles size

I. Introduction

Emulsions are widely used in many branches of food technology. While using aromatic emulsions in non-alcoholic beverages production a series of advantages is observed, in particular the blending time is decreased as there is no need to add aromatizer, to choose dye and stabilizer. The problem of aroma and flavor stability is also solved because in such a case an emulsifier plays a role of aromatic part adsorbent and provides delicate and mild aroma.

In the restaurant business and public catering the emulsions are used for flavoring and coloring the alcoholic beverages, which are prepared on the basis of alcohol, sugar, citric acid and addition of concentrated juices, depending on the recipe of the finished beverage.

The advanced technology of aromatic emulsions is associated with the peculiarities of hydrocolloids application. Constant attention to the research of these compounds is stipulated by their importance for the food industry. However, despite the large number of studies on the physical and chemical properties of hydrocolloids, there is insufficient scientifically based data on their use in food emulsions [1].

Emulsions are thermodynamically unstable. With time they tend to break down into their constituent oil and aqueous phases. The term ‘emulsion stability' therefore refers to the ability of an emulsion to resist this breakdown, as indicated by growth in average size of droplets or change in their spatial distribution within the sample. The more slowly that these properties change, the more stable is the emulsion. In practice, stability is a relative term which depends on the context. For some food emulsions, such as cake batters or cooked sauces, the required time-scale for stability is only a few minutes or hours. But for other products, such as soft drinks and cream liqueurs, emulsion stability must be maintained over a period of several months or years [2].

A hydrocolloid ingredient may act as an emulsifying agent, as a stabilizing agent, or in both of these roles. An emulsifying agent (emulsifier) is a surface- active ingredient which adsorbs at the newly formed oil-water interface during emulsion preparation, and it protects the newly formed droplets against immediate coalescence. Given that polysaccharides are predominantly hydrophilic in molecular character, and most hydrocolloids are not surface-active, they cannot act as primary emulsifying agents. There is really only one hydrocolloid - namely, gum arabic - which is commonly employed as an emulsifying agent. The main emulsifying agents used in food processing arc the proteins, especially those derived from milk or eggs. A stabilizing agent (stabilizer) is an ingredient that confers long-term stability on an emulsion, possibly by a mechanism involving adsorption, but not necessarily so. In O/W emulsions, the stabilizing action of hydrocolloids is traditionally attributed to the structuring, thickening and gelation of the aqueous continuous phase [3].

The functional role of these small- molecule emulsifiers in food technology is typically not for emulsion making, but for other reasons: controlling fat morphology and crystallization; promoting shelf-life through interaction with starch and gum arabic;

and destabilizing emulsions by competitive protein displacement from the oil-water interface [4, 6].

A stable emulsion is one where the droplets remain sufficiently small and well separated that Brownian motion alone keeps them evenly dispersed throughout the continuous phase. The physic-chemical principles of O/W emulsion stability arc based on the classical colloid theories of electrostatic and steric stabilization. Electrostatic stabilization arises from the presence of electrical charge on the surface of the droplets, or more usually on the adsorbed stabilizer layer at the surface of the droplets. The greater the charge density at the surface, and the lower the ionic strength (electrolyte concentration) of the continuous phase, the more stable is the emulsion. Steric stabilization arises from the presence of a polymeric (steric) barrier at the droplet surface. To confer long-term stabilization, this polymer must be present at sufficient concentration to cover the oil-water interface completely, and it must remain permanently attached to the surface, with at least part of the molecule projecting away from the surface into the aqueous medium. Steric stabilization is increasingly supplemented by electrostatic stabilization in emulsions containing adsorbed proteins at pH values well away from the protein's isoelectric point (p)[7].

Whether emulsion droplets will remain dispersed or will tend to stick together depends on the nature of the antiparticle pair potential between the droplet surfaces. Generally speaking, colloidal stability requires that the antiparticle repulsion should be of sufficient range and strength to overcome the combined effects of gravity, convection. Brownian motion and the ubiquitous short-range attractive forces together drive the system towards its final and inevitable phase-separated equilibrium condition (Fig. 1).

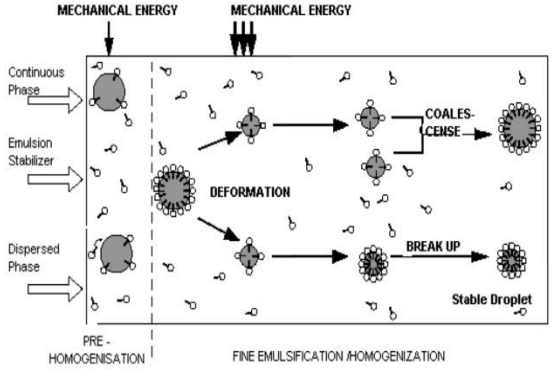

Fig. 1 *Emulsification and stabilization*

The aim is to study particle size effects on the stability of emulsions during storage and use in the manufacture of beverages and their stability during 180 days [5, 8].

II. Materials and methods

As materials for research are prepared samples of drinks with emulsions (O/W) orange, lemon, peach, grapefruit in which use stabilizer (modified starch or gum arabic).

When consistency and stability of the emulsion in the beverage were verified by preparing drinks and placing them in direct sunlight, for at least 72 hours, an oily ring is formed. Then this emulsion is homogenized again for particles to 1 micron. Drink this emulsion based not put on stability during storage as oily ring will increase. If within 72 hours oily ring is formed in drinks, such drinks are investigated for stability following manner.

For studies prepared samples of drinks with emulsions (O/W):

1. Beverages (with starch)

a) non-alcoholic beverages orange (1), lemon (2), peach (3), grapefruit (4)(Table 1)

b) alcoholic beverages orange (5), lemon (6), peach (7), grapefruit(8) (Table 2).

2. Beverages (with gum arabic)

a) non-alcoholic beverages orange (9), lemon (10), peach (11), grapefruit (12)(Table 3)

b) alcoholic beverages orange (13), lemon (14), peach (15), grapefruit(16) (Table 4).

Preparation of drinks

Preparation of the sugar syrup.

a. Weigh the required amount of water into a glass and heated to 50 -80° C.

b. Attach the required amount of sugar and completely dissolve.

Dissolving citric acid and sodium benzoate in water (t=20 ºC). Attach the required amount of sodium benzoate and completely dissolve. Add citric acid and dissolve completely.

Attach the required amount of emulsion and completely dissolve.

Weigh the required amount of ingredients of the drinks add in stirrer, mix at room temperature until ingredients completely dissolved in water with CO_2.

Table 1

Formulations of non-alcoholic beverages (with starch) orange (1), lemon (2), peach(3), grapefruit (4)

The ingredients of the drinks	Content. g/100g			
	Number of drinks			
	1	2	3	4
Emulsion	1	1	1	1
Sugar	100	100	100	100
Citric acid (E330)	2,5	2,5	2,5	2,5
Sodium benzoate	0,15	0,15	0,15	0,15

(E211)				
Water	896,35	896,35	896,35	896,35
Total	1000	1000	1000	1000

Table 2

Formulations of alcoholic beverages (with starch) orange (5), lemon (6), peach (7), grape fruit(8)

The ingredients of the drinks	Content. g/100g			
	Number of drinks			
	5	6	7	8
Emulsion	2	2	2	2
ugar	180	180	180	180
Juice Bx 70%	23	23	23	23
Vodka 40%	450	450	450	450
Citric acid (E330)	2,5	2,5	2,5	2,5
Sodium benzoate (E211)	0,15	0,15	0,15	0,15
Water	342,35	342,35	342,35	342,35
Total	1000	1000	1000	1000

Table 3

Formulations of non-alcoholic beverages (with gum arabic) orange (1), lemon (2), peach(3), grapefruit (4)

The ingredients of the drinks	Content. g/100g			
	Number of drinks			
	9	10	11	12
Emulsion	1	1	1	1
Sugar	100	100	100	100
Citric acid (E330)	2,5	2,5	2,5	2,5
Sodium benzoate (E211)	0,15	0,15	0,15	0,15
Water	896,35	896,35	896,35	896,35
Total	1000	1000	1000	1000

Table 4

Formulations of alcoholic beverages beverages (with gum arabic) orange (5), lemon (6), peach (7), grape fruit(8)

The ingredients of the drinks	Content. g/100g			
	Number of drinks			
	13	14	15	16
Emulsion	2	2	2	2
ugar	180	180	180	180
Juice Bx 70%	23	23	23	23
Vodka 40%	450	450	450	450
Citric acid	2,5	2,5	2,5	2,5
(E330)				
Sodium benzoate (E211)	0,15	0,15	0,15	0,15
Water	342,35	342,35	342,35	342,35
Total	1000	1000	1000	1000

For alcoholic beverages add required amount of vodka 40%.Measure density, pH of the drinks. The results of measurement of each emulsion: density-lab density meter, pH- lab pH meter.

III. Results and discussion

There are four main kinds of instability processes exhibited by O/W emulsions: creaming, flocculation, coalescence and Ostwald ripening. (For W/O emulsions, the processes are the same, except that sedimentation replaces creaming). Flocculation is probably the most subtle and complicated phenomenon to control, because it can be triggered by so many different factors, and the resulting emulsion properties can be quite different depending upon whether the flocculation is weak or strong. In dairy-type O/W emulsions, at or below ambient temperature, instead of the full coalescence of liquid droplets, we have so-called 'partial coalescence' ('clumping') of semi-crystalline globules. In practice, two or more of the phenomena may happen at the same time, and the presence of one mechanism (flocculation) may trigger or enhance another (creaming or partial coalescence). Emulsion phase inversion, as in the shear-induced transformation of cream (O/W), is a multi-mechanism process.

If the particle size is less than 1 micron, the emulsion is highly robust stability and gives some turbidity but less than 1 micron particle size, the less turbidity, if the particle size is not greater than 0.3 micron. The principle of leverage ratio of water and oil phase of emulsions with different stabilizers is the same. In the obtained parameters also affects the nature of emulsions stabilizer.

Investigation of the stability of emulsions was carried out by determining the size of the diameter of the particles by laser granulometry and placement on the stability of soft drink, which was used emulsion for 180 days. During storage of beverages prepared from emulsions studied, there was no formation of oil ring or "creaming" bottled, indicating the stability of emulsion systems.

IV. Conclusions

The use of aromatic emulsions in the manufacture of soft drinks has several benefits, including: reduced duration blending, as there is no need to pick up the flavor, color and taste.

The process of storing drinks not observed the emergence of oil rings on the surface of the drink, there was no change in color, taste and aroma of the drink. Drinks made with the addition of gum arabic emulsions have better storage stability compared with a drink on starch (Fig. 2).

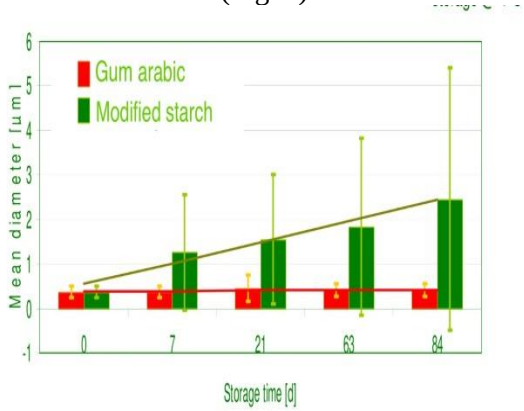

Fig. 2 *Emulsion – long-term stability*

Complete the emulsion must have the following parameters: the size of the oil particles (up to a micron); organoleptic - appearance, color, smell (aroma) and taste according to recipes; density (1,030-1,100), g/cm^3; pH (3, 3 ± 0, 7); stability in the drinks.

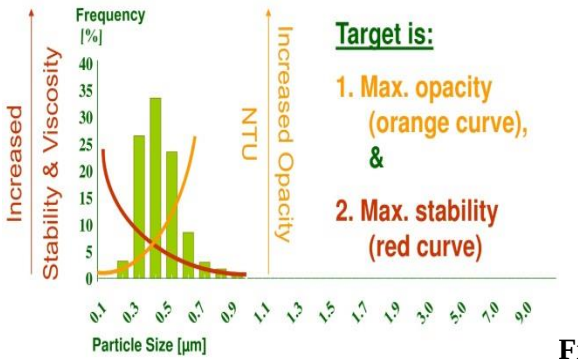

Fig. 3 *Emulsion summary*

The best result of research in emulsions - is to obtain the maximum number of particles of about 1 micron (Fig. 3).

Creating a stable emulsion system is a pressing issue in the food industry, so these studies are useful and important for the development of new food products.

References

[1].BORISENKO O.V., ALEKSEEV J.A., KLIMOV S., Methods of creating highly concentrated flavoring emulsions for soft drinks, food ingredients. *Raw materials and additives*, 2, pp. 18-19, (2002).

[2].PHILLIPS G.O., WILLIAMS P.A., (Eds.) Handbook ofHydrocolloids. Cambridge: Wood Head Publishing, p. 156 (2000).

[3].McKENNA B.M. (Ed.), Texture in Food — Vol. 1: Semi-Solid Foods. — Cambridge: Woodhead Publishing, p. 480 (2003).

[4].BOGACH A., Aromatic emulsion for manufacture of soft drinks,*Food & Drinks. Food & Beverage*, 4 - pp. 10-11, (2003).

[5].STEPHEN P., U.S. Patent for invention № 6576285, Cholesterol lowering beverage, Bader, Fowler, 10.06.2003.

[6].IMESONA. (Ed.), Thickening and Gelling Agents for Food. 2nd Ed., London: Blackie Academic and Professional, p. 408 (1999).

[7].WHISTLERR.L.B., MILLERJ. N., PASCHALL E.F., (Eds.), Starch Chemistry and Technology. 2nd Ed. Orlando, FL: Academic Press, 1984, 3508. Galliard T. (Ed.) Starch; Properties and Potential /Society of Chemical Industry. Chichester, UK: John Wiley and Sons, p. 210 (1987).

[8].ATWELLW.A. THOMAS D.J. Starches. — St. Paul, MN: American Associationof Cereal Chemists, p. 150 (1997).

STUDENTS' HABITS FOR INFORMED CHOICE OF FOOD AND DRINKS INTRODUCTION

M. Petrova[1], N. Ivanova[1], S. Damyanova[1], I. Kostova[1], I. Ivanova[1], G. Nakov[1]

[1]Department of Biotechnology and Food Technologies, University of Ruse "Angel Kanchev", Branch Razgrad, Aprilsko vastanie Blvd. 47, Razgrad 7200, Bulgaria,
e-mail: mgpetrova@uni-ruse.bg

Abstract. *The development of educational activities and events to familiarize students with the ways of healthy eating and their application is an important factor in the positive food culture in the younger generation. The purpose of the survey is to study the eating habits of the students in the last classes in secondary schools and to explain them the necessity of information when they make a purchase of food and drinks.*

Key Words: food labels, a survey, food products, consumers

I. Introduction

Nutrition is one of the most important factors for the health of the coming generation. The relation of eating habits with the development of cardiovascular disease, cancer, diabetes, etc. has been demonstrated by a number of studies. Food is necessary not only for the growth and functioning of the body and is associated with health and quality of life at any age. Particularly sensitive to the composition and quality of food are children in the different age groups [1]. A number of studies show that in our times the number of overweight people increases [2]. An worrying fact for Bulgaria is that the children at younger age have overweight. The number of cardiovascular diseases, diabetes, osteoporosis, myocardial infarction, etc. increases, almost all are related to unhealthy lifestyles and unhealthy diets. [3].

The legislator has taken care by normative acts - through the food label - the consumer to be properly informed and at the same time protected against incorrect and misleading information. [7] Already in 1979 the EU is introduced an unified control of the food-labeling with the Directive 1979/112. In 1990 the nutrition value labeling is introduced. In 2006 it is introduced Regulation 1924/2006, which establishes control of nutrition and health claims. In 2011 it is adopted a new Regulation 1169/2011, which introduces some changes, adds new requirements and repeals some. The Regulation 1969/2011 of practice brings together the requirements imposed in some of the previously adopted regulatory documents.

Consumers benefit from the information on the labels is sometimes uncertain and effectiveness of labeling as a communication tool is questionable. The reasons are different but perhaps the lack of interest to the information on the label by users is the most common. The survey by Alpha Research concludes that each of three people who had difficulties in reading the information on the label is not inclined to believe the label [7]. Even if the consumers have an interest a lot of them consider that it is difficult to cope with the large quantity of information on the label, a part of which is incomprehensible, confusing and is poorly presented. [4] When the product does not allow to put a label on it the trader has to provide the consumer written information by other appropriate way or by providing the relevant documents [6].

The main consideration related to the requirement for the compulsory food information should enable the consumers to identify and to use the food correctly and to make a choice that is suitable to the individual needs of their diet. For that purpose the producers of food products have to make this information more easily accessible to the people with visual disabilities [5].

The foreign experience shows that the supply of goods may use other means of informing consumers than labels, which explain and supplement the data from the label if is required by the decrees. [6]

The development of educational activities and events to familiarize students with the ways of healthy eating and their application is an important factor in the positive food culture in the younger generation. In this connection, in Razgrad town it was conducted explanatory and research activities among the students in the region. The university lecturers from the Branch - Razgrad of the Ruse University "Angel Kunchev" organized visits and activities in the following schools:

- Professional Technical High School "Shandor Petofy";

- Professional High School of Chemical Technologies and Biotechnologies "Marie Curie";
- Mathematics High School "Acad. Nikola Obreshkov";
- Professional High School of Agriculture and Food Technologies "Angel Kanchev", etc.

The undertaken initiative is by the **PROJECT NUTRILAB (Nutritional Labeling Study in Black Sea Region Countries), the Seventh Framework Program, activities Marie Curie (INTERNATIONAL RESEARCH STAFF EXCHANGE SCHEME)**. The purpose of the survey is to study the eating habits of the students in the last classes (XI, XII) in secondary schools and to explain them the necessity of information when they make a purchase of food and drinks.

We conducted a survey among the students to study their habits to follow the information given on the labels of food products.

II. Materials and methods

To conduct the experiment it was used a survey developed by the program MS Excel in an electronic form or on paper. The survey includes 20 questions for follow-up consumer's interest to the information on the food labels. There is only one possible answer for twelve questions. The rest questions have a possibility of choosing among a great number of answers and there are questions requiring a classification of the answers through a numeric scale that is defined in the question. The survey of the each respondent is stored as a file or saved on a paper and then it is used for automated processing of data in the survey (Figure 1).

14	Четете ли всичко, дадено като информация върху етикетите на хранителните продукти.	2	1	Да, чета	1
			2	Чета, но не всичко	2
			3	Не чета	3
15	Класифицирайте информацията от етикетите на хранителните продукти по значение, като поставите числата от 1 до 10 в полето вдясно (счита се **1** за ***най-значимата*** информация, а **10** за *най-незначимата*).	1	1/10	Срок на годност	1/10
		5	1/10	Цена	1/10
		10	1/10	Производител	1/10
		3	1/10	Количество	1/10
		9	1/10	Държава производител	1/10
		8	1/10	Информация за качеството (сорт, марка и др.)	1/10
		2	1/10	Информация за хранителни добавки	1/10
		7	1/10	Начин на приготвяне	1/10
		6	1/10	Енергийни съставки	1/10
		4	1/10	Съдържание на соли	1/10
16	Каква информация според Вас, трябва да има задължително върху етикетите на хранителните продукти?	1	0/1	За опасните компоненти, носещи риск за човешкото здраве	0/1
		1	0/1	Наличие на ГМО	0/1
		0	0/1	Държава, регион на производство	0/1
		0	0/1	Не знам, не съм се замислял	0/1
		0	0/1	Друга информация	0/1
17	Имате ли доверие на информацията от етикетите на хранителните продукти?	1	0/1	Да, доверявам се напълно	0/1
		0	0/1	Да, доверявам се, но не във всичко	0/1
		0	0/1	Много малко се доверявам	0/1
		0	0/1	Не, не се доверявам	0/1

Figure 1

The survey includes questions about the study of the most popular food on the table of the respondents among seven food categories (Figure 2). These questions have two possible answers, only "yes" or "no" depending on the specific food products in the

Figure 2

given category and consumers' preference.

The statistical conclusions are made by statistical estimates of parameters. The presentation and processing of the data is automated and is very fast, using computational and graphic apparatus MS Excel (Figure 3). We use the built-in mathematical and statistical functions for summarizing and displaying the results. The control of the performance is carried out, which includes reporting capabilities for errors.

P	Q	R	S	T	U	V	W	X	Y	Z
в. 12.4	**в. 13. 1**	**в. 13.2**	**в. 13. 3**	**в. 13.4**	**в. 13. 5**	**в. 13.6**	**в. 13. 7**	**в. 14**	**в. 15. 1**	**в. 15.2**
0								**1**	**1**	**10**
								1	**2**	**3**
0								**2**	**1**	**7**
0								**3**	**1**	**8**
0								**2**	**1**	**2**
66								***0***	***0***	***0***
22	33	37	29	29	36	45	25	35	73	38
0	0	0	0	0	0	0	0	63	13	25
0	0	0	0	0	0	0	0	14	6	8
0	0	0	0	0	0	0	0	0	1	4
0	0	0	0	0	0	0	0	0	2	5
0	0	0	0	0	0	0	0	0	4	0

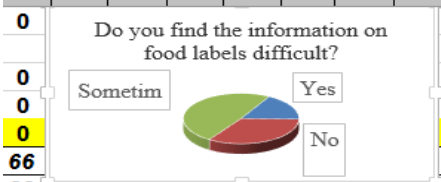

Figure 3

III. Results and discussion

To the question "Does the food influence on your health?" The largest percentage, 24% of students are selected the answer "influences to a great extent", followed by the value 24% where they are selected "influences to a less extent" and in the third place 21% is the answer "influences to a certain extent" (Figure 4).

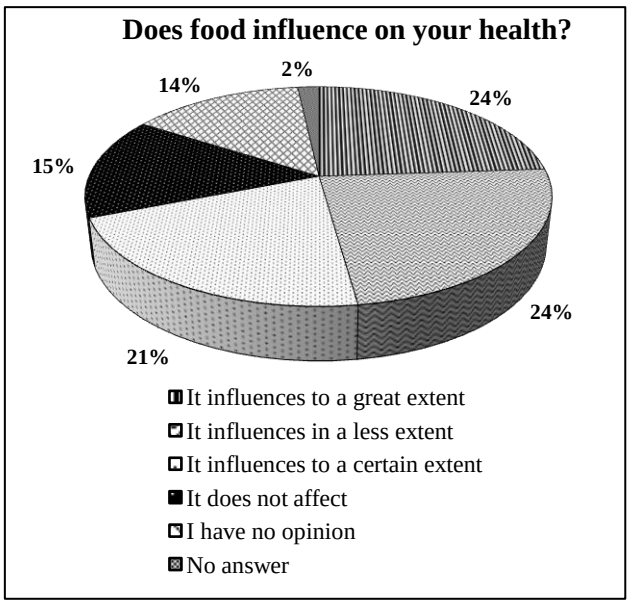

Figure 4

Asked about the purpose when they choose food products - 45% of students are responded "to feed," 39% - "to be healthy", 10%- "to raise the mood" 4% -"other purpose" and 2% - "do not point an answer"?

Through the survey we check in which category falls the students' choice of food (Figure 5). The answer "It depends on the situation" is selected with the highest percentage of respondents -39%, followed by "I like trying new products," chosen by 29% and the third " I expand my choice during the holidays" 18%.

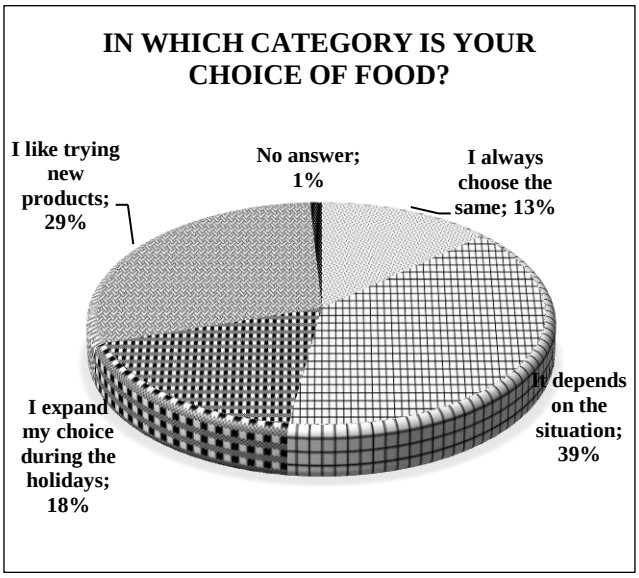

Figure 5

To the question "How do you choose food products in a network of shops?", 37% of students say that they read the labels, 23% go to the stand by habit, 17% read the names of the products on the price lists on the shop windows, 12% rely on their life experience, 9% use other ways which is not pointed, and 2% did not answer the question.

To the question "Do you read everything given as information on food labels?",56% of students are answered "I read but not everything", 31% indicated "yes, I read" 12% chose "I do not read" and 1% did not indicate an answer.

Have the respondents ever met difficulties when they read the information on the food labels it can be seen on the Figure 6. According to the students' responses the classification in descending order shows 44% - "No", 32% - "sometimes" and 24 % - "Yes".

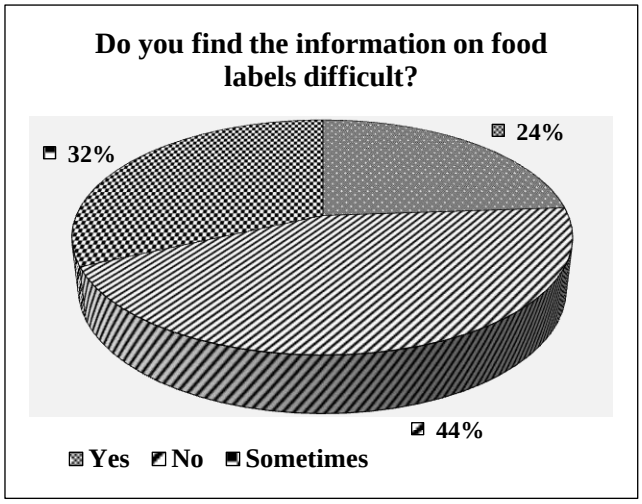

Figure 6

Among the listed in the survey possible difficulties the most are the answer -"The information is pale and illegible" - 50%, "too small print" - 37% and "used a lot of numbers and symbols with incomprehensible meaning" – 26 % (Figure 7).

The question "Classify the information from the

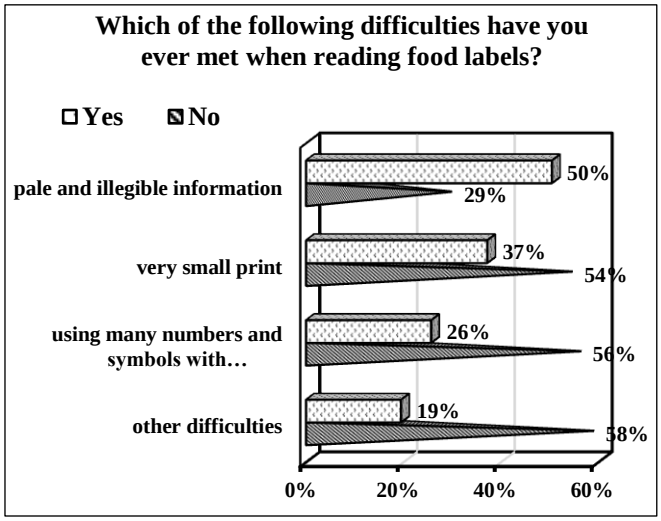

Figure 7

food labels in importance by placing the numbers 1

to 10 in the box on the right (it is considered one of the most important information and 10 for the most unimportant)" defined as:

- ✓ the most important information for students is "expiration date", it is selected by 65% of respondents, "the price by" 34% and information about "nutritional supplements" by 23%;
- ✓ the most unimportant information for students is "producer",it is selected by 19%, "salt content" by 17% and "Country producer" by 14% of the respondents.

The table shows the percentages of the complete results of the classification of the information of food labels in the criteria specified in the leftmost column.

Table 1

Degrees of important information on labels	1	2	3	4	5	6	7	8	9	10	No answer
Expiration date	65%	12%	5%	1%	2%	4%	0%	1%	2%	4%	5%
Price	34%	22%	7%	4%	4%	0%	4%	4%	3%	13%	5%
Producer	17%	8%	12%	8%	7%	6%	3%	2%	9%	19%	9%
Quantity	15%	7%	20%	10%	12%	4%	4%	4%	11%	7%	7%
Country producer	14%	3%	3%	4%	12%	10%	10%	11%	12%	14%	8%
Quality information (sort, brand, etc.)	18%	10%	8%	10%	12%	9%	4%	11%	5%	9%	6%
Information for the food additions	23%	8%	6%	15%	11%	4%	11%	2%	9%	7%	4%
Preparation way	16%	4%	3%	5%	15%	8%	12%	12%	9%	10%	8%
Energy components	16%	4%	8%	8%	9%	13%	12%	10%	7%	8%	6%
Salt content	17%	4%	4%	7%	1%	11%	14%	13%	6%	17%	7%

The following graph presents the respondents' answers of the question "According you what information should be on the food labels?" (Figure 8). The classification of the answers with the highest values in descending order is as follows: 61% of the surveyed students want compulsory to indicate data " About dangerous components which carry a health risk", 56% want to have information about availability of GMO, 33% want to have the opportunity to see the component indicating "Country and region of production".

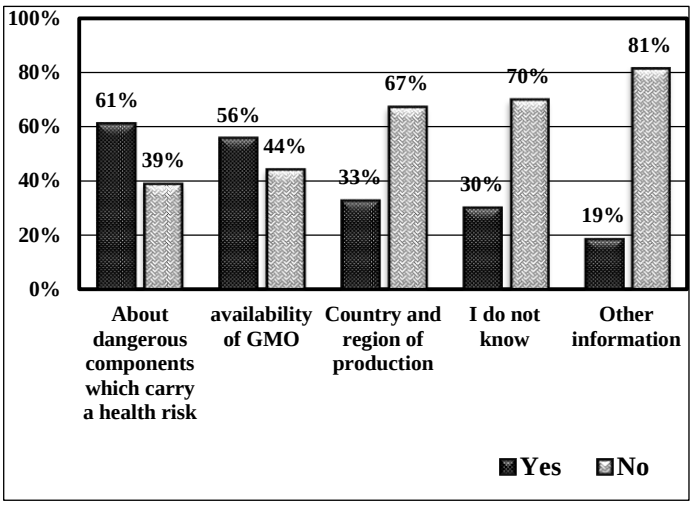

Figure 8

About the degree of confidence of students to the information on food labels with the highest percentage, more than half of the respondents chose the answer "Yes, I trust, but not everything" - 52%, and the answer chosen by the least number of students is "Yes, I trust completely" - 21% (Figure 9).

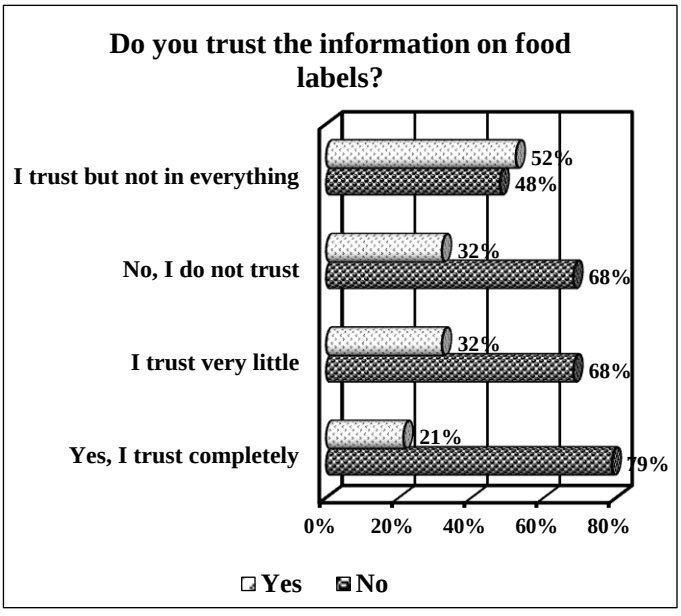

Figure 9

The study examines the information that is unclear, although it is easy to read (Figure10). Arranged in descending order with the highest percentage the respondents are indicated the following answers to unclear information "Some abbreviations" by 40% of the students, "used symbols and signs" by 33% and "Expiration date" by 32%.

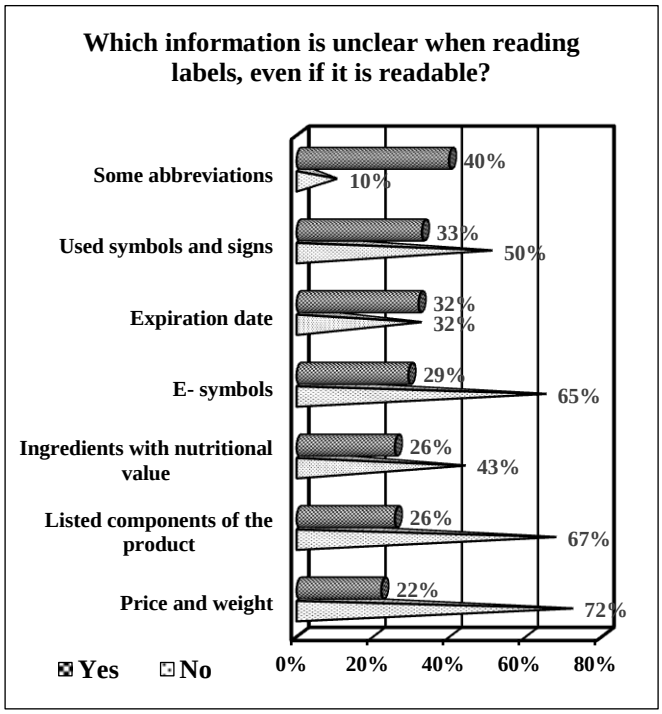

Figure 10

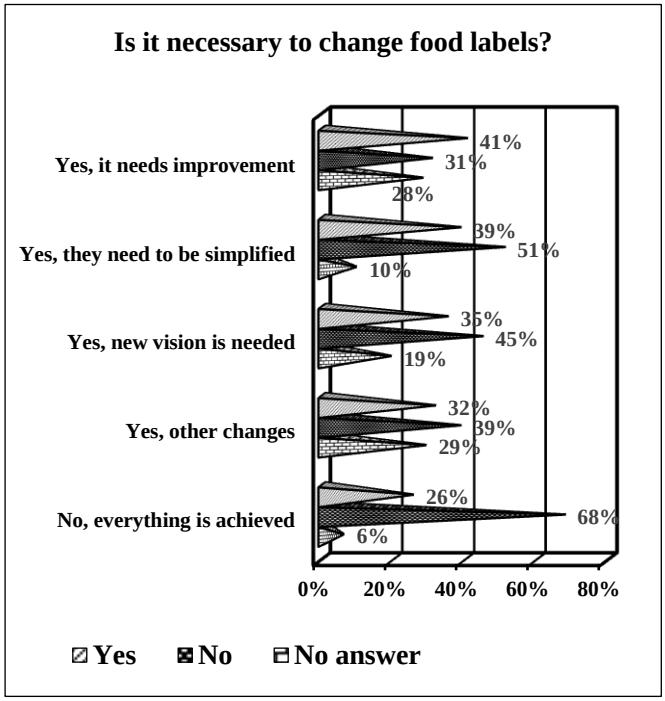

Figure 11

To the question" Is it necessary to change food labels?" among five possible answers 41% of respondents support the need for improvement, 31% do not support it and 28% did not answer the question. According 39% of students the labels should be simplified, but 51% consider it is not necessary, while 10% did not answer the question (Figure 11).

To the next question, "Which of the proposed amendments on the food labels do you offer to be made for convenient shopping?" - 58% of students have chosen on the labels to have "instructions for whom the products are dangerous" 44% want to be specified "for whom the products are intended" and 40% have chosen using of "Special symbols and images" for convenience of the users (Figure 12).

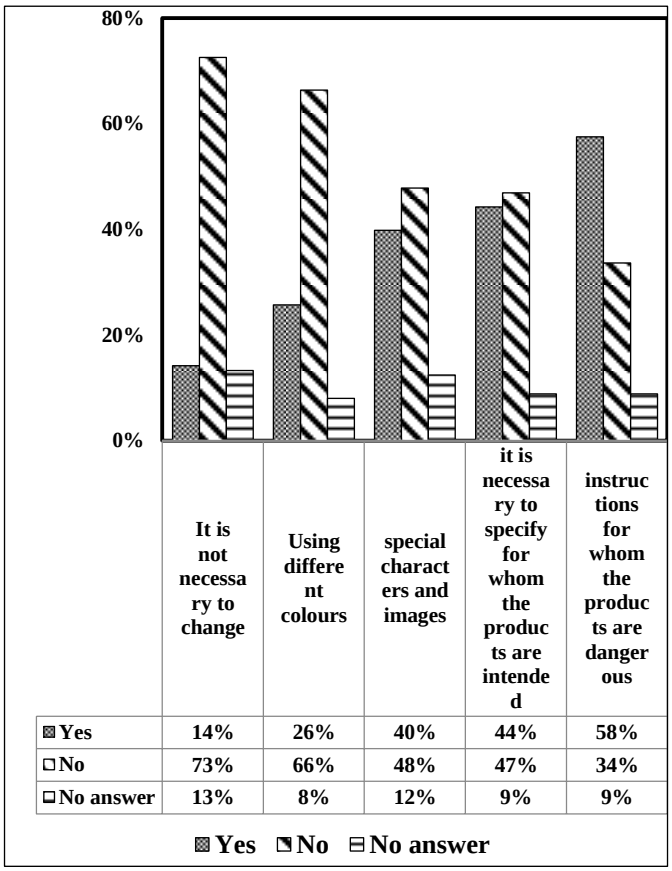

	It is not necessary to change	Using different colours	special characters and images	it is necessary to specify for whom the products are intended	instructions for whom the products are dangerous
Yes	14%	26%	40%	44%	58%
No	73%	66%	48%	47%	34%
No answer	13%	8%	12%	9%	9%

Figure 12

How food labels influence on their choice almost half of the students chose the answer "Yes, always" 49%, followed by the answer " In a less extent " by 36% and on the third position is the answer "it does not affect" 11% (Figure 13).

The survey researches which food products are the most often on the family table. From dairy products the most preferred are yoghurt 74%, 62% yellow cheese, white cheese 57%, milk 46% (Figure 14).

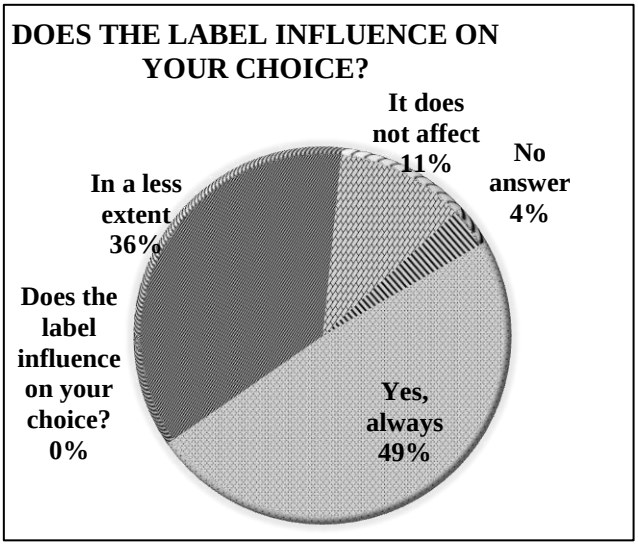

Figure 13

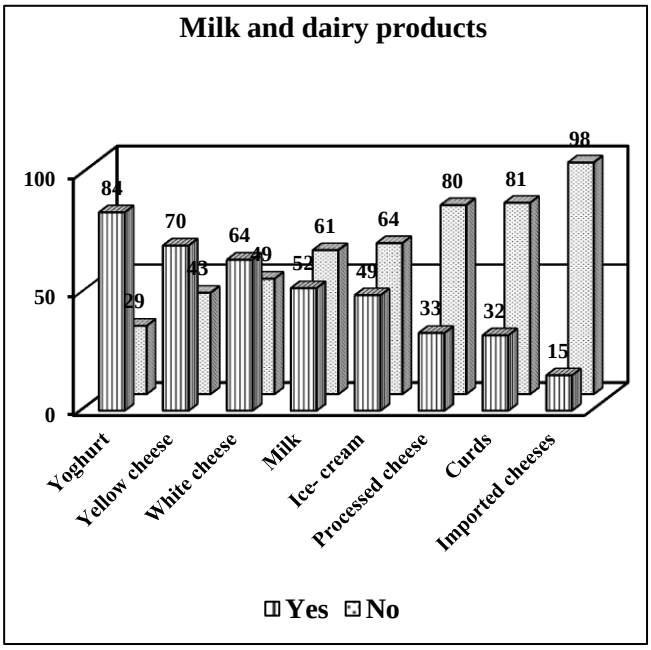

Figure 14

From the category "Bread, baker's goods and pasta" with the highest percentage of a preference on the family table students indicate respectively: "White wheaten bread" by 71% of respondents "pasta" - 61%, "Salty , crackers, crisps "44% and" Dietetic bread " by 42% (Figure 15).

From the category "Meat, meat products and fish" with the highest percentage of a preference the respondents are chosen: "Minced meat " - 68% of the students, "Chicken "- 67% and" Fish "- 64%, the whole graph is given in Figure 16.

From the category "Sugar and confectionery products" the students are indicated as the most preferred "Chocolate and chocolate candies" - 63% - "Yes" and 37%- "No", "Sweets" - 59% "Yes" and 41% - "No", and for "Dessert blocks" - 58%- "Yes" and 42%- "No".

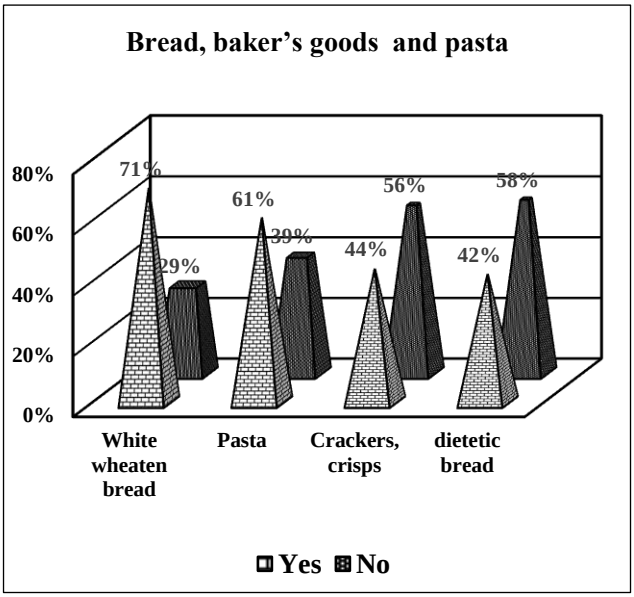

Figure 15

From the next category "Fruits and Vegetables" students are indicated as the most preferred "Fresh fruit" - 72% -"Yes" and 28% - "No", "Fresh vegetables" - 70%- "Yes" and 30%- "No" and "Canned fruits and vegetables" - 35%- "Yes" and 65% - "No". 59 % of the students prefer "Walnuts, almonds, hazelnuts and other nuts ", they give an answer -" Yes "and 41% give answer -" No ".

Among the pulses the preferences are "Rice, beans, lentils" - 61% - "Yes" and 39%- "No" and "Oat flakes, granola" - 38%- "Yes" and 62%- "No".

From the product category "Fats" with the highest

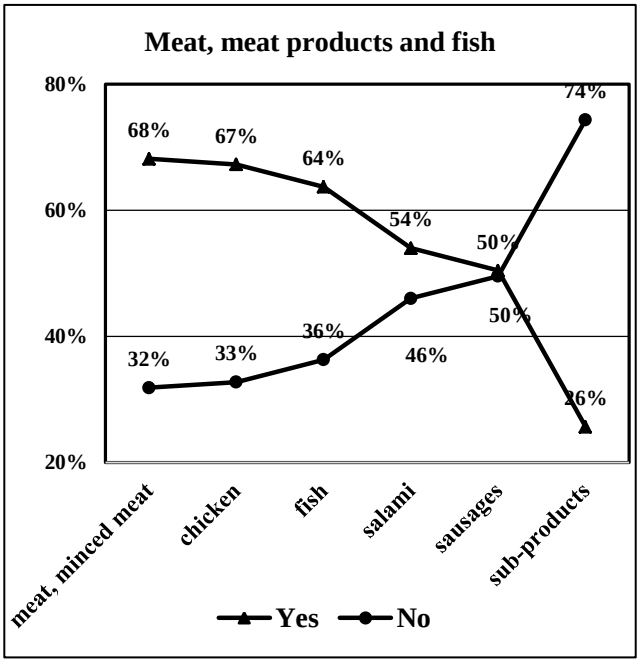

Figure 16

percentage on the family table respondents indicate respectively: Cooking oil" 52%, "Olive oil" 42% and "Butter" 41% (Figure 17).

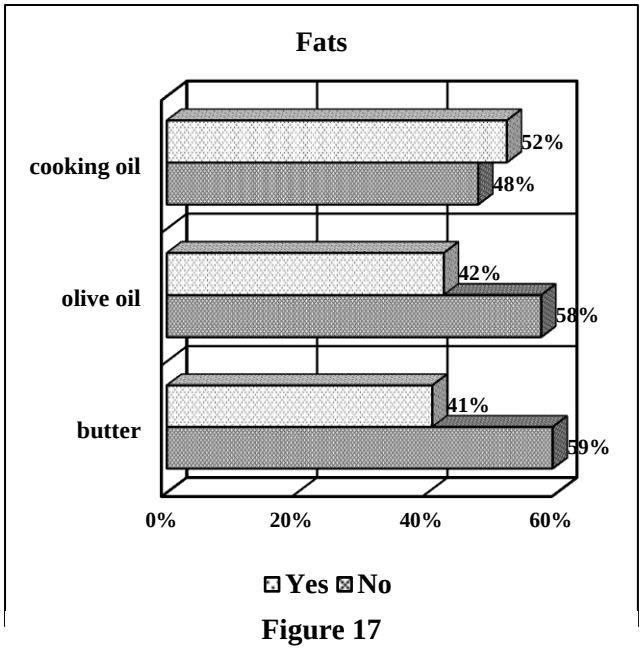

Figure 17

IV. Conclusions

The conducted survey among the students shows that making a better food choice is by improving the culture of shopping, better awareness and desire for a quality lifestyle.

The study shows that 24% of students have difficulties when they read the information on food labels, and 36% "sometimes". 50% of respondents think that the information on food labels is pale and illegible, and 40% have difficulties with some abbreviations whether they are legible.

61% of the surveyed young people believe that it is important that on the labels there should be written the information about the ingredients of the product that are a potential health risk, and 56% of the students are convinced that on the labels should be noted, if there is an availability of GMO even if it is a negligible amount.

There is big approval for the inclusion of new elements on the labels of food products. About 58% of students consider it necessary food labels should include instructions for whom the products are dangerous ", while 44% of respondents are chosen" it is necessary to specify for whom the products are intended".

This research aims to provide bigger awareness and knowledge about a healthy choice of food and drinks by our young generation.

In conclusion, it might be concluded that the welfare and health of the population depends on the level of awareness and shopping culture. This requires a continuous process of modernization in the labeling of foods and drinks, according to the users.

References

[1] Георгиева, С., Рискови фактори при децата в България, Стара Загора, 2008, www.sustz.com/Proceeding08/Papers/MEDICINE/**Georgieva_Stela**.pdf

[2] Долечек, Р., Опасният свят на калориите, Медицина и физкултура, 1980;

[3] Тенев, В., Докторе кажи. „168 часа" ЕООД, Брой 1, ISSN 0861-4067.

[4] Маркова, М., Храненето на възрастните и старите хора, Медицина и физкултура, 1984;

[5] РЕГЛАМЕНТ (ЕС) № 231/2012 НА КОМИСИЯТА от 9 март 2012 година.

[6] Meagan N Vella, Laura M Stratton, Judy Sheeshka, Alison M Duncan, Functional food awareness and perceptions in relation to information sources in older adults, 2014, ISSN 1475-2891.

[7] http://madjarov.bg/blog/2011/07/08/%D1%81%D0%B0%D0%BC%D0%BE39%D0%BE%D1%82%D0%B1%D1%8A%D0%BB%D0%B3%D0%B0%D1%80%D0%B8%D1%82%D0%B5%D1%87%D0%B5%D1%82%D0%B0%D1%82%D0%B5%D1%82%D0%B8%D0%BA%D0%B5%D1%82%D0%B8%D1%82%D0%B%D0%BD%D0%B0/

CONTROL SOURCES OF REACTIVE POWER AS EFFECTIVE METHOD OF INCREASED EFFICIENCY IN POWER SUPPLY SYSTEMS FOR FOOD PRODUCTION

S. Baljuta[1], V. Shesterenko[1], O. Mashchenko[1]

National University of Food Technologies, Volodymyrska str., Kyiv 01601, Ukraine, e-mail oll973@ukr.net

Abstract. *Improve the power factor in power systems by food businesses advisable optimal use capacitors and synchronous motors Reactive power consumption during the day is uneven. Hierarchical structure and high complexity is inherent to the system of reactive power compensation at the enterprises. During the day the generated power should overlap not less than for 80-90% with schedule of consumed reactive power. The paper considers ways to improve effectiveness of reactive power compensation at food enterprises by applying the two-level system of reactive power sources control. The proposed systematic approach to compensation allows improving the economic performance of all reactive power sources significantly. The system of complex compensation provides a shift in the emphasis of compensating device capacity management: from decentralizing to ensuring the system commitment in solving problem that is conceptually related to the optimization of power consumption mode at the industrial enterprises. System of reactive power complex compensation takes into consideration the requirements of power supply system at the interface of power supply systems and consumers' ones, and simultaneously considers power regulation of high-voltage capacity units, batteries for voltage lower than 1000 V, the level of reactive power, which is produced by synchronous engines.*

Key words*:* reactive power, power supply, control system, compensation.

I. Introduction

The main production of food industry enterprises occupies small territory (excluding pumping stations). They have power voltage of 35 ... 10 kV and high-voltage distribution network of 6 ... 10 kV. Power transformers at these plants usually exceed 750 kV·A, thus reactive power compensation needs to be provided.

Power supply organization sets the mode of company's compensating devices work. Capacity of unregulated power batteries is taken as the least reactive load network. Typically, multi-stage regulation should be used. Reactive power adjustment is an ideal method from many points of view. The controller turns on in the power network node. Condensing unit can be multisection and regulation can be maintained with sufficient accuracy according to schedule of reactive load[2,4,6,7,9,12,14,17,18,21].

The criterion of rational solution to the problem of reactive power compensation is the minimum of stated expenses. They include costs of compensating, regulatory and related devices, as well as expenses on reactive power regulation and its transfer through the power supply system elements. These expenses include components that do not depend on the value of reactive power, thus there was developed a methodology of determining compensating devices capacity that does not require considering the absolute costs of power supply system elements [1,3,5,8,10,11,13,15].

Reactive power consumption during the day is uneven. Operation mode of all reactive power sources must meet schedule of reactive power consumption. Power of compensating devices should be changed according to schedule of reactive power consumption. The use of individual compensation capacitor helps to eliminate the use of complex and expensive devices of capacitor installations power control that are needed to complete the centralized compensation installations in transmission substations [1,2,3,7,16,18,19,20].

II. Materials and methods

Mathematical tools of probability theory and mathematical statistics are used.

Hierarchical structure and high complexity is inherent to the system of reactive power compensation at the enterprises. At the industrial enterprises capacitors and synchronous engines are used to compensate reactive load [2,4]. The most widely spread are capacitors. Small mass, absence of rotating parts, minor loss of energy, simplicity of maintenance, safety and reliability in exploitation allow the use of capacitors for reactive power compensation at all levels of power supply [Patent of Ukaine № 34943, H02J 3/12. — Method of connecting individual capacitor condensators having reactive power compensation of induction motor – / Shesterenko V.Y., Siryj O.M., Baluta S.M., Maschenko O.A. – Published on 26.08.2008]. Synchronous engines are widely used

at the enterprises to drive devices that do not require speed control. Engines can run with advanced power factor and compensate reactive power of other power receivers. Compensating ability of engine is determined by the load on its shaft, voltage and excitation current.

In shops with lots of low-power engines individual compensation is not always effective. In such cases, a centralized compensation with capacitors installation near the transformer substation plant is used.

III. Results and discussion

Power factor is generally

$$\cos\varphi = \frac{\frac{1}{T}\int_0^T u\, i\, dt}{U\, I}, \qquad (1)$$

U,I - rms voltage and current.

The low value of power factor suggests incompleteness use power source.

International committee for the improvement of power factor named in 1929 the reactive power component of apparent power

$$Q = \sum_1^{\nu} U_{\nu}\, I_{\nu} \sin\varphi_{\nu} = \frac{1}{2\pi}\sum_1^{\nu}\frac{1}{\nu}\int_0^T U_{\nu}\, di_{\nu} \qquad (2)$$

The physical meaning of this expression has not been agreed, but the decision was made for two reasons: 1) The expression is valid for sinusoidal linear systems, 2) The non-sinusoidal expression systems can be represented as

$$S = \sqrt{P^2 + Q^2 + D^2} \qquad (3)$$

D - power distortion.

A small mass, no rotating parts, minor loss of energy, ease of maintenance, safety and reliability allow the use of capacitors for reactive power compensation at all levels of power supply system.

When compensation is necessary to consider the following general requirements [1,8]:

1) in contrast to the active reactive power can be generated at any point in the network;

2) approximation of reactive power sources to consumers helps unloading the network;

3) balance of reactive power must be maintained for all system units power supply system.

Energy Systems have limited ability to generate reactive power. Thus, generators of 100 MW and above have $\cos\varphi_N = 0.8$.

Much of the generated reactive power consumed by transformers and transmission lines. Therefore, during the peak load power companies may issue a limited number of reactive power with its high cost. Therefore, reactive power transmitted to power consumers, should be reduced (offset) to economic levels [2,3,6].

Average consumption of reactive power is: asynchronous motors - 70%, transformers - 20%, lighting and other power-consuming equipment - I0% [1,5].

Since cosφ generators of power plants and major consumers (inductive motors) coincide and equal to 0.8Power, for a long time it was thought that compensate for reactive power plants do not required.

But in the real world load engines often does not match the nominal capacity. If the motors is running at full capacity, load factor.

$$\beta = 1, \rightarrow \cos\varphi \approx 0.8 \qquad (4)$$

In the case of reducing the load factor power factor decreases:

$$\beta = 0.5, \quad \rightarrow \quad \cos\varphi \approx 0.6$$
$$\beta = 0.25, \rightarrow \cos\varphi \approx 0.4 \qquad (5)$$

Therefore, reactive power generators power is not enough for normal operation of the enterprise, and many factories have installed high-voltage capacitor banks that it is inappropriate for economic performance, because during the transfer of reactive power to consumers experiencing significant active power losses due to the resistance of conductors *r*

$$\Delta P = \frac{Q^2}{U^2}\cdot r \qquad \text{or}$$
$$\Delta P = P^2 \cdot \left(1 + tg^2\varphi\right) \qquad (6)$$

Increasing section leaders because section selected for load current, and the current depends on the reactive power

There are additional voltage loss [4,6,]

$$\Delta U = \frac{Qx}{10 \cdot U_N^2}, \qquad (7)$$

x - reactance elements of the system power supply.

In general, the voltage at the consumers:

$$U = U_{MVS} \pm E - \frac{\Pr + (Q - Q_K)(x_L - x_C)}{U} \quad (8)$$

E – additive voltage generated by regulatory devices;

P, Q – active and reactive power of consumption;

Q_{KV} - reactive power of compensating devices;

$(x_L - x_C)$ - network reactance, r - network resistance;

U_{MVS} – main voltage of enterprise reducing substation.

Therefore, reactive power transmitted to power consumers, should be reduced (offset) to economic levels.

By placing capacitors in a network of industrial enterprises into account that there are individual and centralized reactive power compensation [2,3].

When an individual compensation capacitor installation is connected to the terminals without power-switching devices [2,3,]. This type of compensation should only be used in relatively large power consumers with a large number of annual working hours. Individual compensation allows you to unload all of the reactive power production enterprise network. However, this method requires significant capital investment. In addition, time compensating devices depends on the duration of electro switch for turning off the network with it off and capacitor battery.

Let us consider the individual method of compensation. Typically, fluorescent lamps are equipped with capacitors and lighting networks do not require separate compensation.

As a major consumer of power network reactive power is the induction motor. Due to the large number of types is quite difficult to give clear guidance on the choice of power capacitors. Based on the optimal efficiency condensers, irrational fully compensate reactive power output at its terminals. Power capacitors also limit the phenomenon of self-excitation of the engine. If the engine is switched on again during the self-excitation, developing a powerful transition process as self-excitation phase voltage rarely coincides with the phase voltage electricity network. On the winding and the motor shaft are electromagnetic forces that are several times higher than those encountered in normal operation. This is especially true engine inertia load. Therefore, it is recommended to all engines with individual compensation check for self-excitation process by connecting a voltmeter to the terminals of the motor. When self-excitation voltage at the terminals of the motor is proportional current condenser and rotor speed of the engine. The value of voltage may rise to 160% nominal [1, 3]. A method that avoids self-excitation. This condenser installation of individual reactive power output terminals are connected to the engine via a circuit breaker that is equipped with an electromagnet remote shutdown, parallel clamps connect the relay output maximum voltage control signal to the relay electromagnet serves to fuse and disconnect condenser units at higher voltage directly on the engine as during normal engine operation and during transients shutdowns of the engine from the network [1, 6, 9]. In shops with lots of low-power engines Individual compensation is not always effective. In such cases, a centralized compensation installing capacitors near the transformer substation plant. In the case group and centralized power compensation capacitor is selected based on the active power losses in the power supply system [1, 3]. In the specifications for the design of electricity industry is expected usually full reactive power compensation. This allows you to significantly reduce energy loss and improve the voltage quality. In shops with lots of low-power engines individual compensation is not always effective. In such cases, a centralized compensation with capacitors installation near the transformer substation plant is used.

Reactive power of j station network

$$Q(t) = \sum_{j=1}^{n} \left[Q_j(t) - Q_{K\,i} \right], \quad (9)$$

$Q(t)$ - reactive power of load, Q_K - power capacity of condensing units.

For choosing condensing units their function should be studied.

$$f = \sum_{i=1}^{n} r_i \left[\sum_{j=1}^{i} (Q_j - Q_{K(2j)}) \right]^2 + \sum_{j=1}^{i} \sum_{e=1}^{i} K_{je}, \quad (10)$$

Q_j - mathematical expectation of reactive power of load in *j*–station, K_{je} - correlation moment of random values $Q_j(t)$ and $Q_e(t)$.

Losses of electrical power

$$\Delta W_i = \frac{r_i}{U_N^2} \cdot \sum_{k=1}^{\omega} T_k \left[M_k(P_i^2) + M_k(\mathrm{Q}_i^2) \right] \quad (11)$$

If there are few condensing units at the enterprise, multi-stage regulation of total reactive power is applied by means of different time enabling or disabling individual cells according to the load schedule. Total capacity of unregulated sources should not exceed the consumption power in the hours of low load, because reactive power should not be transferred from the enterprise power network into power supply system.

The analysis of modern Ukrainian and foreign scientific papers on the subject of reactive power compensation is conducted and existing regulatory systems of reactive power are summerised and evaluated.

Optimality criterion in efficient management of compensation is minimum power losses. A significant reserve of efficiency increase may be a system of complex reactive power compensation that is created on the basis of modern technical and computational tools [2,3]. The system allows you to change the emphasis in management of compensating devices capacities from decentralization to ensuring systematic commitment of solving problem that is conceptually related to the optimization of power consumption mode at the industrial enterprise.

System of reactive power complex compensation takes into consideration the requirements of power supply system at the interface of power supply systems and consumers' ones, and simultaneously considers power regulation of high-voltage capacity units, batteries for voltage lower than 1000 V, the level of reactive power, which is produced by synchronous engines. To improve the power factor condenser units are used. By means of the reactive power controller we change the reactive power of capacitor batteries, compensating devices (or synchronous engines).

devices

$$\mathrm{Q}_M = M(\mathrm{Q}_\Sigma) + \beta\delta_2, \quad (14)$$

$M(\mathrm{Q}_\Sigma)$ - mathematical expectation of reactive power, consumed in power supply system, δ_x - the standard deviation of power, β - multiplicity of dispersion extent.

By reducing the transmitted reactive power, losses of active power are reduced to 0.12 kW / $M_k(P_i^2)$ - mathematical expectation of active power, $M_k(\mathrm{Q}_i^2)$ - mathematical expectation of square reactive power, ω - number of intervals of stationarity and ergodicity, T_k - duration of these intervals.

For minimizing losses and accurate fulfillment of power supply system requirements with respect to reactive power, signal that comes to the regulators in the lines of power supply system grows faster over time. Thus here occurs switching of low-power capacitor installations, causing changes in the power factor. If the new factor meets the requirements of power supply system as to the amount of consumed reactive power, power at the output of voltage regulator drops to zero and the signals are also reduced.

Efficiency ratio of compensatory devices use:

$$\Psi = \frac{\sum_{1}^{n} \mathrm{Q_i t_i}}{\mathrm{T} \sum_{1}^{n} \mathrm{Q_i}}, \quad (12)$$

$\mathrm{Q_i}$ - reactive power of compensating devices, quarter;

t - the duration of the compensating device work during the year, hours;

T - the duration of the company work during the year, hours.

By changing the efficiency ratio of reactive power sources use it is possible to increase performance of low efficiency devices.

To choose compensating devices it is enough to minimize the function

$$f = \sum_{i=1}^{n} r_i \left[M^2(\mathrm{Q}_i) + D(\mathrm{Q}_i) \right] \quad (13)$$

$M(\mathrm{Q}_i)$ - mathematical expectation of Q on *i*-site of power supply system, $D(\mathrm{Q}_i)$ - dispersion of this power value.

Maximum capacity of compensating kVAr and depend on the distance to a power source. During compensation it is necessary to consider the following general requirements: unlike active power reactive one can be generated at any point in power supply system; approximation of reactive power sources to consumers facilitates unloading of the system; reactive power balance must be maintained for all nodes of electric power supply.

When switches in the power lines are not enough, in some time the signal will reach the level that will

cause switching in the degree of capacitor installation on the main site (or changes in the operating mode of synchronous engines). After such a switch commutation of low-power installations becomes possible in the lines of power supply system for more accurate support of reactive power required value. If the signal meets the requirements to connect additional section of battery and $tg\varphi$ in line is close to zero, connection will not happen. Additional sections will be connected only in those lines where own reactive power is not completely offset. Thus, close to optimal power factor will be hold up in lines of power supply system. Only when all the capacitor installation power on the main site is used, the growth of signal will be possible to such a level that the condenser units in lines will switch regardless of signal of local deliverer.

A significant advantage of two-level method of reactive power sources regulation is complex control of reactive power flow and simultaneous regulation of all sources of reactive power at the enterprise. However, in contrast to the remote control, where according to the signal from control point switching is done, regardless of $tg\varphi$ in branch, this method proposes to take into account the level of two signals - from the local sensor and from starting regulator. Switching of capacitor batteries sections occurs selectively, in some branches, and only under certain signal levels. Reactive power consumption during the day is uneven. Operation mode of all reactive power sources must correspond to the schedule of reactive power consumption. The smallest specific losses are typical for condenser battery with voltage above 1000 V. The greatest occur in low power synchronous engines. The smaller are losses in compensating devices, the better it is to use them in continuous working mode and vice versa, compensating devices with larger losses should be connected transitorily. For example, to cover reactive loads in the hours of maximum power, and also to cover peaks in the graph [4].

Thus, in the long-term, baseline mode it is better to use high-voltage compensating devices. Regulated compensating devices with voltage of 0.4 kV and synchronous engines with low losses (high power, speed) - to cover the main graphic, synchronous engines with high specific losses - only to offset short-term peaks in the graph.

The system is done on the basis of the NOVAR type controller, Czech made. The work is introduced in Dnipropetrovsk Dairy. Result of implementation is to reduce energy losses by 23% and the amount of reactive power payment by 78%.

For optimal placement of capacitors in a radial network to minimize the function

$$f = \sum_{i=1}^{n} r_i \left[(\mathrm{Q}_{K\,i} - \mathrm{Q}_i)^2 + \delta_{\mathrm{Q}i}^2 \right] \qquad (15)$$

$\delta_{\mathrm{Q}\,i} = \sqrt{D(\mathrm{Q}_i)}$ - standard deviation values of the Q load.

If there are few condensing units at the enterprise, multi-stage regulation of total reactive power is applied by means of different time enabling or disabling individual cells according to the load schedule. Total capacity of unregulated sources should not exceed the consumption power in the hours of low load, because reactive power should not be transferred from the enterprise power network into power supply system.

The analysis of modern Ukrainian and foreign scientific papers on the subject of reactive power compensation is conducted and existing regulatory systems of reactive power are summerised and evaluated.

IV. Conclusions.

1. Reactive power consumption during the day is uneven. Operation mode of all reactive power sources should correspond to the schedule of reactive power consumption. Compensating devices power should be changed according to schedule of reactive power consumption.

2. Hierarchical structure and high complexity is inherent to the systems of reactive power compensation at the enterprises. Optimality criterion in efficient management of compensation is minimum power losses.

3. Significant potential for raising the efficiency of the system can be the system of complex compensation of reactive power that is created on the basis of modern technical and computational tools. The system allows you to change the emphasis in management of compensating devices capacities from decentralization to ensuring systematic commitment of solving problem that is

conceptually related to the optimization of power consumption mode at the industrial enterprise.

4. The system of complex compensation allows you to maintain the flow of reactive power in the elements of power supply system at the optimum level, with maximum effect to use set sources of reactive power, as far as disabling of compensating devices is not allowed in times of reactive power shortage in the power supply system node.

References

[1] Shesterenko V.Ye. (2011), Systemy elektrospozhyvannia ta elektropostachannia promyslovykh pidpryiemstv, Nova Knyha, Vinnytsia.

[2] Shesterenko V.Ye., Siryi O.M. (2003), Rozrakhunky pry proektuvanni ta rekonstruktsii system elektropostachannia promyslovykh pidpryiemstv, ISDO, Kyiv.

[3] Jon H., Wu J., Wu K., Chiang W., and Chen Y. (2005), Analysis of zig-zag transformer applying in the three-phase four-wire distribution power system, IEEE Trans. Power Del., 20(2), pp. 1168-1173.

[4] Shesterenko V., Sidorchuk I. (2013), Reactive power compensation in the combined system of sugar refinery electricity, Ukrainian Food Journal, 2(1), pp.116-122.

[5] Shesterenko V., Sidorchuk I. (2013), Research of the features of reactive power compensation in the combined system of food industry, Ukrainian Journal of Food Science, 1(1), pp. 89- 95.

[6] Shesterenko V.Ye. (2001), Optymizatsiia system elektrospozhyvannia promyslovykh pidpryiemstv, Hlana, Kyiv.

[7] Arrillaga J. and Neville R.W. (2003), Power System Harmonics, Hoboken, NJ, USA, Wiley.

[8] Abhik Banerjee, Mukherjee V., Ghoshal S.P. (2014), Intelligent fuzzy-based reactive power compensation of an isolated hybrid power system , International Journal of Electrical Power & Energy Systems, 57, pp. 164-177.

[9] Binod Shaw, Mukherjee V., Ghoshal S.P. (2014), Solution of reactive power dispatch of power systems by an opposition-based gravitational search algorithm, International Journal of Electrical Power & Energy Systems, 55, pp. 29-40.

[10] V. Shesterenko, O.Danko, O. Shesterenko. (2014), Ukrainian Journal of Food Science, Volume 2, Issue 2, 2014, pp. 273- 280.

[11] Shamtsyan M., Klepikov A. (2014), Some prospects of pulsed electric field treatment in food processing, Journal of Food and Packaging Science, Technique and Technologies, 2(1), pp. 60-64.

[12] Abhik Banerjee, Mukherjee V., Ghoshal S.P. (2013), Modeling and seeker optimization based simulation for intelligent reactive power control of an isolated hybrid power system , Swarm and Evolutionary Computation, 13, pp. 85-100.

[13] Dulce Fernão Pires, Carlos Henggeler Antunes, António Gomes Martins (2012), NSGA-II with local search for a multi-objective reactive power compensation problem, International Journal of Electrical Power & Energy Systems, 43(1), pp. 313-324.

[14] Julia Klymenko, Sergii Baluta (2013), Application of neural network regulator in cascade systems of regulation, Ukrainian Food Journal, 2(1), pp. 111-115.

[15] Salles D., Jiang C., Xu W., Freitas W., Mazin H. E. (2012), Assessing the collective harmonic impact of modern residential loads - Part I: Methodology, IEEE Trans. Power Del., 27(4), pp. 1937-1946.

[16] Jiang C., Salles D., Xu W., and Freitas W. (2012), Assessing the collective harmonic impact of modern residential loads - Part II: Applications, IEEE Trans. Power Del., 27(4), pp. 1947-1955.

[17] Amit Saraswat, Ashish Saini, Ajay Kumar Saxena (2013), A novel multi-zone reactive power market settlement model: A pareto-optimization approach, Energy, 51, pp. 85-100.

[18] V. Shesterenko, I. Izvolensky, O. Mashchenko, O. Shesterenko. Optimization of power supply system at food production enterprises. (2014), Ukrainian Journal of Food Science, Volume 2, Issue 1, pp. 97- 105.

[19] Qingfeng Tang, Jianhua Zhang, Linze Huang (2014), Coordinating Control of Reactive Power Optimization in Distribution Power System with Distributed Wind Energy, AASRI Procedia, 7, pp. 38-44.

[20] Aqeel Ahmed Bazmi, Gholamreza Zahedi (2011), Sustainable energy systems: Role of optimization modeling techniques in power generation and supply - A review, Renewable and Sustainable Energy Reviews, 15(8), pp. 3480-3500.

[21] Omid Alizadeh Mousavi, Rachid Cherkaoui (2014), nvestigation of P–V and V–Q based optimization methods for voltage and reactive power analysis.

THERMOPHILIC METHANE FERMENTATION OF CHICKEN MANURE IN A WIDE RANGE OF SUBSTRATE MOISTURE CONTENTS

A. Salyuk, S. Zhadan, E. Shapovalov

Faculty of Biotechnology and Environmental Control, National University of food technologies, Volodymyrska str. 68, Kyiv, 01601, Ukraine, e-mail: zhadan.nuft@gmail.com

Abstract. *One of the effective ways of environmental management in poultry waste that allows the increase of energy-saving and reduction of negative environmental impact is methane fermentation. Methane fermentation process is possible in three temperature modes: psychrophilic, mesophilic and thermophilic. Methane fermentation of chicken manure in thermophilic mode is less studied in comparison with mesophilic mode. The article presents the results of the study of methane fermentation of these wastes. The process was carried out in thermophilic conditions at 50 °C. Substrate moisture values varied from 72% to 99%. Biogas production ranged from 10,6 ml / g VS to 382,3 ml / g VS, methane production – from 1,8 ml / g VS to 207,9 ml / g VS. The maximum yield of biogas and methane per unit of mass was reached with the substrate moisture content of 92%. Production of methane from chicken manure in the thermophilic mode with low moisture level of the substrate was also possible despite the high content of ammonia nitrogen and free ammonia. However, with a decrease of the substrate moisture content lower than 80% efficiency of methane fermentation was at the same level and very low.*

Key Words: chicken manure, anaerobic digestion, biogas, ammonia, inhibition

I. Introduction

In market conditions there is a serious struggle for a market niche among producers whose outcome is largely determined by the cost of production. Energetic and environmental factors such as the cost of electricity and fees for environmental pollution impact the cost of production. One of the effective ways of environmental management in poultry waste that allows the increase of energy-saving and reduction of negative environmental impact is methane fermentation.

Methane fermentation process is possible in three temperature modes: psychrophilic, mesophilic and thermophilic. Waste treatment and wastewater treatment in industrial scale is carried out mainly in mesophilic or thermophilic conditions. Most of the works on methane fermentation of chicken manure were carried out in mesophilic mode.

Studies of anaerobic digestion of chicken manure report that high nitrogen content in poultry manure often creates problems of ammonium toxicity for anaerobes. It is believed that concentration of ammonia nitrogen is the limiting factor for the dilution coefficient [11]. In its turn, the increase of influent concentration is economically valuable as it leads to reduction of reactor volume and lowers consumption of water and energy for its heating, the amount of effluent, the cost of transportation and storage.

The periodic process with substrate moisture content ranging from 82 to 94% at 50 °C has been carried out by the authors in their previous work with the aim to investigate high-solid methane fermentation of chicken manure in the thermophilic mode [13].

Since methane fermentation took place in all range of substrate moisture values, the purpose of this study was to investigate the process at lower moisture values to find the value at which it is still possible. The process was also conducted at high dilution of the material in order to establish general regularities of methane fermentation of chicken manure.

II. Materials and methods

The experiments were carried out in thirty three 60 ml syringes three times in a row. Moisture content of the substrate was 72%, 74%, 76%, 78%, 80%, 82%, 84%, 94%, 96%, 98% and 99%. Manure was diluted with tap water to get the desired moisture level. Each syringe contained 20 g of substrate. Mass fraction of anaerobic sludge was 10%. The syringes were placed in a dry-air thermostat TC 80 M2. The process was carried out in the thermophilic mode at 50 °C. The amount of produced biogas was determined by deviation of the syringe piston. The concentration of carbon dioxide was measured by passing the biogas through 2% NaOH solution. The burnability of biogas was also checked. Chicken manure was obtained from Vasilkovska poultry farm where the egg-laying hens were kept in battery cages. Excessive anaerobic active sludge obtained from methane tanks of Bortnychi aeration station (where sludge from the primary clarifiers is processed) was used as inoculum. The sludge was clarified and the obtained liquid was decanted.

Chicken manure and anaerobic active sludge were stored in a refrigerator at 4 °C.

The content of total solids (TS) was measured by drying the sample in a drying oven at 105 °C to constant weight. To determine the volatile solids (VS), dry residue was heated in a muffle furnace at 600 °C. The pH level was measured using a pH meter pH-150 МИ. Electric conductivity was determined using PHYWE cobra4 mobile-link with module «Conductivity». The concentration of ammonia nitrogen and volatile fatty acids (VFA) was determined by distillation.

The content of free ammonia was calculated basing on concentration of ammonia nitrogen by the formula [5]:

$$NH_3(mg\ /\ l) = NH_4^+ - N(1 + 10^{(pK_w - pK_b - pH)})^{-1}$$

where pK_w is a constant of water ionization at 50°C that equals 13.262 [3], pK_b is a constant of ammonium dissociation at 50 °C that equals 4.723 [4].

The content of free VFA was calculated basing on the concentration of VFA by the formula [4]:

$$Free\ VFA(mg\ /\ l) = \frac{VFA \cdot 10^{(pK_a - pH)}}{1 + 10^{(pK_a - pH)}}$$

where pK_a is a constant of dissociation of acetic acid that is 4.787 at 50 ºC.

III. Results and discussion

Chicken manure obtained as a natural output of bird's vital activity has moisture level of 75%. During the first stage of the experiment the moisture content was 72.2% and during the second – 71.4%.

Chicken manure contains a larger proportion of organic matters, capable of biological decomposition, than other animal wastes [6]. The content of VS in the manure during the first stage of the experiment was 70%, and during the second – 69.8%. In the study of Webb and Hawkes (1985) the content of VS varied from 60 to 70.59% [14], in the work of Huang and Shih (1981) – 76% [7], Niu and al. (2013) – 73.84% [9, 10].

The characteristics of substrate with different moisture values (during the first and the second stages of the experiment) before methane digestion are given in Table 1 and after methane digestion – in Table 2.

Table 1. *Characteristics of chicken manure before methane digestion*

Primary moisture, %	General nitrogen, mg / l	$N\text{-}NH_4^+$, mg / l	NH_3, mg / l	VFA, mg / l	Nondissociated VFA, mg / l	pH	Electric conductivity, µS / cm
99	475	143	0,25	145	13,10	5,79	1200
98	950	285	0,60	290	22,60	5,86	2533
96	1900	570	1,34	580	40,63	5,91	3992
94	2652	796	2,05	831	53,44	5,95	4871
92	3536	1061	3,06	1140	65,78	6,00	5811
90	4420	1326	4,09	1449	78,33	6,03	6420
88	5304	1591	5,14	1757	90,93	6,05	8107
86	6188	1856	6,89	2066	93,75	6,11	7887
84	7072	2122	8,63	2374	98,64	6,15	8457
82	7956	2387	11,14	2683	97,62	6,21	8120
80	9500	2850	14,25	2898	98,64	6,24	8257
78	10450	3135	18,82	3188	90,78	6,32	8533
76	11400	3420	21,01	3478	96,84	6,33	8436
74	12350	3705	27,33	3767	87,65	6,41	8771
72	13300	3990	32,24	4057	86,27	6,45	8964

Table 2. *Characteristics of chicken manure after methane digestion*

Primary moisture, %	General nitrogen, mg / l	$N\text{-}NH_4^+$, mg / l	NH_3, mg / l	VFA, mg / l	Nondissociated VFA, mg / l	pH	Electric conductivity, µS / cm
99	451	451	164,97	60	0,02	8,30	3964
98	903	902	379,44	210	0,05	8,40	6990
96	1805	1804	830,5	420	0,09	8,47	11455
94	2522	2522	1978,37	885	0,04	9,10	13244
92	3363	3222	2831,98	3210	0,08	9,40	15807
90	4199	3082	2608,43	7080	0,23	9,28	15160
88	5037	4483	3617,27	6840	0,29	9,16	20380
86	5879	3362	1229,79	8100	2,49	8,30	19840
84	6720	3642	2554,72	7140	0,54	8,91	28180
82	7558	4644	2404,84	14990	2,47	8,57	21480
80	9358	5648	155,17	12230	76,16	6,99	25372
78	10293	6168	8,92	9281	1010,49	5,70	21376
76	11229	6760	4,68	12700	2582,66	5,38	21370
74	12165	7269	4,00	16315	3967,93	5,28	21280
72	13101	7816	4,72	13582	3078,47	5,32	19780

With a decrease in the substrate moisture content from 99% to 92% biogas and methane yield from VS increased, and from 90% to 80% - decreased. In the range from 72% to 82% biogas and methane yield were relatively at the same level. Biogas production ranged from 10.6 ml / g VS to 382.3 ml / g VS and methane production – from 1.8 ml / g VS to 207.9 ml / g VS. The maximum yield of biogas and methane per unit of mass was 382.3 ml / g VS and 207.9 ml / g VS respectively with the substrate moisture content of 92% (Figure 1).

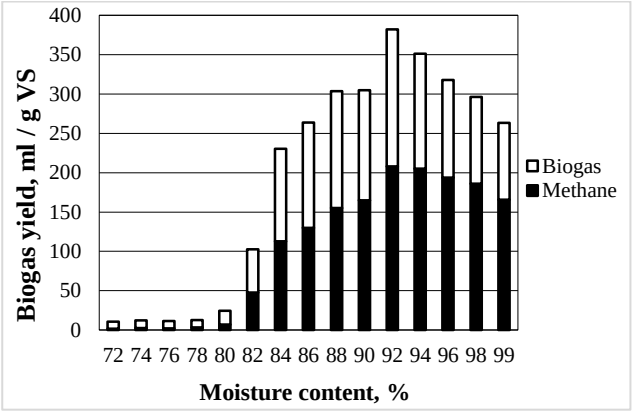

Figure 1. *Gas yield from VS with different moisture values of substrate*

With a decrease in the substrate moisture content from 99% to 84% biogas yield per unit of volume increased, and from 82% to 80% – decreased. In the range from 72% to 80% biogas and methane yield was relatively at the same level. Biogas production ranged from 2.2 ml / ml to 25.8 ml / ml, and methane production – from 0.4 ml / ml to 13 ml / ml. The maximum gas yield was 25.8 ml / ml with the substrate moisture content of 86% and methane yield - 13 ml / ml with the substrate moisture content of 88% (Figure 2).

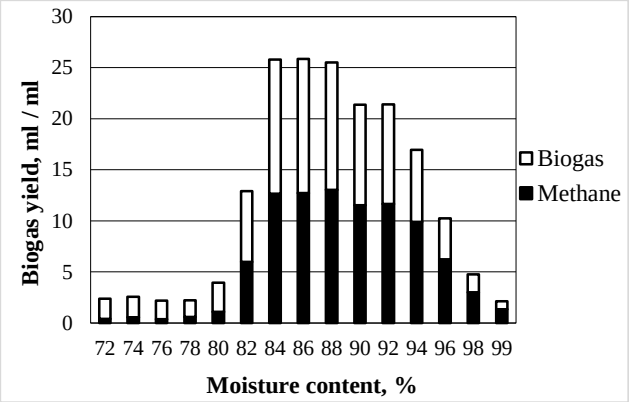

Figure 2. *Gas yield from the volume with different moisture values of substrate*

In the range of moisture values between 84% and 80% biogas and methane yield per unit of mass and unit of volume decreased sharply.

The concentration of methane in the biogas increased with an increase in the substrate moisture content. The content of methane in the produced gas ranged from 16.8% to 62.9%. Substrate moisture content of 80% led to a sharp decrease in the concentration of methane in the produced gas (Figure 3).

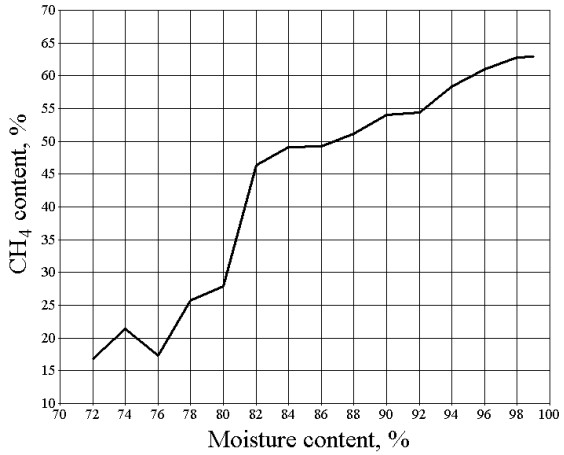

Figure 3. *The proportion methane / biogas with different moisture values of substrate*

Increasing of methane concentration in the biogas from the beginning of the experiment was faster with greater moisture content of the substrate.

The maximum rate of methanogenesis increased with an increase in the substrate moisture content. Its maximum value was 37 ml CH_4 / (g VS • day). The growth was exponential in nature. In the range of the moisture content values from 72% to 78% maximum rate of methanogenesis was relatively at the same level (Figure 4).

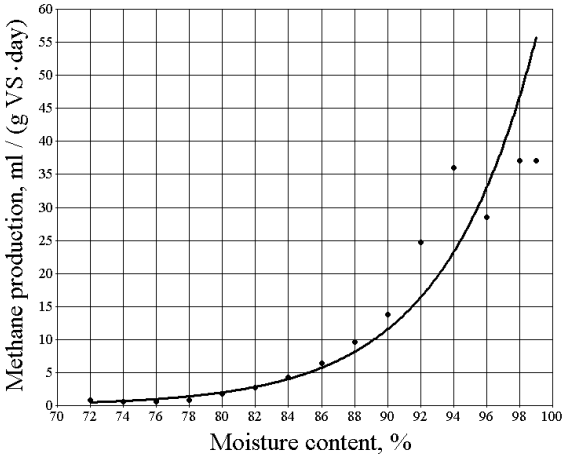

Figure 4. *The maximum rate of methanogenesis with different moisture values of substrate*

Mass of the substrate at the end of the experiment was lower than at the beginning due to its partial transition to the mass of gas.

After the methane fermentation a decrease in substrate viscosity was observed due to the conversion of organic matter of chicken manure into biogas.

The degree of destruction of TS and VS of chicken manure resulting from methane fermentation was proportional to the yield of biogas per unit of mass. In this regard, its values changed with a decrease in the substrate moisture content values similar to values of biogas production per unit of mass. The degree of decomposition of TS ranged from 1.28% to 67.59% and VS – from 1.83% to 96.55%. Maximum decomposition of TS and VS was with substrate moisture content of 92% and amounted to 67.59% and 96.55% respectively (Figure 5). Under different process conditions Webb and Hawkes (1985) obtained the decomposition of VS, ranging from 48.97% to 66.5% [14], Huang and Shih (1981) – 66% [7], Safley (1987) – 53.1% [12].

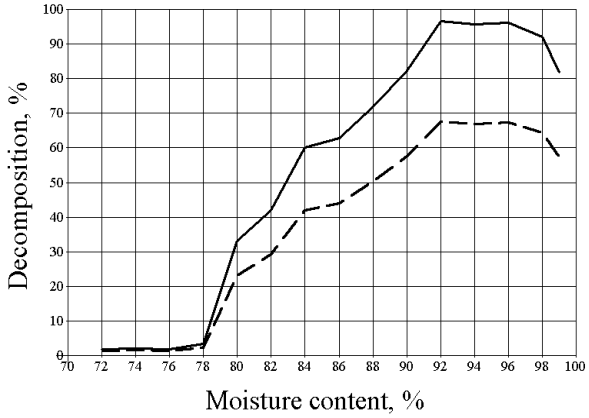

Figure 5. *Decomposition of VS and TS resulting from methane fermentation*

In our study pH of the substrate decreased with an increase in the manure moisture content from 6.45 to 5.79, which corresponds to an increase in ammonia nitrogen content. After the methane fermentation pH increased with a decrease in the substrate moisture content from 99% to 92%, and decreased with the further reduction in the moisture content from 90% to 72%. With the substrate moisture content ranging from 72% to 78% pH value was lower than at the beginning of the process, which can be explained by the accumulation of significant amount of VFA. Safley and al. (1987) noted an increase of pH from 7.2 to 8.05 as a result of anaerobic processing of poultry manure with moisture content of 94% in a continuous process at 35 ºC and 22-day duration [12].

Electrical conductivity of the substrate increased with the decrease in moisture content from 1200 to 8964 μS / cm. As a result of methane fermentation electrical conductivity increased due to mineralization and ranged from 3964 μS / cm to 28180 μS / cm. Safley and al. (1987) noted an increase in the electric conductivity from 22802 μS / cm to 26855 μS / cm [12].

During the second stage of the experiment, the content of ammonia nitrogen in poultry manure was 14.25 mg / g TS, while during the first stage it was 13.26 mg / g TS. Ammonium concentration with a decrease in the substrate moisture content increased from 143 mg / l to 3990 mg / l. As a result of methane fermentation the content of ammonia nitrogen increased and ranged from 451 mg / l to 7816 mg / l. McCarty (1964) indicated that when ammonia nitrogen concentration exceeds 3000 mg / l, the anaerobic digestion processes are inhibited at any pH [8].

The toxic effect of ammonia nitrogen is associated with nondissociated ammonia. It has been shown that it diffuses into the cell membrane and is ionized to form ammonium ions NH_4^+, leading to pH imbalance inside and outside the bacterial cell. It negatively affects both the transport of substances and the enzyme activity [9]. The content of nondissociated ammonia in the substrate ranged from 0.25 mg / l to 32.24 mg / l. After methane fermentation the concentration of ammonia increased due to ammonification and increasing pH. However, with the substrate moisture content ranging from 72% to 78% ammonia content was lower than at the beginning, as pH decreased as a result of methane fermentation. The concentration of ammonia varied from 4 mg / l to 3617 mg / l.

With the decrease in moisture content of the substrate VFA content increased and amounted from 145 mg / l to 4075 mg / l. After the methane fermentation with the substrate moisture content ranging from 96% to 99% VFA concentration was lower than at the beginning of the experiment, and from 72% to 94% – higher. VFA content ranged from 60 mg / l to 16315 mg / l. Safley and al. (1987) reported a decrease of VFA content from 8447 mg/l to 3403 mg/l [12]. Pechan and Knappovfi (1987) reported an increase in the content of VFA up to 4600-9300 mg / l as a result of semicontinuous methane fermentation of chicken manure with moisture content values ranging from 85.9% to 88.7% in case of duration of the process 27-58 days in mesophilic conditions [11].

VFA can exist in solution as unionized molecules. Similarly to free ammonia the unionized form of VFA can also be toxic. Its concentration increases with a decrease of pH solution [5]. Inhibitory levels can be as low as 10 mg / l as acetic acid, however, acclimations in the range of 30-60 mg / l as acetic acid were reported [2]. The concentration of nondissociated VFA at the beginning of the process ranged from 13.1 mg / l to 98.64 mg / l. After the methane fermentation, with the substrate moisture content ranging from 82% to 99%, concentration of free VFA was lower than at the beginning of the experiment, and from 72% to 80% – higher. The content of nondissociated VFA ranged from 0.02 mg / l to 16315 mg / l.

IV. Conclusions

1. The regularities of methane fermentation of poultry manure in batch mode in thermophilic conditions depending on the moisture content of the substrate in a wide range of values have been determined.

2. Production of methane from chicken manure in the thermophilic mode with the low moisture level of the substrate is possible, despite the high content of ammonia nitrogen and ammonia. Moisture content

value of the substrate, ceasing the production of methane, was not detected.

3. With a decrease in the substrate moisture content lower than 80% efficiency of methane fermentation was relatively at the same level and very low.

References

[1] Abouelenien F. Dry mesophilic digestion of chicken manure for production of methane by repeated batch culture / F. Abouelenien, N. Nishio, Y. Nakashimada // J. Biosci. and Bioeng. - 2009. - № 107(3). - pp. 293-295.

[2] Anaerobic treatment process stability / E.J. Kroeker, D.D. Schulte, A.B. Sparling, H.M. Lapp // Journal of Water Pollution Control Federation. – 1979. - № 51(4). – pp. 718-727.

[3] Bandura A.V. The ionization constant of water over wide ranges of temperature and density / A.V. Bandura, S.N. Lvov // J. Phys. Chem. Ref. Data. - 2006. - Vol. 35, № 1. - pp.15-30.

[4] Bates R.G. Acidic Dissociation Constant of Ammonium Ion at 0° to 500 C, and the Base Strength of Ammonia / R.G. Bates, D.P. Gladys // Part of the Journal of Research of the National Bureau of Standards. - 1949. - Vol. 42. - pp. 419-430.

[5] High solid anaerobic digestion of chicken manure / G. Bujoczek, J. Oleszkiewicz, R. Sparling, S. Cenkowaski. // J. Agric. Eng. Res. - 2000. - № 76(1). - pp. 51-60.

[6] Hill D.T. Simplified Monod kinetics of methane digestion of animal wastes / D.T. Hill // Agricultural Wastes. - 1983. - № 5. - pp. 1-16.

[7] Huang J.J.H. The potential of biological methane generation from chicken manure / J.J.H. Huang, J.C.H. Shih // Biotech. and Bioeng. - 1981. - № 23(10). - pp. 2307-2314.

[8] McCarty P.L. Anaerobic waste treatment fundamentals III / P.L. McCarty // Public Works. – 1964. – № 95. – p. 91.

[9] Mesophilic methane digestion of chicken manure at a wide range of ammonia concentration: Stability, inhibition and recovery / Q. Niu, W. Qiao, H. Qiang [et. al.] // Bioresource Technology. - 2013. - № 137. - pp. 358–367.

[10] Microbial community shifts and biogas conversion computation during steady, inhibited and recovered stages of thermophilic methane fermentation on chicken manure with a wide variation of ammonia / Q. Niu, W. Qiao, H. Qiang, Y.-Y. Li // Bioresource Technology. - 2013. - № 146. - pp. 223–233.

[11] Pechan Z. Anaerobic Digestion of Poultry Manure at High Ammonium Nitrogen Concentrations / Z. Pechan, O. Knappovfi // Biological Wastes. - 1987. - №20. - pp. 117-131.

[12] Safley L.M.J. Operating a full-scale poultry manure anaerobic digester / L.M.J. Safley, R.L. Vetter, D. Smith // Biol. Wastes. - 1987. - № 19(2). - pp. 79-90.

[13] Salyuk A. Thermophilic methane digestion of chicken manure / A. Salyuk, S. Zhadan, E. Shapovalov. // Ukrainian Food Journal. - 2014. -Vol. 3(4). – pp. 587–594.

[14] Webb A. R. Laboratory scale anaerobic digestion of poultry litter: Gas yield-loading rate relationship / A.R. Webb, F. R. Hawkes // Agric. Waste. - 1985. - № 13(1). - pp. 31-49.

METHODICS FOR CALCULATION AND CONTROL OF PURIFICATION LIME CONSUMPTION IN RAW CANE SUGAR PROCESSING

Pashamov E.R., T.G. Djurkov, M. Dzhivoderova

University of Food Technologies, Bulgaria, Plovdiv
26 Maritza Street,4002 Plovdiv, Republic of Bulgaria

Abstract: *The effect of lime quantity on the purification of raw cane sugar of different colouring is analyzed. It is established that this effect can be determined by the adsorption isotherm equation. Methodics for calculating the optimal lime consumption for raw remelt sugar syrup purification are suggested.*

Keywords: methodics, lime milk, liming, carbonation.

I. Introduction.

The commonly applied purification process flow in raw cane sugar processing for white sugar production includes liming and carbonatation. Liming is the process in which non-purified remelt sugar syrup is treated with lime /CaO/ in the form of lime milk /$Ca(OH)_2$/. Carbonatation is the process of saturating limed remelt sugar syrup with carbon dioxide /CO_2/, which produces a deposit of calcium carbonate /$CaCO_3$/ on which part of the non-sugars and especially the pigments are adsorbed.

The most important factor determining the efficiency of raw remelt sugar syrup purification with lime milk and carbon dioxide in raw cane sugar processing is the quantity of the purifying lime consumed. This factor depends on the quality of processed raw cane sugar but mostly on the colouring of the raw material which, in turn, determines the colour of non-purified remelt sugar syrup.

II. Discussion.

In the course of several consecutive raw cane sugar processing campaigns at the sugar-processing plant in Gorna Oryahovitsa, we conducted experimental research on the effect of purification lime quantity on the colour of purified remelt sugar syrup in view of the initial colouring of raw remelt sugar syrup. The results from the study are presented in Fig. 1.

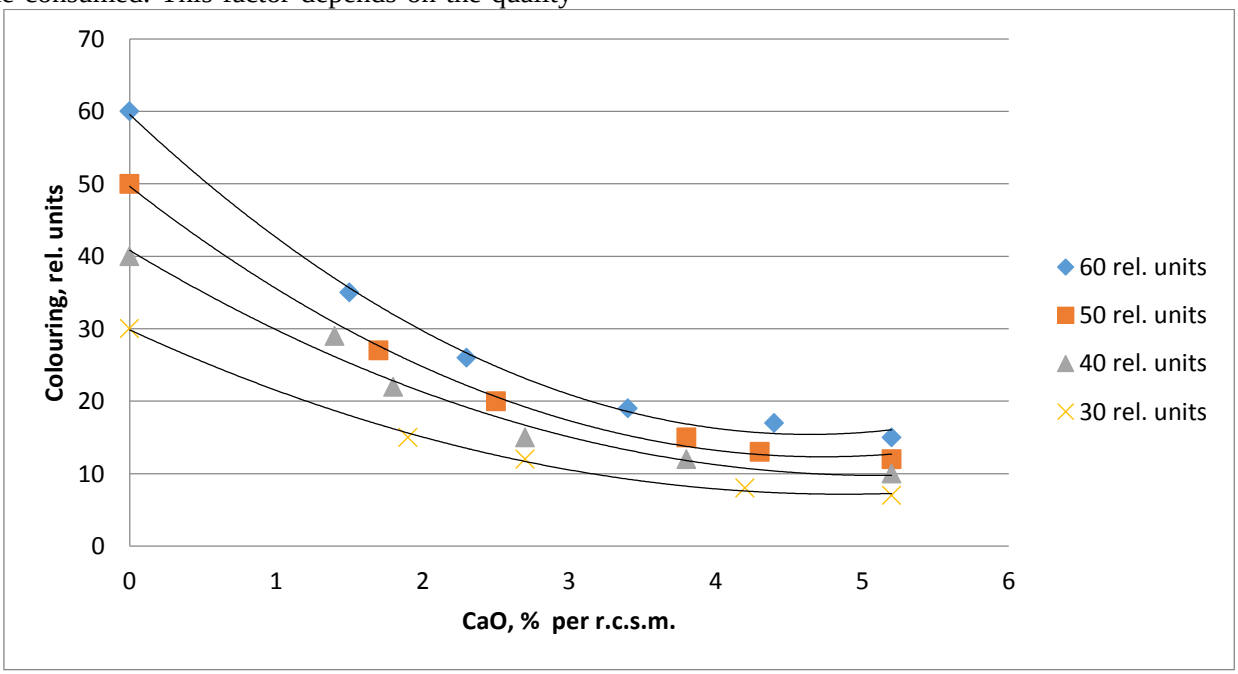

Fig.1. *Modifications in the colour of purified remelt sugar syrup depending on raw remelt sugar syrup colour for lime consumption concerning four types of non-purified remelt sugar syrup with the following initial colouring: 60, 50, 40 and 30 rel. units*

The analysis of the data shows that in order to obtain purified remelt sugar syrup with the technologically desirable colour of 15 rel. units for non-purified remelt sugar syrup colour of 60, 50, 40 and 30 rel. units, it is necessary to consume different quantities of lime, namely: 4.4; 3.7; 2.7 and 1.9 % CaO in accordance with raw cane sugar mass (per r.c.s.m.). The lime quantity increases with the intensification of non-purified remelt sugar syrup colour and raw cane sugar colour.

The processing of the data demonstrates that the type of colour modifications in purified remelt sugar syrup in accordance with the purifying lime quantity are determined sufficiently well by the adsorption isotherm equation with the k = 0.85 and n = 0.89 coefficients.

The adsorption isotherm equation is suitable for establishing the theoretical optimal purification lime consumption depending on non-purified remelt sugar syrup colour and the technologically desirable purified remelt sugar syrup colour of 15 rel. units.

Therefore, the Freundlich equation is expressed as:

$$X = \left(\frac{Y}{k}\right)^{\frac{1}{n}}. \qquad (1)$$

Then, it is transformed into:

$$\frac{L}{100} = \frac{(Y_0 - Y_1)}{(Y/k)^{\frac{1}{n}}}. \qquad (2)$$

Thus, the equation determining the theoretical optimal purification lime consumption assumes the following expression:

$$L = \frac{100(Y_0 - Y_1)}{(Y_1/k)^{\frac{1}{n}}}, \qquad (3)$$

where:

L – is the quantity of CaO, in percentages, in accordance with the mass of non-purified remelt sugar syrup;

Y_0, Y_1 – is the colouring of non-purified and purified remelt sugar syrup, rel. units;

k, n – are invariable coefficients (k = 0.85, n = 0.89).

In order to calculate the quantity of CaO in percentages depending on raw cane sugar, we apply the following equation:

$$L_1 = L.0{,}01.M_{NRSS}, \qquad (4)$$

where:

M_{NRSS} – is the quantity of non-purified remelt sugar syrup per 100 kg of raw cane sugar;

Example: Determine the theoretical optimal lime consumption for purifying raw non-purified remelt sugar syrup with a colour of 37 rel. units in order to obtain purified remelt sugar syrup with a colour of 15 rel. units.

Substituting with the values in equation (3), we get:

$$L = (100.(37{,}0 - 15{,}0))/(15/85)\text{^}(1/0{,}89) = 0{,}9\ \%\ per\ r.c.s.m. \qquad (5)$$

If the quantity of non-purified remelt sugar syrup amounts to 290 kg per 100 kg of raw cane sugar, then the consumption of CaO in percentages in accordance with the mass of raw sugar will be:

$$L_1 = 0{,}9.0{,}29 = 2{,}5\ \%. \qquad (6)$$

In practice, sugar-processing plants control the consumption of purification lime via measurements of remelt sugar syrup alkalinity. Knowing the lime quantity necessary for purification, we can determine the alkalinity of limed remelt sugar syrup corresponding to a specific lime quantity. In this case, the following equation is applied:

$$A_{LRSS} = \frac{100.L_1.C_{LM}}{M_{NRSS}.C_{LM} + 100.L_1}, \qquad (7)$$

where:

A_{LRSS} - is the alkalinity of limed remelt sugar syrup, in percentages, depending on product mass;

L_1 – is the quantity of lime consumed in purification, % CaO per r.c.s.m.;

C_{LM} – is the amount of CaO in lime milk, % . For lime milk density of 1.17 g/cm^3, C_{LM} = 19.8 %.;

M_{NRSS} – is the quantity of non-purified remelt sugar syrup, % per r.c.s.m..

In this example, substituting with the values in equation (7), we get:

$$A_{ДК} = \frac{100.2{,}5.19{,}83}{290.19.83 + 100.2{,}5} = 0.83\%\ CaO\ per\ m.r.s.s. \qquad (8)$$

In fact, since we determine the titratable alkalinity of the remelt sugar syrup, i.e. the lime content of limed remelt sugar syrup, in percentages depending on its volume, then to express the titratable alkalinity, we apply this equation:

$$TA_{LRSS} = A_{LRSS}.D_{NRSS} \quad , \qquad (9)$$

where:

TA_{LRSS} – is the titratable alkalinity of limed remelt sugar syrup, in % according to remelt sugar syrup volume;

D_{NRSS} – is the density of non-purified remelt sugar syrup, g/cm^3. For a dry matter content of non-purified remelt sugar syrup amounting to 50 %, D_{NRSS} = 1,223 g/cm^3.

In the example examined by us, we get:

$$TA_{LRSS} = 0{,}83.1{,}223 = 1{,}0\ volume\ \%\ CaO \qquad (10)$$

In this example, during raw cane sugar processing, in order to produce purified remelt sugar syrup with a colour of 15 rel. units from non-purified remelt sugar syrup with a colour of 37 rel. units, it is necessary to maintain a titratable alkalinity of limed remelt sugar syrup amounting to 1.0 % CaO.

If we know the titratable alkalinity of limed remelt sugar syrup, then we will be able to calculate purification lime consumption by the formula:

$$L_1 = \frac{M_{NRSS}.C_{LM}.TA_{LRSS}}{(C_{LM}.TA_{LRSS}).100}, \%\ CaO\ per\ r.c.s.m. \qquad (11)$$

The calculations of purification lime consumption in raw cane sugar processing are based solely on the colouring of raw remelt sugar syrup and the desired colour of purified remelt sugar syrup. The suggested methodics do not take into account the effect of non-sugar content in raw cane sugar on the filterability of remelt sugar syrup. In view of this, the necessary modifications in lime consumption and, hence, in titratable alkalinity, can be made experimentally only, at the beginning of the processing campaign.

III. Conclusions

1. The paper presents methodics suggested for calculating the theoretical optimal quantity of calcium oxide to purify raw remelt sugar syrup in raw cane sugar processing.
2. The methodics allow for the calculation of the titratable alkalinity of limed remelt sugar syrup, on the basis of which the consumed quantity of calcium oxide for purification is controlled.

References:

[1] Bugaenko I. F., N. A. Chernysheva, *Technology of the Production of Sugar from Gur*, Soyuzrossahar, Moscow, 2002 (*Технология производства сахара из сырца*, Москва, Союзроссахар, 2002).

[2] Bugaenko I. F., *Special Tehnological Calculations in Sugar Production*, Moscow, 2003 (Специальные технологические расчеты сахарного производства, Москва, 2003).

[3] Bugaenko I. F., *Production of Sugar and Sugar Products*, Rusagro-Sahar, Moscow, 2006 (*Производство сахара и продуктов из него*, Москва, ООО „Русагро – Сахар", 2006) .

[4] Marinova N. D., *Technology of Sugar*, HIFFI Acad. Publishing House, Plovdiv, 2002 (*Технология на захарта*, АИ на ВИХВП, Пловдив, 2002) .

[5] Sapronov A. R., *Technology of Sugar Manufacture*, "Kolos", Moscow, 1998 (*Технология сахарного производства*, Москва, „Колос", 1998).

[6] Slavyanskiy A. A., S. P. Gol'denberg, V. I. Tuzhilkin, Calculation of Product Flows in Sugar Production, Moscow, MGUPP, 2004 (Расчет материальных потоков сахарного производства, Москва, МГУПП, 2004).

PROCESS FLOW WITH TWO WHITE AND THREE YELLOW PRODUCTS IN THE CRYSTALLIZATION COMPARTMENT

Pashamov E.R., T.G. Djurkov, M. Dzhivoderova

University of Food Technologies, Bulgaria, Plovdiv
26 Maritza Street ,4002 Plovdiv, Republic of Bulgaria

Abstract: *A pneumatic system for molybdenum concentrate drying was designed and launched into operation. Molybdenum concentrate is a raw material in the manufacture of molybdenum which is a major component of the stainless steel used in food industry and biotechnology. The dryer throughput is 730 kg/h moist product and the energy efficiency is 79.2%.*

Keywords: molybdenum concentrate, pneumatic vortex dryer, scrubber

I. Introduction

The processing of raw cane sugar in the crystallization compartment of the "Zaharni Zavodi Gorna Oryahovitsa" sugar-processing plant utilizes a four-product process flow with one white and three yellow products (Fig. 1) [5].

Following the process flow, the white (A) massecuite is obtained from concentrated and purified remelt sugar liquor, white liquor and part of the green liquor. The quantity of the green liquor is experimentally determined in accordance with the desired colour of white crystal sugar. At the sugar-processing plant, the acceptable colour of white sugar is not more than 45 ICUMSA.

High-raw (B) massecuite and low-raw (C) massecuite are obtained from white liquor, A-green and B-green syrup, respectively, and green liquor. The quantities of the liquors with corresponding purities are calculated by equations with predefined purities [5].

II. Discussion

The technological parameters of white (A) massecuite and the A-green and A-white syrups obtained after its centrifugation according to the technological operations utilized in the plant, are shown in Table 1.

Table 1.*Technological parameters of white (A) massecuite, green liquor, and white liquor*

№	*Parameters*	*Measured in*	*Products*		
			White (A) massecuite	*Green liquor*	*White liquor*
1.	Dry matter content	%	91,5 ± 0,5	78,0 ± 80,0	75 ÷ 77
2.	Purity	%	95,5 ± 96,5	90,0 ± 91,5	91 ÷ 93
3.	pH value	pH units	7,5 ÷7,8	7,5 ÷7,8	7,5 ÷7,8
4.	Colour	0St/100g DM	-	≤ 55	≤ 45

In the processing of raw cane sugar with sucrose content between 99 - 99.4 %, the purities of white (A) massecuite, A-green, and A-white syrup are higher than the desired ones in the technological operations.

The results for the technological parameters of raw cane sugar, white (A) massecuite, and the white and green syrups obtained in centrifugation in different processing campaigns, are given in Table 2.

Table 2.*Technological parameters of raw cane sugar, white (A) massecuite, A-green, and A-white syrup*

Technological parameters				*Cane-processing campaigns*				
№	Name	Parameter	Measured in	2010	2011	2012	2014	2014
				IV-VI	IX	VII-VIII	III	VIII

1	Raw cane sugar	Bx	%	99,855	99,892	99,780	99,931	99,840
		Pol	%	99,111	99,298	98,846	99,370	99,180
		Q	%	99,252	99,405	99,060	99,440	99,340
2	White (A) massecuite	Bx	%	91,110	90,860	91,160	90,620	90,800
		Pol	%	88,050	87,940	88,180	87,780	88,110
		Q	%	96,640	96,790	96,730	96,870	95,700
		pH	pH units	7,860	7,520	7,630	7,410	7,620
3	A-green syrup	Bx	%	76,501	75,610	76,660	78,330	77,750
		Pol	%	70,813	70,570	71,030	73,100	72,940
		Q	%	92,050	93,340	92,660	93,340	91,400
		colour	^{0}St/100g DM	56,630	56,630	53,980	64,950	55,400
		pH	pH units	7,500	7,430	7,560	7,290	7,510
4	A-white syrup	Bx	%	75,233	74,590	74,530	74,880	74,660
		Pol	%	70,788	70,610	70,100	71,290	71,440
		Q	%	93,830	94,660	94,060	94,680	95,250
		colour	^{o}st/100g DM	32,880	36,590	37,830	42,580	37,340
		pH	pH units	7,500	7,430	7,560	7,320	7,510

In order to optimize processing in the crystallization compartment, during the VIII 2014 campaign a new process flow with two white and three yellow products was suggested and implemented (Fig. 2).

The introduction of the new process flow has the following advantages:

- Reduction of the passage of part of the high-purity green liquor;
- Reduction of the purity of white (A) massecuite and the liquors obtained from it;
- Reduction of losses in sucrose, which results in an increase in white sugar yield;
- Reduction in waste vapour.

The new process flow produces two white products. The first white massecuite is obtained from concentrated and purified remelt sugar liquor, white liquor, and part of the green liquor.

The second white massecuite is obtained from concentrated remelt sugar syrup and A-green syrup from the first white massecuite by a formula with predefined purities [5]. The predefined purity of the second white massecuite is 94.0 % and the quantities of the remelt sugar syrup and the green liquor with their purities are calculated by the respective equations [5].

The second white massecuite is mixed with the first white massecuite in the white (A) massecuite mixer. When the two white massecuites are mixed, the purity of the mixed white massecuite is lowered from an initial value of 97.4 % to 95.5 – 96.5 %, so that it remains within the specified limits for the technologically predetermined purity of white (A) massecuite. When the desirable purity of white (A) massecuite is reached, the production of the second white massecuite ceases. The processing is then reversed to the conventional process flow with one white and three yellow products. Table 2 demonstrates that the VIII 2014 processing campaign achieved and maintained a mean value of the purity of white (A) massecuite amounting to 95.7 %, which is within the technologically predefined purity limits at the plant.

Table 3 shows the yield and the relative waste vapour during the processing campaigns. The data manifest that in the VIII 2014 campaign, when the new process flow was implemented, the yield was at its highest, whereas the relative waste vapour was at its lowest.

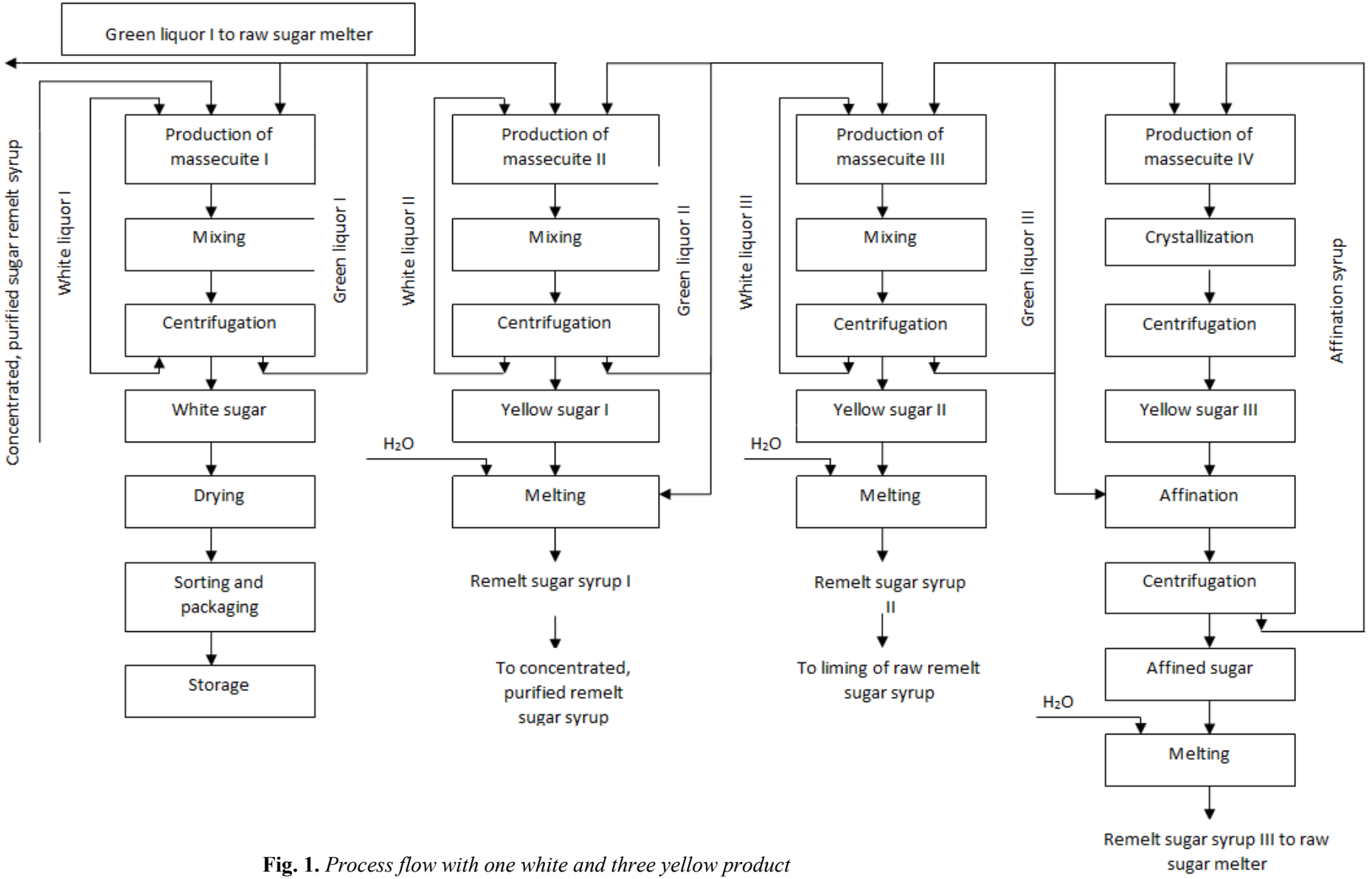

Fig. 1. *Process flow with one white and three yellow product*

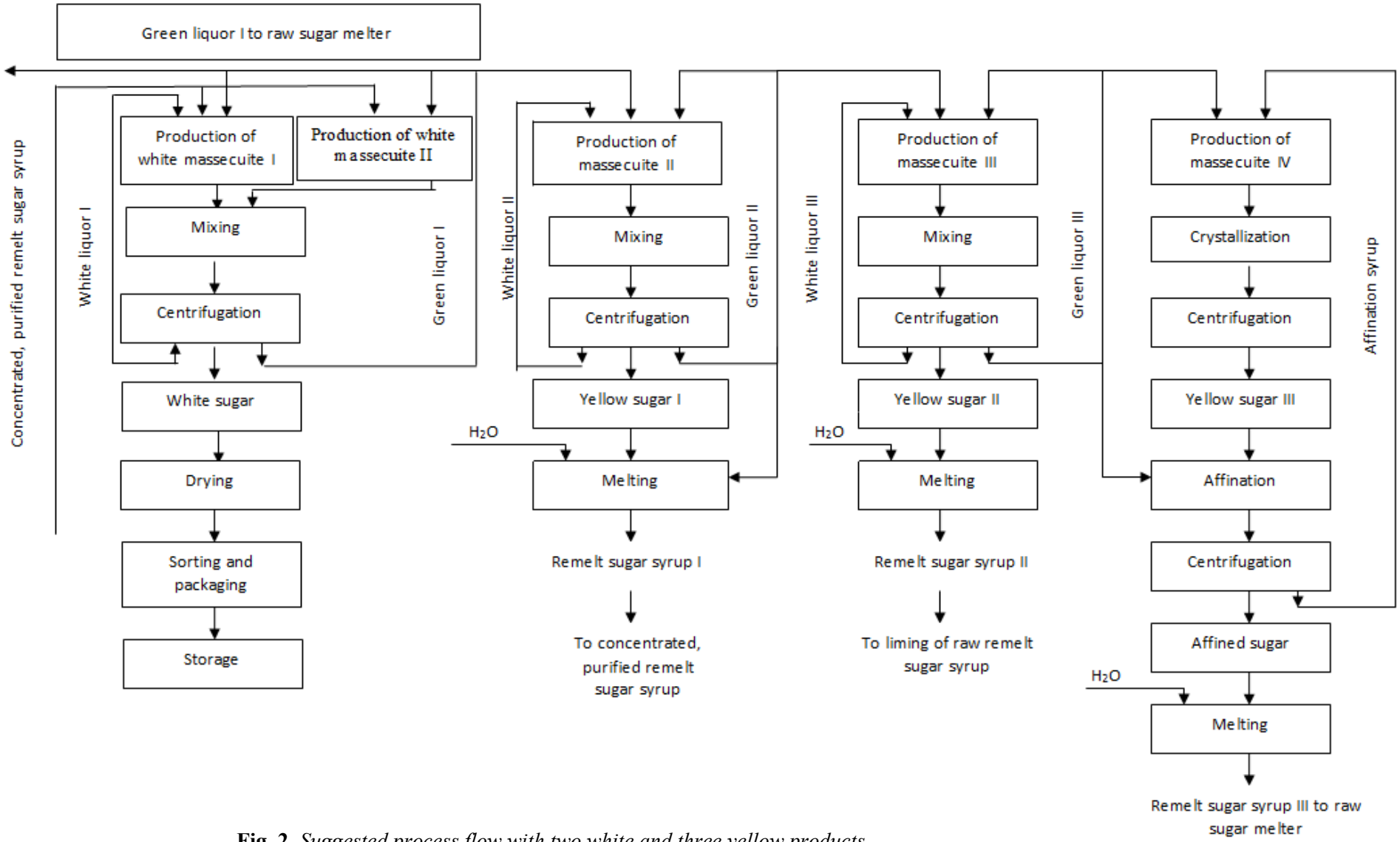

Fig. 2. *Suggested process flow with two white and three yellow products.*

Table 3.*Yield and relative waste vapour*

№	Name	Measured in	Cane-processing campaigns				
			2010	2011	2012	2014	2014
1.	Yield	%		95.92	95.10	96.27	96.58
2.	Relative waste vapour	MWh/t.w.s.	1.084	0.968	0.925	0.882	0.856

III. Conclusions

1. A new process flow with two white products was suggested and implemented.

2. The new process flow allows for a reduction in the passage of part of the green liquor, which is used to obtain a second white massecuite. This reduces sucrose losses from alkaline thermal degradation. The mixing of the two white massecuites brings about a decrease in and maintenance of the purity of white (A) massecuite within the technologically specified limits at the plant.

3. The practical results from the implementation of the new process flow show that it achieves a higher yield and lower vapour wastes.

References:

[1] Bugaenko I. F., N. A. Chernysheva, *Technology of the Production of Sugar from Gur*, Soyuzrossahar, Moscow, 2002 (*Технология производства сахара из сырца*, Москва, Союзроссахар, 2002).

[2] Bugaenko I. F., *Production of Sugar and Sugar Products*, Rusagro-Sahar, Moscow, 2006 (*Производство сахара и продуктов из него*, Москва, ООО „Русагро – Сахар", 2006) .

[3] Marinova N. D., *Technology of Sugar*, HIFFI Acad. Publishing House, Plovdiv, 2002 (*Технология на захарта*, АИ на ВИХВП, Пловдив, 2002) .

[4] Pashamov et al., *Massecuite crystallization methodics with predefined purity*, Scientific Works of the UFT Plovdiv, Plovdiv, vol. LIX, 2012 (*Методика за сваряване на захарни маси по предварително зададена чистота*, Пловдив, Научни трудове на УХТ, том LIX, 2012, стр. 324 – 329).

[5] Sapronov A. R., *Technology of Sugar Manufacture*, "Kolos", Moscow, 1998 (*Технология сахарного производства*, Москва, „Колос", 1998).

DATA INFORMATION SYSTEMS AND THEIR APPLICATION IN SEMI THEORETICAL APPROACH FOR TECHNOLOGICAL PROCESS DEFINITION

H. Dinkov[1], N. Bozukov[2], S. Madzharova[2]

[1] *Faculty of Economics, University of Food Technologies, Bulgaria, Plovdiv 26 Maritza Str.,4002 Plovdiv, Republic of Bulgaria, e-mail: hristo.d@dir.bg*

[2] *Faculty of Economics, University of Food Technologies, Bulgaria, Plovdiv 26 Maritza Str.,4002 Plovdiv, Republic of Bulgaria*

Abstract. *This paper presents an easy practical approach to the solution of common commercial situations in the food and canning industry that need prompt decisions. This study provides an example from the food sterilization industry. At times, due to customer or market demand, manufacturers need to vary the type, material and volume of product packages. The different thermal penetration properties lead to the need for a prompt reaction towards suitable changes in the scheduled time-temperature process. The necessary technical equipment, specific tools and practical algorithm have been presented. As a base of the given example is presented simple structure of a PC based 1-Ware buss measurement and data storage system. The specific software needed for that case of practice is also presented.*

Keywords: Data, temperature measurement, 1-Wire buss

I. Introduction

According to the dynamic changes in market demands, the producers of canned food are often forced to change their products – their volume, shape and the material of the containers. This always differs from the familiar and appropriate manufacturing practices concerning the time-temperature schedule and creates an urgent need for correction. The lack of practical experience in using new packages with different thermal penetration characteristics and changed volume makes that process relatively complicated. An adequate heating process is essential: if insufficient, it can affect the safety or shelf life of the product; if overextended, the product quality will deteriorate and energy losses will be incurred. On the other hand, food safety demands and good manufacturing practices (ISO and HACCP systems) force producers to implement and use computer-based measurement and backup systems in their industrial practice [1]. In any case, the availability of an appropriate validated on-line measurement system makes the above task much easier [4, 5]. Having the necessary equipment, it is fully possible and quite ease to determine a new time-temperature heating curve which will both cover the demands of the specified food safety (target lethality - F_0 should be achieved), and reduce undesirable over-processing and energy losses.

II. Equipment, materials and methodology

In our study, we accepted the following initial conditions:

- On-line measurement and file recording system in use;
- Experience in thermal sterilization processes in the manufacture of certain products and packages;
- Qualified food technologist and retort operator;
- Specially designed device for on-line measurement of the so-called “cold spot” within the package placed in the retort package container, and a measuring device for the retort temperature.

Equipment and software:

A. PC-based measurement and recording 1-Wire bus system used under industrial conditions. The structure of a system is presented below:

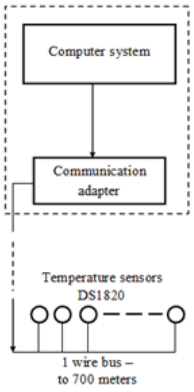

Figure 1. *Sumplified block diagram of the system*

B. Apart from the standard Windows-based software, software for on-line visualisation and

calculation of accumulated lethality (F_0 value at the cold spot) was defined, designed and used for that purpose. Briefly, we can define the function ability and main characteristics of this software module as follows:

- Dynamic table generation for all sensors connected to the system;
- A daily, weekly or another time interval report, either in table or graphic format;
- Document printing ability;
- Database storage (in text format);
- On-line view of the selected temperature points, and calculation and graphic presentation of the accumulated lethality (F_0-value).

In this case, we will not discuss in details the structure and hardware ingredients of the system because any system which has the above abilities can serve this purpose well. The presented one is only for the purpose of the very low cost and simplicity.

Having in mind that the data is recorded in text format, it is easy for any experienced employer to import and process the collected data in Excel, and then not only to present them graphically, but to make some correction in the time-temperature profile.

C. Industrial Retort

D. Familiar, already manufactured canned food, the processing parameters of which have to be achieved under the new conditions: changed shape, material and/or volume of the package (container). Standard products such as peas and tomato paste were used in the examples given in the article.

The pressure level was set at 200 bar as is above the critical pressure of the CO_2 solvent (73,8 bar), and as suggested by previous workers for extraction of phenolic compounds from plant material. Temperature of 50 ^{0}C is above the critical temperature for CO_2 (31,06 ^{0}C) and this temperature is generally used in the extraction of plant materials by SC-CO_2. The selected value of the temperature (50 ^{0}C) was low enough to avoid the damage of heat sensitive compounds.

Algorithm and step sequence of the approach for defining new and actual heating and cooling temperature retort profile:

Placing the measuring device into the jar or another package at the place corresponding to the so-called "cold spot", and of the package so prepared – at the coldest spot position of the retort rack (basket).

Defining the target F_0 value (accumulated lethality) – known for almost all of the processed products.

Defining the proper temperature profile for the retort (the usual one for the product).

Starting the sterilization process and controlling the process evaluation – retort and product temperatures and F_0 value on the monitor. *(when it is possible)

Starting the cooling procedure after reaching about 90% of the target F_0 value. (90% value is only as an example and could vary depending on temperature transfer velocity).

In some cases it is possible to inflict the need of repeating the above listed routine.

III. Results and discussion

Let us suppose that because of customer demand, the package needs to be changed to a relatively bigger or smaller one. Evidently, this situation will make it necessary to re-adjust the processing conditions as a result of the different thermal penetration and geometrical characteristics of the package, and the quantity of the raw material filled.

In accordance with the proposed algorithm, the sterilisation process of tomato paste in T_O 0.250 jars was processed under the conditions known as suitable for the product (cooking temperature, Z-value and F_0 aimed to about 25 conditional minutes). The calculated data are graphically presented in Fig. 2. The data showed that the product was in acceptable limits: F_0 was equal to about 30 minutes.

The F_0 value was calculated for corresponding temperature and time at 1-minute intervals. As reported in many scientific sources, the sufficient F_0 target value is about 25 minutes, which may differ slightly depending on the country demands, according to a base temperature of 93.3 ^{0}C and z=8.8 [3]. By reducing or extending the heating time depending on the expected value, we can reach the desired value.

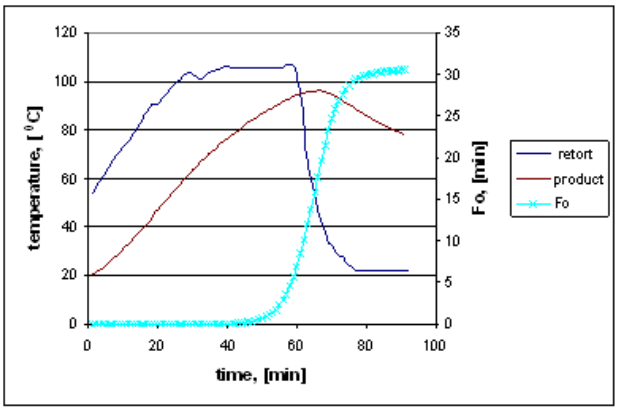

Figure 2. *Sterilization process*

The example shown above demonstrates the proposed algorithm availability. This approach was tested again for different products under industrial

conditions. The next example shown in Fig.3 illustrates the process of green pea sterilisation, where the heating process was insufficient with regard to food safety (the F_0 value was 3.8 instead of the recommended approximately 6.2 conditional minutes). This experiment was undertaken only for the need of expectance check.

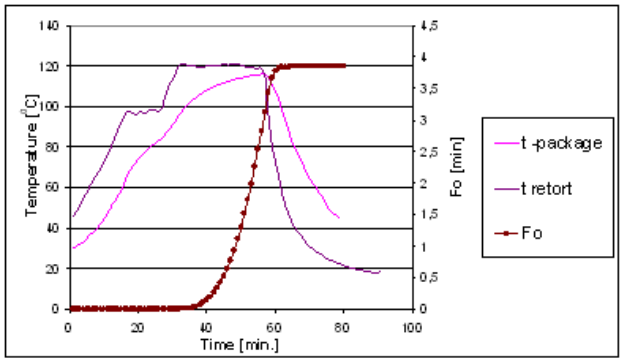

Figure 3. *Pea sterilization – proposed process*

In this case, we reprocessed the batch again extending the heating time interval where the temperature was relatively constant following the proposed procedure until the target F_0 value of about 6 minutes was reached. We need to be fully aware that the time-temperature curve we define will practically yield a little bit greater F_0 value under the same conditions. The inconvenience and inaccuracy of the method can be overcome by a repetition of the same method, followed by another correction, instead of process modeling, which is possible but complicated. The final result is presented in Fig.4 and illustrates the practical effect of the corrected process when the steps of the proposed procedure are followed.

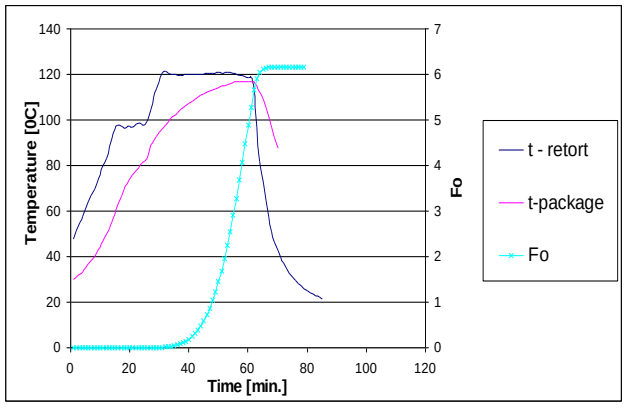

Figure 4. *Practical result of the time-temperature curve correction*

IV. Conclusions

Experiments with other products replicated the expected results and the observed accuracy remained within 10% to 15% of the target F_0 value. In our opinion, for express practical solutions, the proposed approach is simple and easily applicable for process correction in order to meet the demands for safe production and energy efficiency.

Overall, any process deviations concerning the initial product temperature or the time-temperature profile of the retort lead to mistakes. The proposed approach is reliable when the processing conditions are stable and repeatable. It may be used for process condition and temperature profile definition but will not guarantee the result in the event of process deviations.

References

[1] Динков Хр. 2012. Системите за температурен контрол и архивиране на данни по отношение управлението на качеството и безопасността на храните. Научни трудове на УХТ- Пловдив, Том LIX-2012, pp. 694-696.

[2] Динков Хр. и съавтори. 2012. Приложение на информационно-архивиращите системи за оптимизиране на режимите и снижаване на енергийните разходи при топлинна стерилизация на храни., Научни трудове на УХТ- Пловдив, Том LIX-2012, pp. 694-696.

[3] Хайдутов М., Н. Пенов, Ст. Делкинова. 2005. Режими на стерилизация , F0 – стойности и тяхното влияние върху безопасността, качеството и енергоемкостта на стерилизирани консерви., Пловдив,Академ. изд. на УХТ.

[4] Simpson R., A. Teixeira, S. Almonacid, 2007. Advances with intelligent on-line retort control and automation in thermal processing of canned foods. J. Food Eng.,vol. 18, July 2007, pp. 821-833.

[5] Simpson R., I. Figueroa, D. Llanos, A. Teixeira, 2007. Preliminary validation of on-line correction of process deviations without extending process time in batch retorting: Any low-acid canned foods, Food control, vol. 18, Issue 8, pp. 983-987.

[6] Norohna, J., Hendrickx, M., Van Loey, A., & Tobback, P. 1995. New semi-empirical approach to handle time-variable boundary conditions during sterilization of nonconductive heating foods. J. Food Eng., 24(2), pp. 249–268.

MATHEMATICAL MODELING OF DEFORMATION DURING THE FLAT CARDBOARD CREASING

Poliezhaiev[1] I., A. Gavva[2]

[1] Department of Printing Machines and Automated Complexes, Institute of Publishing and Printing, National Technical University of Ukraine "Kyiv Politechnic Institute", 37, Prospect Peremohy, Kyiv, Ukraine, e-mail: ivan.poliezhaiev@gmail.com

[2]Chair of technical mechanics and packing technique, Faculty of engineering mechanics and packing technique, National University of Food Technologies, Volodimirs`ka St., 68 - Kiev, Ukraine

Abstract: *The relevance and the way of flat paperboard creasing mathematical modeling with the finite element method are described in the article. The quality of creasing is influenced by many factors, the main ones are the physical and mechanical properties and structure of paperboard, shape and size of creasing tools and parameters of creasing matrix. Mathematical model of creasing allows predicting the influence of these factors on the process of creasing and quality, and selecting rational parameters.*

Keywords: creasing, cardboard, paperboard deformation, paperboard folding.

I. Introduction

The need to compliance with the optimal values of the load in the contact zone of cardboard with abundant running tools and prevent damage to the material during creasing justifies the importance and relevance of research.

The purpose of the study is to determine the rational parameters of creasing a flat paperboard using mathematical modeling.

II. Materials and methods

The main properties of cardboard are: appearance and performance characteristics. The exterior is characterized by suitability for printing, laundry, tidying up paint and resistance to abrasion. Operating properties are associated with the physical and mechanical properties of cardboard. These properties relate to how the board will withstand the surrounding factors. [1]

Cardboard has a linear elastic behavior to a given boundary - Yield. This means that the force applied to the cardboard is proportional to the deformation caused by the applied force. If the action of force stops, cardboard restores its original size. This is summarized in Hooke's law described below.

Cardboard is deformed beyond the elastic showing the elastic-plastic properties. This means that the applied force is no longer proportional to strain, see Figure 1. When the action force stops cardboard does not restore its original size. The value of the elastic limit is usually 0.2% elongation. [2]

Feature fibers and cardboard production determine the physical and mechanical properties of the material, which can be regarded as very close to orthotropic.

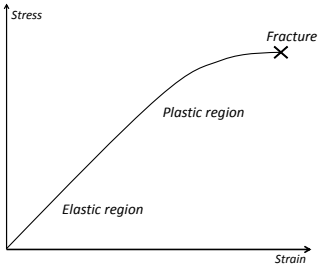

Figure 1. *The elastic and plastic properties of a typical paperboard*

This means that the materials will have different properties in three orthogonal directions: paperboard fiber direction coincides with the longitudinal (machine direction) - MD, direction perpendicular to the fiber paperboard machine running - CD and ZD - thickness direction, as shown in Figure 2.

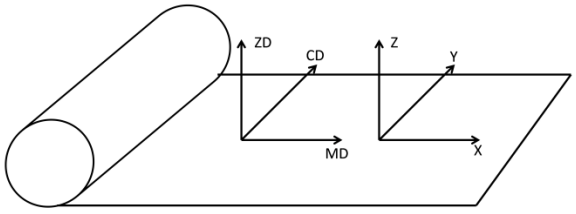

Figure 2. *The main directions of stress perception cardboard*

To ensure correct and line quality and reduce bending force to be put to bending, cardboard slabs are subjected to preliminary processing - creasing. [3]

The process of creasing - a preliminary application to the material through a bend in the form of grooves particular profile is the process of pulling out local material. Creasing is used to reduce the stiffness of sheet cardboard pieces on line bending, significant facilitation of fold formation and improve quality parameters of cartons, especially in its forming machines automatic action.

Creasing can be divided into three stages. In the first phase cardboard blank, when lowering blanking dies, elastic fixed position presses on counter-matrixes. In the second stage creasing tool (with the standard, narrowed or thickened molding head) draws a blank cardboard into two axis directions. In the third stage there is a compression board under creasing tool and counter-matrixes.

Creasing tools put pressure on the work piece so that the board is deformed by just buried matrix elements, with the formation of sharp lines creasing. The macro graphic of creasing process is shown in Figure 3. [4]

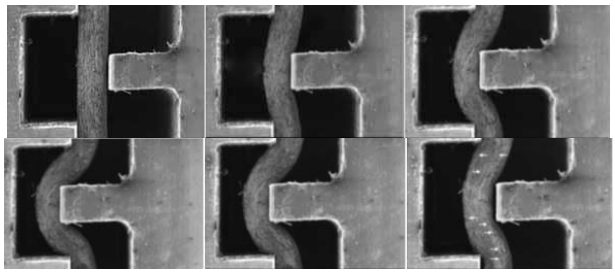

Figure 3. *Macroscopic image of creasing process.*

When creasing, fibrous connections between layers of cardboard are destroyed and damaged, fibers of plastic deformation occurs in cardboard layers. There are creasing high strain shear and compression in the area. Layering shift is caused by layers of cardboard, which reduces its bending stiffness in further assembly. Thanks to local damage in the area, creasing cardboard ideally behaves like a hinge that will improve the quality and productivity of the process assembly. Thus, after creasing the quality can be judged by the ease of folding, i.e. assembly. To assess the quality of creasing, you need to consider many factors that affect it, such as moisture cardboard, width of creasing groove, depth of penetration tools and so on. However, it has been experimentally found that the most significant factor is the thickness of the cardboard. Thicker slabs require wider range and groove. Therefore, they are less sensitive to inaccurate case between the ruler and the groove.

Macroscopic image running them and drawn samples are shown in Figure 4. Based on these images, two important conclusions can be taken into account when constructing mechanical models of creasing.

Firstly, plastic deformation occurs in the area of creasing. Plastic deformation projects thickness of cardboard, ZD, starts after creasing 5% below the creasing line. A special form of creasing zones, after interaction with the tool is caused not only by plastic deformation in the plane ZD, but also by stress and shear stress of the outer layer and stretching towards MD.

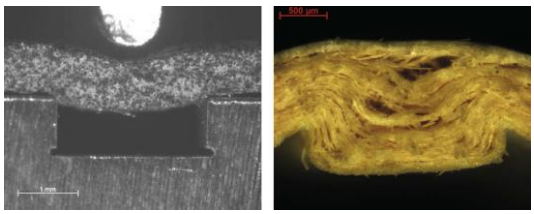

Figure 4. *Macroscopic image of cardboard blanks after creasing (left) and folding (right)*

Secondly, microscopic images are obtained after assembly lines are running to show that the inner layer of cardboard was separated from the outer layers - especially from the upper layer. The very inner layer is divided into several layers of paper. The lower layers were bent and curved inward, as shown in Figure 4 b. [5]

The number of such layers is about eight, without taking into account a number of ultrafine. This behavior detachment is a natural phenomenon for cartons, although the number of layers formed may vary.

During the creasing in the area between the tools and running the creasing groove matrix, the coplanar tension compression and shear stresses are not coplanar. In the industrial creasing (as it is shown in Fig. 5), in the field next to the creasing area, there is the tension in the plane of the work piece. [6]

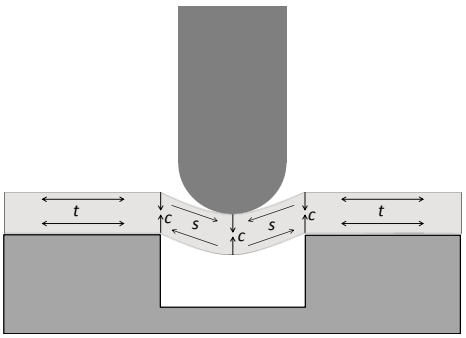

Figure 5. *Diagram of the deformation and stress state in the creasing zone during creasing: t - tension, c – compression, s - shear.*

Not outside of the bend formed tension, but inside it – there is a compression to create a rounded bottom layer. Moreover, the ability to flake board is a very important property for its assembly. Layering

is a mode of destruction of paper or paperboard, where the surface is refracted parallel to the plane of the sheet. This type of damage takes place in case of a positive cardboard folding mechanism since it can reduce stress on the outside of the bend, which will enable to reduce the risk of cracks on the outside of the bend. Compilation of cardboard is largely based on the workpiece ability to the internal stratification to compression stresses occurring inside the bend formed by the inner relief. When the separation takes place, stress arising in place of the workpiece, usually 50 to 100 times smaller than the tension arising in the preparation of blanks without prior creasing. [7]

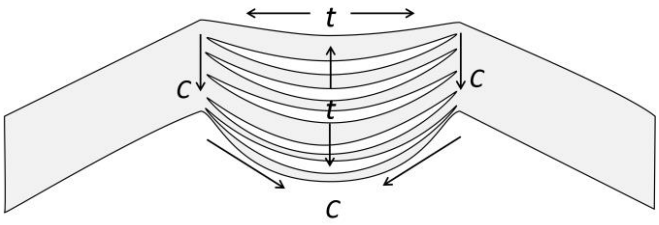

Figure 6. *Diagram of the deformation and stress state in the creasing zone during folding: t - tension, c – compression.*

During the drafting board, its inner layers are easily bending because they have curved shape and are in a compressed state (Fig. 6). As the thin layers in the area of creasing are easier to bend than cardboard outside creasing, bending occurs only along the lines of creasing. However, some non-planar tension may arise within the fold through fibers that took off the surfaces and are in the extended position. The outer layers, including the top layer are under tensile stress, which can lead to cracking and fracture of the upper layer of the workpiece. Thus, creasing and folding must be done so that the tension in the plane of the upper layer is minimized.

Accurate modeling of creasing lines behavior is a key factor in the development of models and approximate mathematical modeling process of creating cardboard packaging.

To predict the behavior of cardboard under the influence of various parameters of creasing we have created a mathematical model. This model should be constructed in such a way that it could be relatively easily implemented in a computer program using the finite element method. To simulate the cardboard we used a holistic model that describes the behavior of cardboard material combined with stratification model to explain the formation of different layers of paper. The most important elements of the mathematical model are elastic-plastic composite materials.

Needless to say, the process of creasing results in lower elasticity, rigidity and strength of cardboard. This deterioration is due to the combined effect of separation, the width W field and creasing cardboard thickness δ. The geometric effect is achieved by creasing permanent deflection of cardboard layers. Depending on the intensity j, creasing, more or less significant changes in cardboard are observed after creasing, which reduces the stability of compressed layers bending.

Based on the observation of physical processes occurring at creasing, it provides:

- The strength and stiffness for reduced crease line of creasing, creasing process in proportion to the intensity measured by the initial nominal shear strain γ, defined in equation (1);

$$\gamma = \frac{2h}{W}$$

(1) where h- value recess creasing tool, W - width of the groove.

- Increased depth penetration (above γ) of creasing tool has got two main consequences: is a bundle of thinner layers of cardboard; remains more out of plane deflection (Figure 7.)

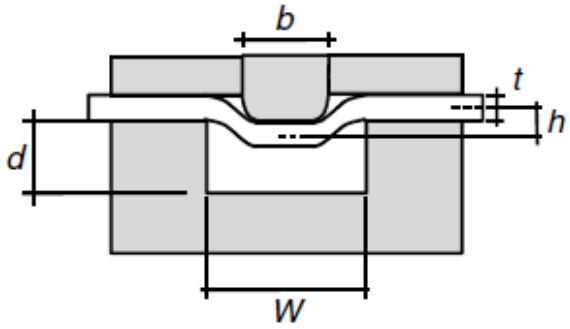

Figure 7. *Geometrical parameters of penetration creasing tool,*
where h - depth of penetration creasing tool and W is the width of the groove, b - width of creasing tool, d - depth of the groove, t - thickness of the paperboard.

- Deterioration of mechanical properties of cardboard in place of creasing is the result of reducing the thickness and the permanent deflection stratified elements. [8]

The finite element method (FEM) (its practical application is often known as finite element analysis (FEA)) is a numerical technique for finding

approximate solutions of partial differential equations (PDE) as well as integral equations. The solution approach is based either on eliminating the differential equation completely (steady state problems), or rendering the PDE into an approximating system of ordinary differential equations, which are then numerically integrated using standard techniques such as Euler's method.

In solving partial differential equations, the primary challenge is to create an equation that approximates the equation to be studied, and is numerically stable, meaning that errors in the input and intermediate calculations do not accumulate and cause the resulting output to be meaningless. The finite element method is a good choice for solving partial differential equations over complicated domains [3].

FEM uses a complex system of points called nodes forming elements which make a grid called a mesh. The elements of the mesh are programmed to contain the material and structural properties, which define how the structure will react to certain loading conditions. Nodes are assigned at a certain density throughout the material depending on the anticipated levels of stress of a particular area and they transfer the stress from element to element. Points of interest may consist of: fracture points, fillets, corners, complex details, high stress areas, etc.

The finite element method is originated from the need for solving complex elasticity and structural analysis problems in civil and aeronautical engineering. Its development can be traced back to the work by Hrennikoff. While the approaches used by these pioneers are different, they share one essential characteristic: mesh discretization of a continuous domain into a set of discrete sub-domains, is usually called elements. Starting in 1947, Zienkiewicz from Imperial College gathered those methods together into what would be called the Finite Element Method, building the pioneering mathematical formalism of the method. [2]

III. Results and discussion

The equations of elastic-plasticity in traditional tensor notations are as follows:

$$\begin{cases} \partial_t \sigma = E : (\partial_t \varepsilon - \partial_t \varepsilon_p) \\ \partial_t \varepsilon = (\partial_x v)_s \\ \partial_t \varepsilon_p = H(\|\sigma\| - \sigma_s)\lambda(\sigma, \varepsilon) : \partial_t \varepsilon \\ \rho \partial_t v = \partial_x \sigma \end{cases} \quad (2)$$

Experimental data show the presence of the diagrams strain softening paperboard areas where there is a voltage drop with increasing deformation. Through these softening initial boundaries value problems are incorrect (broken Hadamard criterion):

$$\partial_t \sigma : \partial_t \varepsilon > 0 \quad (3)$$

This test is called the stability criterion of material or Drakker criterion. Thus, increasing damage to the elastic properties of the material (elastic modulus and yield strength) is reduced to zero, which means complete destruction of structured material.

To simulate the process of creasing system board there must be equations of the theory of elastic-plastic deformation strength for small supplement kinetic equation for the initial nominal shear strain and elastic modulus and the dependence of the yield strength of the original nominal shear strain. This system of equations will look like:

$$\begin{cases} \rho \partial^2 U = \nabla \sigma \\ \sigma = E(\gamma) : (\varepsilon - \varepsilon_p) \\ \partial_t \varepsilon_p = \lambda_p \dfrac{\partial F_p}{\partial \sigma} H(F_p) H(\sigma : \partial_t \varepsilon) \\ \partial_t \gamma = H(F_d) \Gamma(\varepsilon, \varepsilon_p, \gamma) + r_\gamma \\ \varepsilon = 1/2(\nabla \otimes U + (\nabla \otimes U)^T) \\ F_p(\sigma) = 3/2(\sigma' : \sigma')/\sigma_p^2 - 1 \\ F_d = F_d(\varepsilon, \varepsilon_p, \gamma) \end{cases} \quad (4)$$

where ρ - density of paperboard; U - displacement vector creasing tool; σ - stress tensor; $\sigma' = \sigma$ - (σ :I)I/3 - deviator stress; $E(\gamma)$ - tensor of elasticity modules, which is a function of the initial nominal shear strain γ; ε - strain tensor paperboard; ε_p - plastic deformation of tensor paperboard; λ_p - coefficient of law of plastic yield stress, defined by plasticity: $F_p(\sigma) = 0$, Symbol «⊗» contains external tensor product; F_p - load function; H - Heaviside's function equals to zero for negative values of the argument and ones otherwise; σ_p - limit of elasticity paperboard; I - tensor unit; F_d - function by provided destruction inherent value which allows the accumulation of initial nominal shear strain; r_γ - not thermomechanical source of primary shear strain, Symbol «:» contains double scalar product of tensors.

The initial conditions that complement this system of equations will have the form:

$$U\big|_{t=0} = 0$$
$$\partial_t U\big|_{t=0} = 0$$
$$\varepsilon_p\big|_{t=0} = 0 \qquad (5)$$
$$\gamma\big|_{t=0} = 0$$

In order to solve this problem it is necessary to supplement the main (kinematic) or natural (dynamic) boundary conditions. Boundary conditions depend on the specific task and are critical to address it.

IV. Conclusions

Finite Element Modeling using a system of equations of the theory of elastic-plastic deformation strength for small considering the kinetic equation for the initial nominal shear strain and elastic modulus and the yield strength dependence on the original nominal shear strain, will determine the optimal parameters for quality creasing process, providing certain key and natural boundary conditions.

References

[1] Kaverin V. A., Feklin K. P. Vyibor, izgotovlenie, ispyitaniya taryi i upakovki. — M.: MGUP, 2002, p. 260.

[2] Juan Crespo Amigo,- Stiffness design of paperboard packages using the finite element method.,- Department of solid mechanics, Stockholm,Sweden 2012

[3] L.G.J. Gooren,- Creasing behavior of corrugated board. An experimental and numerical approach.,- Technische Universiteit Eindhoven Department Techanical Engineering Materials Technology .Eindhoven, February 2006.

[4] Hui Huang. - Numerical and Experimental Investigation of Paperboard Creasing and Folding - Licentiate Thesis No. 111, 2011,KTH School of Engineering Science , Department of Solid Mechanics ,BiMaC Innovation , Royal Institute of Technology,SE-100 44 Stockholm Sweden.

[5] Manufacturing of paperboard and corrugated board packages. Pulp and Paper Chemistry and Technology - Volume 4, Paper Products Physics and Technology.

[6] L.A.A. Beex, R.H.J. Peerlings, - An experimental and computational study of laminated paperboard creasing and folding* Department of Mechanical Engineering, Eindhoven University of Technology, P.O. Box 513, 5600 MB Eindhoven, The Netherlands, 25 August 2009.

[7] Shreder V. L., Yovanovich K.S. Karton. Tara i upakovka. — K.: IATs «Upakovka», 1999, p. 192.

[8] A. Giampieri , U. Perego , R. Borsari ,- A constitutive model for the mechanical response of the folding of creased paperboard,- Department of Structural Engineering, Politecnico di Milano, Piazza L. da Vinci, 32, 20133 Milan, Italy

[9] Efremov N. F. Tara i eYo proizvodstvo: Ucheb. posob. M.: MGUP, 2001, p. 312.

[10] DerenIvska A.V.,Maslo M.A.,ValIulIn G.R.,- DoslIdzhennya operatsiyi biguvannya zagotovki kartonnoyi upakovki.

STUDY OF THE INFLUENCE OF ION NITRIDING ON THE ROUGHNESS OF MECHANICALLY TREATED SURFACES

I. Zumbilev [1], M. Petkova[2], A. Zumbilev [1]

[1] *Sofia Technical University, Plovdiv Branch, e-mail: zumbilev@mail.bg*
[2] *Faculty of Mathematics and Informatics, Plovdiv University, Plovdiv 4000*

Abstract. *The aim of this paper is to study the influence of ion nitriding on the roughness of the surfaces of the following types of tool steels: 3Cr2W8V (BH21), 4Cr5MoVSi (BH11), 3Cr3Mo3V (BH10). The obtained results illustrate the relationship between the parameters temperature of nitriding, pressure of ammonia in the chamber, duration of the process, temperature of annealing on the one hand, and the roughness of the nitride surfaces, on the other hand. It has been established that after ion nitriding of steels with surface roughness Ra=0,27-0,35 μm, measured in transverse direction with respect to the traces from the last mechanical treatment, the roughness of the nitrided surface does not change considerably but stays within Ra=0,28-0,32 μm and depends on the mode of treatment.*

Key words: ion nitriding, surface roughness, tool steels

I. Introduction

The state of the surfaces of various details considerably influences their wearing, and therefore roughness control is of great significance especially for big contact areas [2, 3, 10, 11].

The roughness of treated surfaces depends on the chemical composition of the material, the type of thermal treatment, as well as on the technological peculiarities of the process of saturation with nitrogen. Iron-carbon alloys, which are not quenched (ferrite structure), are characterized by torn surfaces and high roughness [2]. It has been established in [3] that the surface roughness decreases together with increase in the treated material's hardness up to 400HB. Any further increase of hardness does not influence considerably the height of the roughnesses. Nitriding is the last operation in most technological processes and no additional treatment is applied after it. It is of great importance, therefore, to study its influence on the roughness of the treated surfaces.

The surface roughness of the details after nitriding depends directly on their initial state. Thus, when cast-iron samples are nitrided, their roughness increases considerably compared to the case with steel samples. The availability of graphite inclusions in the structure leads to a different thickness of the (combined) zone, which, in turn, causes considerable increase in the roughness of the surface layer.

At high initial surface roughness after ion nitriding, a decrease in roughness is observed. It does not change when Ra is within 0,8-0,63μm and it decreases to 0,32 μm at values of roughness lower than the given interval [1, 4, 5, 8]. According to [6, 7, 9] ion nitriding retains its initial roughness when Ra is within 0,16-0,04 μm, while classical gas nitriding decreases it. There is no consensus in the cited literature on the issue of how the technological factors of nitriding influence the surface roughness.

This study aims at establishing the influence of nitriding in smouldering discharge plasma on the surface roughness of the following tool steels: 3Cr2W8V, 4Cr5MoVSi, 3Cr3Mo3V.

II. Methodology of the study

Materials for studying and mode of thermal treatment and ion nitriding

Three types of tool steels were selected for studying: BH11 (4Cr5MoVSi - ГОСТ) and BH10 (3Cr3Mo3V - ГОСТ) with raised thermal stability and resilience, and also BH 21 (3Cr2W8V - ГОСТ) – with high thermal stability. The steels given as BH10, BH11 and BH 21 are denoted by BS4659.

The chemical nature of the steels listed above was studied by the automatic analytic equipment "SPECTROTEST", produced by the company SPECTRO Analytical Instruments GmbH. The results are given in Table 1.

The steels were thermally treated in a "Degussa" furnace by the modes, given in Table 2.

The samples were quenched in a vacuum furnace with the help of the gas argon under the pressure of 6 bar. All the samples from the tree types of steels were subjected to annealing in a vacuum furnace at a temperature of 760^0C.

Table 1. *Chemical composition of the steels*

Steels	Chemical elements, wt %								
	C	Cr	Mo	V	W	Si	Mn	Ni	S
3Cr2W8V BH21	0,30	2,70	-	0,29	8,01	0,18	0,26	-	0,015
4Cr5MoVSi BH11	0,38	4,50	1,2	0,47	-	0,98	0,22	0,14	0,006
3Cr3Mo3V BH10	0,28	3,24	2,74	0,55	-	0,45	0,2	0,13	0,01

Table 2. *Modes of preliminary thermal treatment and results from measuring the roughness of the thermally treated surfaces*

Steels	$t_{hard.}$, ^0C	$t_{temp.}$, ^0C	HRC	direction transverse Ra, μm	longitudinal direction Ra, μm
3Cr2W8V	1100	600	46	0,28	0,11
3Cr2W8V	1100	650	44	0,31	0,12
3Cr2W8V	1100	700	32	0,32	0,14
4Cr5MoVSi	1030	600	51	0,27	0,13
4Cr5MoVSi	1030	650	46	0,31	0,14
4Cr5MoVSi	1030	700	29	0,35	0,16
3Cr3Mo3V	1050	600	50	0,29	0,11
3Cr3Mo3V	1050	650	46	0,30	0,13
3Cr3Mo3V	1050	700	30	0,33	0,14

During the process of steel nitriding a complete factor experiment of the type 2^4 at input (control) factors: temperature of nitriding (X_1), ammonia pressure (X_2), duration of the process (X_3), and temperature of annealing (X_4) was conducted. Based on these input factors, intervals of varying and zero level were used, as shown in Table 3.

Table 3. *Intervals of varying of the input factors*

factors / levels	$t_{nitr.}$ ^0C	P Pa	τ h	$t_{temp.}$ ^0C
	X1	X2	X3	X4
Zero level (0)	530	300	7	650
Interval of varying (1)	20	150	3	50
Upper level (+1)	550	450	10	700
Lower level (-1)	510	150	4	600

The samples were nitrided in the installation "ION – 20" according with the modes, given in Table 4.

Study of the surface roughness

For measuring the surface roughness a profile-meter – profile-graph "Surtranic-3" was used, produced by the company "Taylor-Hobson". The device is intended for defining the surface roughness by the parameter Ra. It works on the basis of the contact methods of assessing roughness, in which the examined surface is felt by a diamond needle. Due to the roughnesses, the needle carries out reciprocating motion in a direction, normal to the examined surface.

Table 4. *Modes of ion nitriding*

№ mode nitriding	Technological factors			
	X1	X2	X3	X4
1	-1	-1	-1	-1
2	1	-1	-1	-1
3	-1	1	-1	-1
4	1	1	-1	-1
5	-1	-1	1	-1
6	1	-1	1	-1
7	-1	1	1	-1
8	1	1	1	-1
9	-1	-1	-1	1
10	1	-1	-1	1
11	-1	1	-1	1
12	1	1	-1	1
13	-1	-1	1	1
14	1	-1	1	1
15	-1	1	1	1
16	1	1	1	1

According with BDS ISO 4287-2:1995, the value of 0.25mm was used for a basic length at defining Ra. The roughness of the three thermally treated and ion nitrided steels - 3Cr2W8V, 4Cr5MoVSi and 3Cr3Mo3V - was measured after grinding. Five measurements were done to each sample, and the average value of the parameter Ra was defined afterwards. All measurements were done at room temperature.

III. Experimental results and analysis

Roughness of thermally treated surfaces

The results from the surface roughness measurements of the three steels for the different temperatures of annealing are given in Table 2. From Table 2 it can be seen that there are no considerable differences in the values of the parameter Ra for the various steels and the individual temperatures of annealing. It can be noted, though, that there are tendencies for increase in the surface roughness together with the increase in the temperature of annealing. This can be explained by the presence of larger particles of ferrite and cementite, formed in the structure of the annealed steel at a higher temperature of annealing.

Surface roughness of thermally treated, grinded and ion-nitrided steels

The results from the surface roughness measurements of the samples from the three steels (3Cr2W8V, 4Cr5MoVSi and 3Cr3Mo3V), done longitudinally and transversely to the traces from the last mechanical treatment (grinding), are given in Table 5.

Table 5. *Roughness of thermally-treated and ion-nitrided surfaces*

№ mode (table5)	3Cr2W8V		4Cr5MoVSi		3Cr3Mo3V	
	Ra, μm longitudinal direction	Ra, μm direction transverse	Ra, μm longitudinal direction	Ra, μm direction transverse	Ra, μm longitudinal direction	Ra, μm direction transverse
1	0,14	0,33	0,23	0,41	0,21	0,28
2	0,18	0,33	0,39	0,50	0,15	0,27
3	0,17	0,24	0,17	0,29	0,14	0,35
4	0,27	0,53	0,20	0,24	0,18	0,30
5	0,28	0,37	0,26	0,30	0,46	0,67
6	0,21	0,30	0,53	0,53	0,50	0,58
7	0,14	0,44	0,33	0,40	0,27	0,38
8	0,26	0,45	0,36	0,45	0,09	0,26
9	0,16	0,30	0,29	0,42	0,13	0,46
10	0,25	0,53	0,33	0,43	0,31	0,42
11	0,13	0,36	0,22	0,50	0,26	0,45
12	0,32	0,53	0,20	0,48	0,18	0,26
13	0,29	0,39	0,27	0,55	0,36	0,63
14	0,36	0,48	0,31	0,41	0,58	0,74
15	0,16	0,52	0,27	0,55	0,21	0,42
16	0,33	0,55	0,27	0,41	0,29	0,46

The obtained results from measuring the parameter Ra were introduced into a personal computer and by means of a suitable programme the coefficients of the regression equations were defined, as well as their significance and adequacy.

The following significant and adequate equations of surface roughness were derived:

a) steel 3Cr2W8V

$$\begin{aligned} Ra = {} & 0.41134 + 0.0424X_1 - 0.0231X_2 \\ & + 0.0139X_3 + 0.0389X_4 + 0.0131X_1X_2 \\ & - 0.0346X_1X_3 + 0.0124X_1X_4 - 0.0174X_2X_4 . \end{aligned} \quad (1)$$

After recalculating the coefficients of equation (3.1), we obtain the mathematical-statistical model for Ra in a natural state:

$$\begin{aligned} Ra = {} & 1.17318 - 0.0032191 t_{\text{nitr.}} - 0.00095073\, p \\ & + 4.323\times10^{-6}\, t_{\text{nitr.}} p + 0.307164\,\tau \\ & - 0.0005709\, t_{\text{nitr.}}\tau - 0.005098 t_{\text{temp.}} \\ & + 0.0000124 t_{\text{nitr.}} t_{\text{temp.}} - 2.2968\times10^{-6}\, p t_{\text{temp.}} \end{aligned}$$

$$\begin{aligned} Ra = {} & 0.2194 + 0.0481X_1 - 0.0144X_2 \\ & + 0.0294X_3 + 0.0256X_4 - 0.0319X_1X_2 \\ & - 0.0169X_1X_3 + 0.0119X_1X_4 - 0.0219X_2X_3 \\ & - 0.0056X_2X_4 + 0.0006X_3X_4. \end{aligned} \quad (2)$$

The equations refer to the roughness of the nitrided surface of steel 3Cr2W8V, measured in a transverse (1) and longitudinal (2) direction of the traces from the last mechanical treatment. Considerable influence on the roughness proves to have the temperature of nitriding - X_1. From both equations it can be seen that the rest of the factors (temperature of annealing, ammonia pressure and duration of nitriding) have less influence.

b) steel 4Cr5MoVSi

$$\begin{aligned} Ra = {} & 0.4409 + 0.0116X_1 - 0.0231X_2 \\ & + 0.0378X_3 + 0.0453X_4 - 0.0278X_1X_2 \\ & + 0.0134X_1X_3 - 0.0253X_1X_4 + 0.0184X_2X_4. \end{aligned} \quad (3)$$

After recalculating the coefficients of equation (3), we obtain the mathematical-statistical model for Ra in a natural state:

$$\begin{aligned} Ra = {} & -9.38074 + 0.0182439\, t_{\text{nitr.}} + 0.00313104\, p \\ & - 9.174\times10^{-6}\, t_{\text{nitr.}} p - 0.104709\,\tau \\ & + 0.0002211\, t_{\text{nitr.}}\tau + 0.013579\, t_{\text{temp.}} - 0.0000253\, t_{\text{nitr.}} t_{\text{temp.}} \\ & + 2.4288\times10^{-6}\, p t_{\text{temp.}} \end{aligned}$$

$$\begin{aligned} Ra = {} & 0.2931 + 0.0381X_1 - 0.0331X_2 \\ & + 0.0394X_3 - 0.0156X_4 - 0.0256X_1X_2 \\ & + 0.0119X_1X_3 - 0.0231X_1X_4 \end{aligned} \quad (4)$$

$$+ 0.0231X_2X_3 + 0.0106X_2X_4 - 0.0219X_3X_4$$

Equations (3) and (4) concern steel 4Cr5MoVSi. The strongest influence on the parameter Ra, measured transversely to the traces from the last mechanical treatment (equation (3)) has the temperature of annealing, while the duration of nitriding, temperature of nitriding and ammonia pressure have less influence again.

The roughness of the nitrided surface, measured longitudinally to the traces from the last mechanical treatment (equation (4)), is substantially influenced by the time of treatment and the temperature of nitriding.

c) steel 3Cr3Mo3V

$$\begin{aligned} Ra = {} & 0.428 - 0.0269X_1 - 0.0681X_2 \\ & + 0.0794X_3 + 0.0419X_4\,0.0131X_1X_2 \\ & + 0.0094X_1X_3 + 0.0069X_1X_4 + 0.0594X_2X_3. \end{aligned} \quad (5)$$

After recalculating the coefficients of equation (5), we obtain the mathematical-statistical model for Ra in a natural state:

$$\begin{aligned} Ra = {} & 4.47591 - 0.0082351\,t_{nitr.} - 0.0036541\,p \\ & + 4.323\times10^{-6}\,t_{nitr.}p - 0.095205\,\tau + 0.0001551\,t_{nitr.}\tau \\ & + 0.000129373p\tau - 0.002819t_{temp.} + 6.9\times10^{-6}t_{nitr.}t_{temp.} \end{aligned}$$

$$\begin{aligned} Ra = {} & 0.2638 + 0.0088X_1 - 0.0613X_2 \\ & + 0.0688X_3 + 0.0138X_4 - 0.0263X_1X_2 \\ & + 0.0288X_1X_4 - 0.0563X_2X_3 \\ & + 0.0188X_2X_4 - 0.0113X_3X_4. \end{aligned} \quad (6)$$

Equations (5) and (6) refer to steel 3Cr3Mo3V. In both directions of measuring the strongest influence on the roughness of the nitrided surfaces have the time of nitriding and ammonia pressure, while the temperature of annealing and the temperature of nitriding influence to a lesser extent. From the analysis of the regression equations it can be noted that at a shorter duration of treatment – X_3 - a lower roughness Ra of the surface layer is obtained. This is probably due to the fact that the thinner combined zones produce fewer pores and have a higher density.

It is characteristic for the three studied steels that at lower temperatures of annealing (600°C) nitrided layers with lower roughness of the nitrided surfaces are obtained. The lower roughness in this case is probably due to the higher hardness of the nitrided layer, obtained for structures, formed at temperature of annealing 600°C. Decrease in surface roughness is also observed at higher pressures (450Pa) of ammonia. This can be explained by the smaller coefficient of sputtering at such pressures, as a sequence of which the heights of the micro-roughnesses on the surface decrease. The influence of the temperature of nitriding is mixed and depends on the type of steel.

In the analysis of the equations, some common patterns can be established for the surface roughness of various steels. In all three types of steels the decrease in the roughness of the nitrided surfaces is accompanied by decrease in the temperature of nitriding. The explanation is probably in the fact that the decreased roughness of the surface is at the expense of the plastic deformation, caused by grinding, which, at heating to the temperature of nitriding, restores to a larger extent its original dimensions.

For the three types of steels the shorter time of nitriding leads to a lower roughness of the nitrided surfaces. This can probably be explained by the following: the shorter the time of nitriding, the smaller the probability for growth of nitrides on the surface of the details, what favorably influences the parameter Ra.

The increase in ammonia pressure in the chamber for the three types of steels leads to decrease in the roughness of the nitrided surface. At high ammonia pressure the coefficient of cathode sputtering is smaller, which means that the surface is saturated with a big amount of nitrogen, and a lot of disperse nitrides are formed.

In most cases ion nitriding is applied after mechanical treatment – grinding or polishing. It can be noted that after nitriding the hardness of the surface layer is higher than of the basic material, but lowest roughness of the nitrided surface is not always obtained. In case of additional treatment of the steels, considerable influence of the basic factors of the process of ion nitriding (temperature of nitriding, ammonia pressure and duration of nitriding) on the surface roughness is observed (Figure.1).

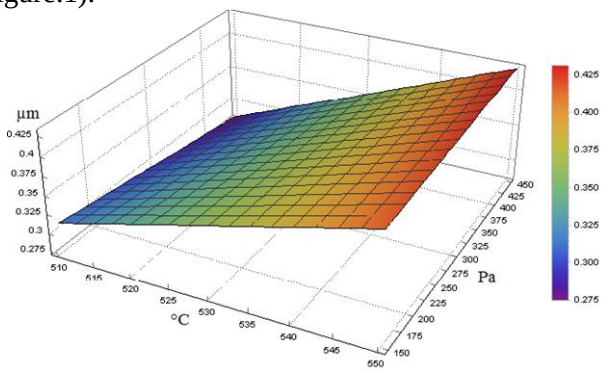

a

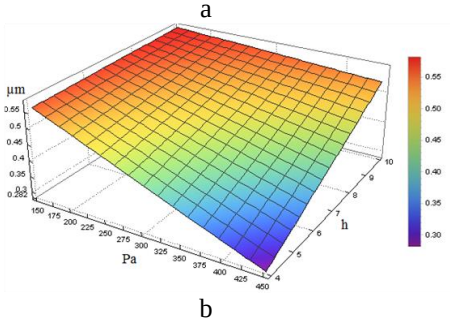

b

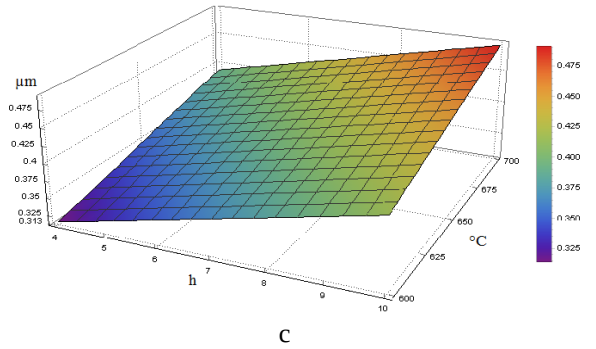

c

Figure 1. *Cross-sections of the multi-factor space a-steel 3Cr2W8V , b – steel 3Cr3Mo3V , c - steel 4Cr5MoVSi*

IV. Conclusions

1. Regression equations have been derived for the transverse and longitudinal direction of the traces from the last mechanical treatment, and these equations reflect the relationship between the temperature of nitriding, ammonia pressure, duration of the process, temperature of annealing, on the one hand, and the roughness of the nitrided surfaces, on the other hand.

2. It has been established that after ion nitriding of a thermally treated surface with Ra=0,11-0,16 µm, measured in longitudinal direction of the traces from grinding, the roughness of the surface is within Ra=0,14-0,74 µm.

3. It has been proved that after ion nitriding of a surface with Ra=0,27-0,35 µm, measured in transverse direction of the traces from the last mechanical treatment, the roughness of the nitrided surface does not change substantially but stays within Ra=0,28-0,32 µm and depends on the mode of treatment

References

[1] Bohotski A., Krastev Ts., Influence of the ion nitriding on the noise characteristics, roughness and geometry of gears, Conference ELTERM-AT 87, Albena, Bulgaria, 28-30 May 1987.
[2] Buchkov D., Toshkov V., Ion nitriding, S., Technics, 1990.
[3] Dimitrov D., Interchangeability, standardization and technical measurements, S., Technics, 1987.
[4] Fisher-Chatteijee P., W Eysell, u.a., Nitrieren und Niirocarburien, Sindelfingen, Expert Verbag, 1994.
[5] Geller Y., Tool steels, M., Metallurgy, 1968.
[6] Lahtin Y. at al., Steel nitriding, M., Machine building, 1976.
[7] Lampe Tomas. Plasmawarmebehandlung von Eisen wertoffen in stickstoff- und kohJentoffhaltigen Gasgemischrn. Dusseldorf, VDI- Verlag, 1985.
[8] Michev V. at al., Chemical and thermal treatment of steels, S., Technics, 1981.
[9] Pashov S., Petkov M., Reference book in mechanical treatment for technologists, S., Technics, 1990.
[10]Patarinski P., Mechanical engineering technologies, part I and part II, S., Technics, 1981.
[11] Popov S., Metal cutting, S., Technics, 1975.

CARBONITRING 37CR12MN8NI8MOVNB STEEL IN GLOW DISCHARGE PLASMA

I. Zumbilev

Technical University of Sofia – Branch Plovdiv, BULGARIA

Abstract: *The aim of the present paper is to study the influence of the process of carbonitriding in low-temperature plasma in an actuating medium of ammonia and gas corgon (82% Ar and 18% CO_2) on the surface micro-hardness and total thickness of the carbonitrided layer in 37Cr12Mn8Ni8MoVNb austenitic steel. The obtained results show that at the higher pressure (P =700Pa) of both gases – corgon and ammonia – layers with higher micro-hardness (1200$HV_{0.1}$) are formed and the thickness of their combined zone is 2 μm. It has also been established that during the process of ion nitriding layers without a combined zone are formed, while in carbonitriding the combined zone reaches up to 2 μm.*

Key Words: carbonitriding, austenitic steel , layers

I. Introduction

Nitriding and carbonitriding are basic processes for surface hardening of details and tools made of iron-carbon alloys, during which either nitrogen only or both carbon and nitrogen are simultaneously introduced into the surface layer.

In case of conducting these two processes in conventional gas furnaces or salt baths, it is impossible to regulate in a reliable way the thickness and the composition of the obtained layers, what necessitates varying with the potentials of carbon and nitrogen in the gas mixture or in the liquid medium. The percentage of nitrogen and active carbon is defined by a small number of parameters – temperature and composition of the gas medium - and the possibilities for variation are limited.

In the processes of carbonitriding and nitriding in glow-discharge plasma these difficulties are resolved, and this is the major advantage of the method. The use of glow electric discharge for treating details is a perspective method of material nitriding and carbonitriding in modern machine building.

Works [1,2,3,5] considermainly the mechanism of building, the structure and the properties of the nitrided layers, obtained in low-temperature plasma,while [3,4,6] discuss basic problems related to carbonitriding in conventional gas furnaces and [7,9,10,11,12,13] speculate on carbonitriding in glow electric discharge. There is lack of data about carbonitriding in glow-discharge plasma in anactuating medium, consisting of ammonia and corgon (82% Arand 18% CO2), and the available information of comparative in vestigations between the two processes – nitriding and carbonitriding – is also insufficient.

It has been established in works [4,7,8] that, when in the process of carbonitriding propane-butane isusedas a carbon-carrier, the phase composition of the combined zone in the carbonitrided layer could not be precisely regulated. Better resultsare obtained in result ofusing a mixture of methane and argon [7]. In metal welding the role of the protective gas is often taken by corgon, which contains both argon and carbon dioxidein a particularratio.

The objective of the present paperis to investigate the possibility to usen corgon not only in welding but also a sanindirect carbon-carrier in the process of simultaneous saturation of the metal surface with nitrogen and carbon (carbonitriding) atlow temperatures. The small percentage of (18%) carbon dioxide in the gas corgon makes it possible to regulate the amount of carbon, in troduced into the vacuum chamber. There is no data in the considered literature about nitriding and carbonitriding in glow-discharge plasma in an actuating medium consisting of ammonia and corgon (82% Ar and 18% CO2). The 37Cr12Mn8Ni8MoVNb steel is with austenitic structure and it is used for producing turbinedisc, valves forengines, wheels with bandage, and other details work in gat up to 800°C. In order to achieve a stable austenitic structure, nickel and manganese are introduced additionally.

The aim of the present workis to in vestigate the in fluence of nitriding and carbonitriding in low temperature plasma, in anactuating medium, consisting of ammonia and gas corgon (82% Ar and 18% CO2), up on the surface hardness and the total thickness of the nitrided and carbonitrided layers of the austenitic steel 37Cr12Mn8Ni8MoVNb.

II. Investigated materials and modes of treatment

Austenitic steel 37Cr12Mn8Ni8MoVNb (GOST) is subjected to investigation. Its chemical composition is checked by the equipment for automatic analysis "Spectrotest" and given in Table 1.

Table 1.*Chemical composition of the steel*

Type	**Chemical elements, percentage**									
	C	Si	Mn	Cr	Ni	S	P	Nb	V	Mo
37Cr12Mn8Ni8MoVNb	0,37	0,3	7,7	13,2	6,2	0,02	0,025	0,03	1.69	0.7

The requirement for a preliminary the maltreatment is imposed mainly by the following consideration: for a chieving the desired mechanical parameters and structure, enabling uniform distribution of nitrogen and carbon in depth and favorable course of diffusion.

Test samples are made of 37Cr12Mn8Ni8MoVNb steel with dimensions 15X15X10mm, and they are treated thermally in a chamber furnace in an oxidizing medium under modes, given in Table 2.

Table 2. *Modes of preliminary treatment*

Steel	**Quenching t_{quen}, ^oC**	**Cooling medium**	**Tempering $t_{temp.}$, ^oC**	**Cooling medium**
37Cr12Mn8Ni8MoVNb	1170	water	650 780	air air

The samples from the investigated steel are nitrided and carbonitrided in the installation "Ion – 20" according to the modes, given in Table 3. Ammonia (NH_3) and corgon are used as saturating gases in different percentage ratio. The temperature of treatment is 550^{o}C.

Table 3. *Modes of nitriding and carbonitriding*

№ of the mode	**Treatment**	**τ h**	**P_1 NH_3 Pa**	**P_2 corgon Pa**	**P total Pa**
1	carbonitriding	2	350	350	700
2	carbonitriding	6	350	350	700
3	carbonitriding	2	360	40	400
4	carbonitriding	6	360	40	400
5	carbonitriding	2	280	120	400
6	nitriding	4	400	-	400

III. Methodology of investigation

In order to clear out the morphological peculiarities of the nitrided and carbonitrided layers, metallographic analysis has been performed.

When defining the structure and the thickness of the obtained nitrided layers a microscope – Axioscop – has been used and metallographic pictures taken.

The thickness of the nitrided layer has been defined by the depth, at which hardness, equal to the core plus 50, has been achieved.

Measuring the micro-hardness of the nitrided samples has been accomplished by means of a micro hardness-meter "Shimadzu" at a load of 0,98 N, following the Vickers' method.

IV. Experimental results and analysis

Preliminary thermal treatment. The results from measuring the hardness after the thermal treatment are given in Table 4.

Table 4. *Results from the preliminary thermal treatment*

Steel	**Hardness, HRC**	
	Quenching	**Tempering**
37Cr12Mn8Ni8MoVNb	21	33(650 °C) 39(780°C)

During the process of quenching the 37Cr12Mn8Ni8MoVNb steel, homogeneous alloyed austenitic structure with low hardness – 21 HRC – has been fixed. During the subsequent double ageing the steel hardens (first ageing – 33 HRC, second ageing – 39 HRC, Table 4) as a result of the separation of disperse carbides in the grain boundary of the supersaturated austenitic structure.

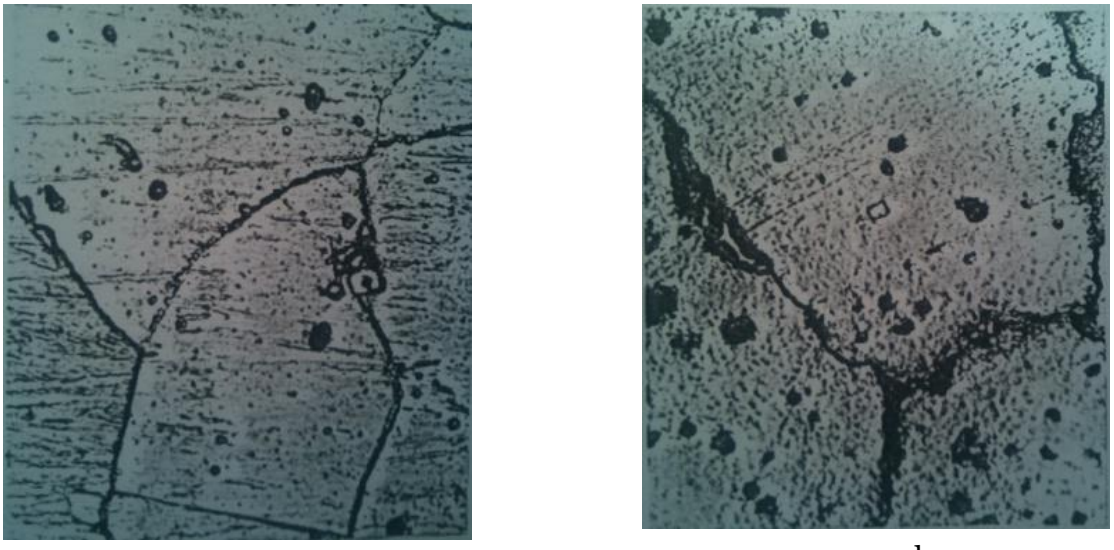

a b

Figure 1. *Micro-structure of 37Cr12Mn8Ni8MoVNb steel after quenching and double tempering X500, a- tempering at 650 °C, b- tempering at 780°C*

Ion carbonitriding

The maximum thickness - $HV_{0.1}$– and the total thickness – δ_{tot} - of the nitrided and carbonitrided layers have been defined by means of measuring the micro-hardness of the thermally treated and ion nitrided and carbonitrided samples in-depth, while the thickness of the combined zone ($\delta_{c.z.}$) of both layers has been defined with the help of a metallographic microscope. The obtained results are given in Table 5.

Table 5. *Results from ion carbonitriding and ion nitriding of the steel*

№ of the mode in Table 3	**37Cr12Mn8Ni8MoVNb**		
	$HV_{0,1}$	**δ_{tot}, µm**	**$\delta_{c.z}$, µm**
1	900	15	Not observed
2	1200	30	2
3	800	20	Not observed

4	1180	50	traces
5	1100	40	traces
6	1100	55	Not observed

After ion carbonitriding the obtained layer is easily seen on the surface of the austenitic steel – Figure 2.

In the process of nitriding 37Cr12Mn8Ni8MoVNb steel under the mode 6 from Table 5 (temperature 550˚C, ammonia pressure 400Pa, time 4h), a layer with 55μm thickness and $1100HV_{0,1}$micro-hardness is obtained. A nitride (white) zone is not observed on the surface – Figure 2a.

After introduction of 10% of gas corgon into the ammonia medium of the working chamber (Table 5, modes 3 and 4), a carbonitrided layer with higher surface micro-hardness ($800\text{-}1180HV_{0.1}$) and total thickness (20-50 μm) is obtained. At longer duration of the treatment (Table5, mode 4) a layer with higher micro-hardness $1180HV_{0,1}$,and greater total thickness - 50μm – is formed on the surface of the 37Cr12Mn8Ni8MoVNb steel. Traces of a carbonitride zone are found in the layer – Figure 2.

Ion carbonitriding of 37Cr12Mn8Ni8MoVNb steel with higher pressure of the gas corgon(P_2 = 350Pa) and ammonia(P_1= 350Pa) and time of treatment 2h leads to obtaining a layer with total thickness of 15μm and maximum surface micro-hardness $900HV_{0.1}$. With prolongation of the time of carbonitriding to 6h in the same saturation medium, the surface micro-hardness of the layer increases to $1200HV_{0,1}$and its total thickness goes up to 30 μm. A carbonitride zone is formed on the surface of the layer, which is 2 μm thick – Figure 2.

It can be noted that after ion nitriding and ion carbonitriding of 37Cr12Mn8Ni8MoVNb steel at the same mode of treatment (temperature 550 ˚C, total pressure of the two gases in the vacuum chamber 400Pa and time of treatment 4h), the surface micro-hardness is almost the same ($1100\text{-}1180HV_{0,1}$). The low total thickness of the layers, obtained after nitriding and carbonitriding, is seen from Table 5. It is explained by the austenitic structure of the 37Cr12Mn8Ni8MoVNb steel, in which the coefficient of nitrogen and carbon diffusion is smaller.

After treating the 37Cr12Mn8Ni8MoVNb steel by an additionally introduced carbon-containing gas(corgon) in ammonia medium at different percentage ratio, carbonitrided layers with lower total thickness are obtained, compared to the layers, formed in the process of nitriding. This is due to the increased content of carbon on the surface, indirectly delivered from CO_2. Apparently the availability of carbon on the surface impedes the diffusion of nitrogen in the interior of the metal.

Only after conducting the process of ion carbonitriding at higher pressure - 700Pa – of both gases – corgon and ammonia (mode 4, Table 5) layers with carbonitride zone thickness of up to 22μm are obtained. Apparently ammonia and corgon pressure in the chamber plays an important role in delivering bigger amount of nitrogen and carbon on the surface for 6h time of carbonitriding. The metallographic analysis of the nitrided 37Cr12Mn8Ni8MoVNb steel does notdetect the presence of white(connected)zone on the surface of the steel.

Counterparts and slip lines are well seen in the surface layer, which serve as intersections between the slip planes and the outer surfaces of the crystals. The availability of slip lines influences favorably nitrogen and carbon diffusion into the volume of the grains [1].

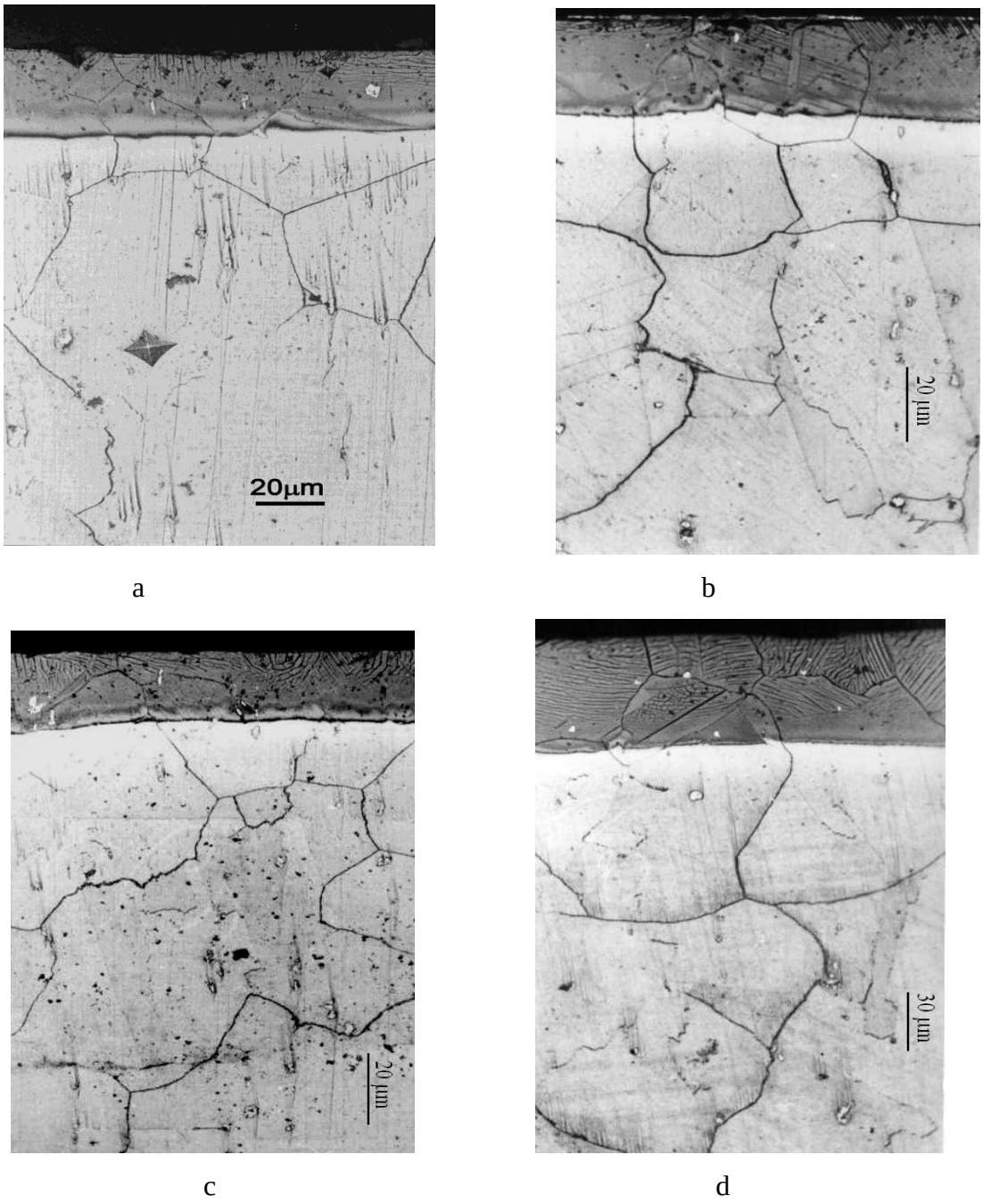

Figure 2. *Micro-structure of 37Cr12Mn8Ni8MoVNb steel after treatment at t= 550˚C: a- P_{NH3} = 350Pa , $P_{82\% Ar +18\% CO2}$ = 350Pa, τ = 2h ; b-P_{NH3} = 350Pa , $P_{82\% Ar +18\% CO2}$ = 350Pa, τ = 6h c- b-P_{NH3} = 360Pa , $P_{82\% Ar +18\% CO2}$ = 40Pa, τ = 6h; d- P_{NH3} = 400Pa, τ = 4h,*

V. Conclusions

It has been established that after ion carbonitriding of 37Cr12Mn8Ni8MoVNb steel at: : t = 550˚C; P_{1NH3}=350Pa ; $P_{2corgon}$=350Pa; τ = 6h, a layer with highest surface hardness of 1200$HV_{0.1}$and thickness of the combined zone 2 μmis formed.

It has been proved that at the same temperature and duration of treatment but for different composition of the saturating gas medium [NH_3 , (82 % Ar + 18 % CO_2)], at total pressure of 400Pa, the formed layers after ion carbonitriding of 37Cr12Mn8Ni8MoVNb steel are with lower thickness and micro-hardness, compared to the layers formed after ion nitriding.

It has been established that during the process of ion nitriding layers without a combined zone are formed, while in the process of carbonitriding the combined zone reaches up to 2 μm.

References

[1] Тошков В., Теоретични и практически аспекти на азотирането на желязо и желязо въглеродни сплави в нискотемпературна плазма, Дисертация, София, 1997.

[2] Тошков В., Азотиране в нискотемпературна плазма , Кинг, 2004.

[3] Fisher-ChatterjeeP.,W.Eysell,u.a.,Nitrieren und Nitrocarburieren, Sindeifingen, Expert Verbag, 1994 .

[4] Русев Р., Теоретично-експериментален анализ на системата Fe-N-C и приложението му в карбонитриращите технологии, Дисертация, Варна, 1998.

[5] Hochman R., Effects of Nitrogen in Metal Surfaces, Proceeding of an Internacional Conference on lon Nitriding, Clevland, Ohio, USA 15-17, September 1989, pp 23-30.

[6] Русев Р., Особености, механизъм на образуване и морфология на карбонитрирани слоеве, получени в среда от амоняк и въглероден оксид, Дисертация, Варна, 1979.

[7] Върхошков Е., Карбонитриране на стомани в тлеещ разряд, Дисертация, София, 1985.

[8] Лахтин Ю., Диффузионные основы процесы азотирования, МиТОМ, № 7, 1995, с.14-17.

[9] Зюмбилев А., К. Николов, Азотиране и карбонитриране на стомани 20 и 25ХГСНМА, Amtech 9-11 November 2005, Rousse.

[10] Huchel U.,J.Crummenauer,S.Stramke, Nitrocarburieren und Oxidieren im Plasma, ELTRO GmbH , Baesweiler, 2003.

[11] Nitriding and Nitrocarburising, Contract Heat Treatment Association,Aston University, Birmingham, 1996.

[12] Gontiyo L., R.Machado, L. Casteletti and P. Nascente, Evaluation of the Effect of Cooling Speed fn the Layer Formation fn Stainless Steel by Plasma Carbonitriding, Acta Microscopica, Volume 12 , № 1, December , 2003.

[13] Lampe Thomas, Plasmawärmebehandlung von Eisenwerkstoffen in stickstoff-und kohlenstoffhaltigen Gasgemischen, VDI-Verlag GmbH, Düsseldorf, 1985.

DIGITAL CONTROL OF ELECTRO-HYDRAULIC STEERING TEST BENCH

A. Mitov[1], J. Kralev[2], I. Angelov[3]

[1]TU-Sofia, Faculty of Power Engineering and Power Machines, Department: „HAD and HM", e-mail:alexander_mitov@mail.bg
[2]TU-Sofia, Faculty of Automatics, Department: „Systems and Control", e-mail:jkralev@yahoo.com
[3]TU-Sofia, Faculty of Power Engineering and Power Machines, Department: „HAD and HM", e-mail:ilangel@tu-sofia.bg

Abstract: *The paper presents design solution and physical implementation of a system for examination of electro hydraulic steering based on OSPE 200 components. The implementation is based on synthesis of required hydraulic and structure parameters, presented in a previous paper. Now we present the interconnection of the digital control system and the closed-loop flow diagram. A formal description of embedded software is presented too, which supports operation of PI control algorithm in real-time. Experimental results for transient response prove the quality of the system.*

Keywords*:* digital control system, electro hydraulic steering, PI closed-loop performance

I. Introduction

Increasing application of mobile machines in industrial environments stimulates development of their basic power drive – hydraulic system. Important element in implementation of hydrostatic systems for mobile applications is the hydraulic networks. Therefore the application field of digital control technology expands based on its embedding capability in control loops of last generation EHSU (electro-hydraulic steering unit). For example in the last decade Danfoss PVE technology is largely used in their OSPE EHSU. These factors together with recent utilization of such mobile machines in our country form an argument to study EHSU for practical and scientific interests.

An experimental test bench system for examination of electro-hydraulic steering devices OSPE 200 is designed and implemented in the Department of Hydro-aerodynamics and Hydraulic Machines of Technical University of Sofia. The implementation is based on synthesis of required hydraulic and structure parameters of the hydraulic system elements, presented in previous our paper [1].

The purpose of this paper is to present implemented digital control system, where an industrial joystick generates the reference signal. The paper contains schematic representation of basic system components, closed-loop control system signal flow graph, and formalization of software implementation of digital PI regulator. The closed-loop performance is demonstrated by reference trajectory response of the driven servo-cylinder.

Design solution and physical implementation of EHSU test bench

For assessment of EHSU functionality, the test bench system should provide measurement capabilities of energetic (pressure and flow) and steering device for direction control. It allows for control of the vehicle in several ways, depending on the generation of control signal: mechanical by steering wheel, electro-mechanical by joystick, remote based on GPS and communication mechanical (position and velocity) physical variables. Measurement devices should be accurate enough to reliably estimate dynamic behavior of physical variables. Figure 1 shows hydraulic shematics of the test bench system, described in detail in [1].

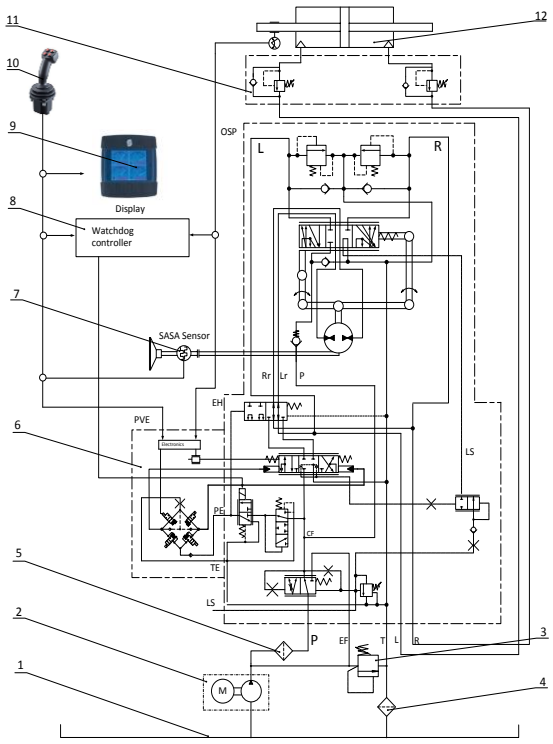

Figure 1. *Hydraulic schematics of EHSU test bench with pressure loading.*

Figure 2 shows 3D model and corresponding picture of the test bench system. Construction and packaging of the test bench system are in line with modern requirements for examination of electro-hydraulic steering devices with various loadings. Pressure loading system is composed of a hydraulic block with pressure reliefs valves (pos. 11, Fig. 1), which are connected to the working chambers of the servo-cylinder.

Figure 2. *3D model and implementation of test bench EHSU.*

Concept of operation of test bench system of EHSU in digital control mode

Concepts of operations description of the test bench system is based on key component – OSPE 200 LSRM EHSU. Its schematic view is presented on Figure 3 [1, 3].

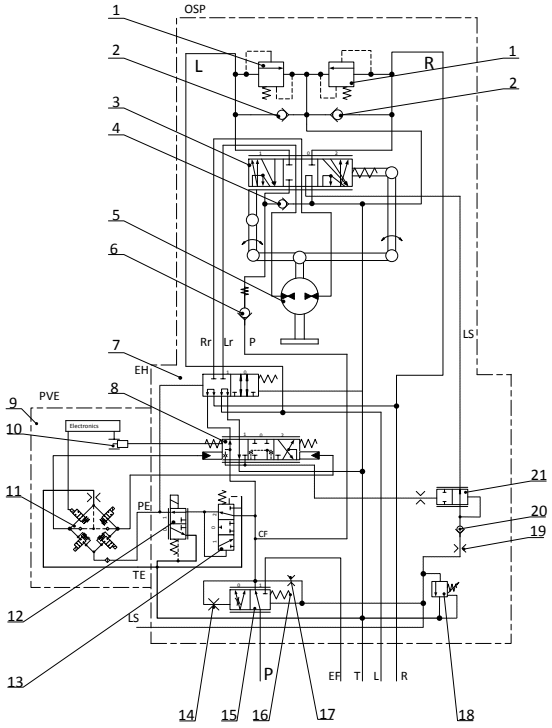

Figure 3. *Hydraulic schematics of EHSU OSPE 200.*

Necessary condition for the work of EHSU hence the whole test bench system in digital joystick control mode (through EH – electro-hydraulic control block for OSPE) is feeding an electrical signal on control valve for mode change (12). When the valve (12) is switched in position '1' control pressure signal is required (12 bar) supported by the reduction valve (13). That signal is fed through control valve for mode selection (12) towards connected in parallel bridge 2/2 valves, which are part of digital control block (PVE, 11). Simultaneously a pressure signal is fed towards main valve, which determine the mode of control (7). It switches to position '1' and connects electro-hydraulic directional valve (8) with L and R lines to corresponding chambers of the servo-cylinder. Directional valve (7) breaks the connection with lines Rr and Lr, as well as with working pair piston/ bush (3). Therefore the mechanism of steering wheel control (OSP) is isolated.

When input electrical signal from the microcontroller is received in the PWM valve controller PVE (9) (in our case the signal is for steering in right direction), parallel electromagnetic controlled 2/2 valves are activated (depending on PWM signal) and electro-hydraulic directional valve (8) switches to position '1'. In the LS-contour connected to directional valve (8) the pressure level is regulated by feeding the working fluid to valve (21), to be able to move the servo-cylinder in desired direction (right).

Valve (21) function is to limit the flow in LS-contour in relation to pressure drop in orifice (17) of priority valve (15). The pressure in the LS-contour acting upon priority valve (15) will correspond to required pressure in the case of control with electro hydraulic directional valve (8). Therefore the position of the priority valve (15) changes in relation to required working pressure in this mode.

II. Implementation of digital control system

Digital control system is developed upon microcontroller *MC012-022* and electrical joystick *JS6000* for control of electro-proportional block PVE (embedded in EHSU *OSPE 200*), which through embedded directional valve (pos.8, Fig.3) executes a control of plant's position – servo-cylinder with equally shaped chambers. Electrical connections between components of the control system are shown in Figure 4.

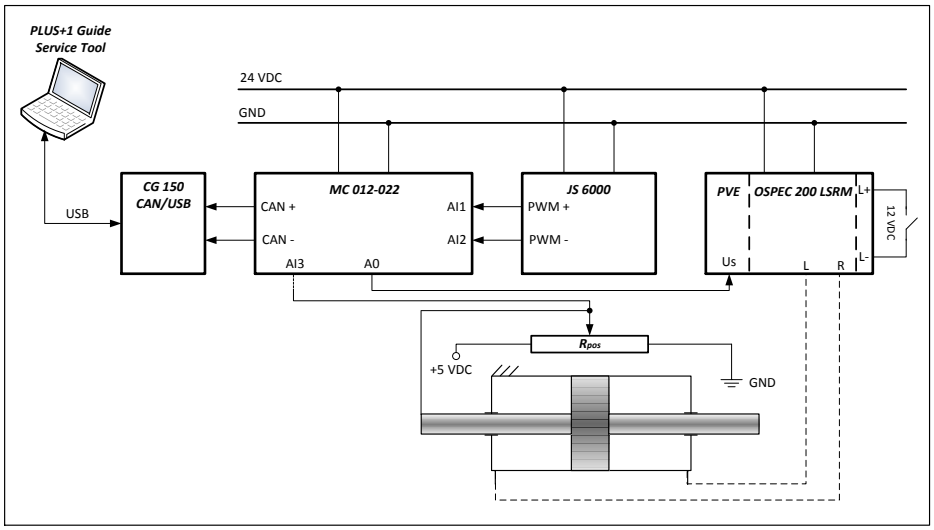

Figure 4. *Conceptual representation of electrical connections of the control system*

The joystick, which generates PWM signal for desired cylinder velocity, feeds correspondent analog input pins of the microcontroller. Embedded software calculates error between position feedback signal (R_{pos}) and reference signal. Analog output of the microcontroller is connected to the electro-hydraulic block with 2/2 valves (*PVE*). Its purpose is sending control voltage signal for EHSU *OSPEC 200 LSRM*. Standard CAN-network [2] is exploited for downloading of microcontroller program and data acquisition of dynamical responses. Workstation for software development accesses CAN-network through USB/CAN - device (CG150) [6].

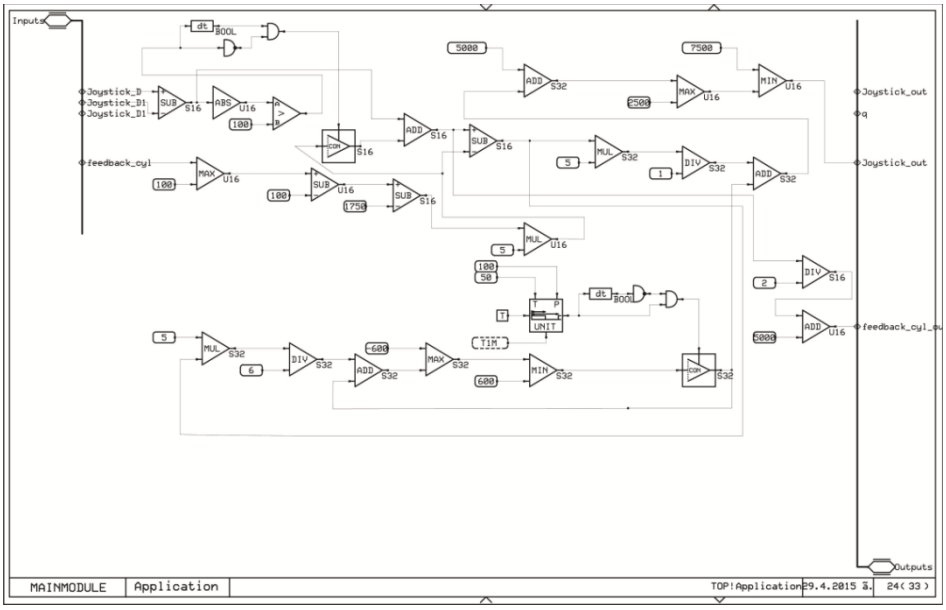

Figure 5. *Software model of digital control system*

We use proportion-integral control law for the position y of the piston of execution servo-cylinder. Human operator generates the reference signal x_{ref} through utilization of electronic joystick [5]. Control signal u represents voltage input for electronic block of steering device (EHSU), which drives the main cylinder. The microcontroller calculates control signal in sample times $m\,T_S$, with sample interval $T_S = 100ms$.

$$u(m\,T_S) = k_p e(m\,T_S) + k_i \sum_{j=0}^{m} e(m\,T_S) \quad (1)$$

$$e = x_{ref} - y \quad (2)$$

We've developed custom program (Fig. 4) in software development environment (PLUS+1 Guide) [2] of microcontroller *MC012-022* [4], to compute control signal. The program is composed of functional blocks connected by data lines. After that the IDE generates executable file which is

downloaded and ran on the microcontroller. Only integer data types are supported. The compiled model runs as idle thread in the microcontroller with clock period assumed $\tau < 100ns$. The sample time is $T_S = 100ms \gg \tau$, we can assume the microcontroller time to be continuous variable t.

The value of reference signal x_{ref} is defined by following expressions:

$$x_{ref} = x_J + y_R \tag{3}$$

$$y_R(t) = \begin{cases} y(t) & S_J(t-\tau) \wedge \overline{S_J(t)} = 1 \\ y_R(t-\tau) & S_J(t-\tau) \wedge \overline{S_J(t)} = 0 \end{cases} \tag{4}$$

$$S_J = \begin{cases} 1 & |x_J| > J_{LO} \\ 0 & |x_J| \le J_{LO} \end{cases}, \quad J_{LO} = 100 \tag{5}$$

The joystick signal x_J increases linearly, with constant derivative proportional to displacement of the stick. In neutral position of the stick $x_J = 0$. Current position of main cylinder y is saved at register y_R, when joystick signal disappears $x_J = 0$. Then the control algorithm stops the movement of the main cylinder at its current position. The event of disappearance of x_J is recognized through detection of falling edge of a signal S_J.

The output signal *y* is obtained by measuring the position of the piston of the main cylinder by means of a potentiometric transducer (*Rpos* , Figure 4). His resistance R_fb vary from 0 to 3,7 kΩ.

$$y = K_y(y_{sat} + A_y), \; K_y = 5, \; A_y = -1850 \tag{6}$$

$$y_{sat} = \begin{cases} R_{fb} & R_{fb} > R_{LO} \\ R_{LO} & R_{fb} \le R_{LO} \end{cases}, \quad R_{LO} = 100 \tag{7}$$

Output signal value is assessed by biasing and scaling of measured resistance, such that zero output to correspond to middle position of the cylinder.

Parameters of PI regulator are k_p – proportional gain and k_i – integral gain. Integer arithmetic of the microcontroller *MC012*-022 restricts these gains to be represented as rational numbers:

$$k_p = \frac{k_{p,N}}{k_{p,D}} \qquad k_i = \frac{k_{i,N}}{k_{i,D}} \tag{8}$$

Integrator element is implemented by the following two expressions.

$$x_i(t) = \begin{cases} x_i(t-\tau) + k_i e(t) & \overline{S_i(t-\tau)} \wedge S_i(t) \\ x_i(t-\tau) \end{cases} \tag{9}$$

$$S_i(t) = \begin{cases} 0 & 0.05(2m-1) < t < 0.1m \\ 1 & 0.1(m-1) < t < 0.05(2m-1) \end{cases} \tag{10}$$

A register x_i accumulates scaled value of the error signal $k_i e$. Register value is updated in equal sample intervals T_S. This is achieved through square wave signal S_i with period 100 ms and duty cycle 50 %. A logical function $\overline{S_i(t-\tau)} \wedge S_i(t)$ detects rising edges of the impulses by generating high level signal for one interval τ. Such an interval is enough to allow accumulation of a new value.

Proportional and integral gains of the regulator are tuned so as to guarantee typical performance indices for such class systems.

Based on structure of the test bench system and technical documentation available we've suppose the following approximate model of the open-loop plant.

$$y(t) = \frac{K_C}{s} e^{-s\,L} F_1(u), \quad s \in C \tag{11}$$

The plant is serial interconnection of a memoryless nonlinearity F_1 and a linear dynamical transfer function $W(s)$.

$$W(s) = \frac{K_C}{s} e^{-s\,L} \tag{12}$$

$$F_1(u) = \begin{cases} 0 & |u| < u_0 \\ u & u_0 < |u| < u_m \\ u_m sign(u) & |u| > u_m \end{cases} \tag{13}$$

To support tuning of regulator gains and scaling factors of the digital control system elements we've developed a numerical model for simulation in MATLAB/Simulink environment – presented on Figure 6.

III. Experimental results

Implemented digital control system provides capabilities for real-time data acquisition of dynamical characteristics such as: transient starting or stopping response of the cylinder; and desired trajectory tracking. The trajectory is selected by human operator through the joystick. It is possible to record simultaneously the control signal from the microcontroller to the *PVE* block, which is indicator of energy efficiency, and is often considered when tuning PI regulators. Experimental data are processed in M-script fain in MATLAB, which allows comparison of different experiments through figures or numerical measures. Usually we compare reference and output signals (R_{pos}). Figure 7 shows one experimental result of output signal dynamics.

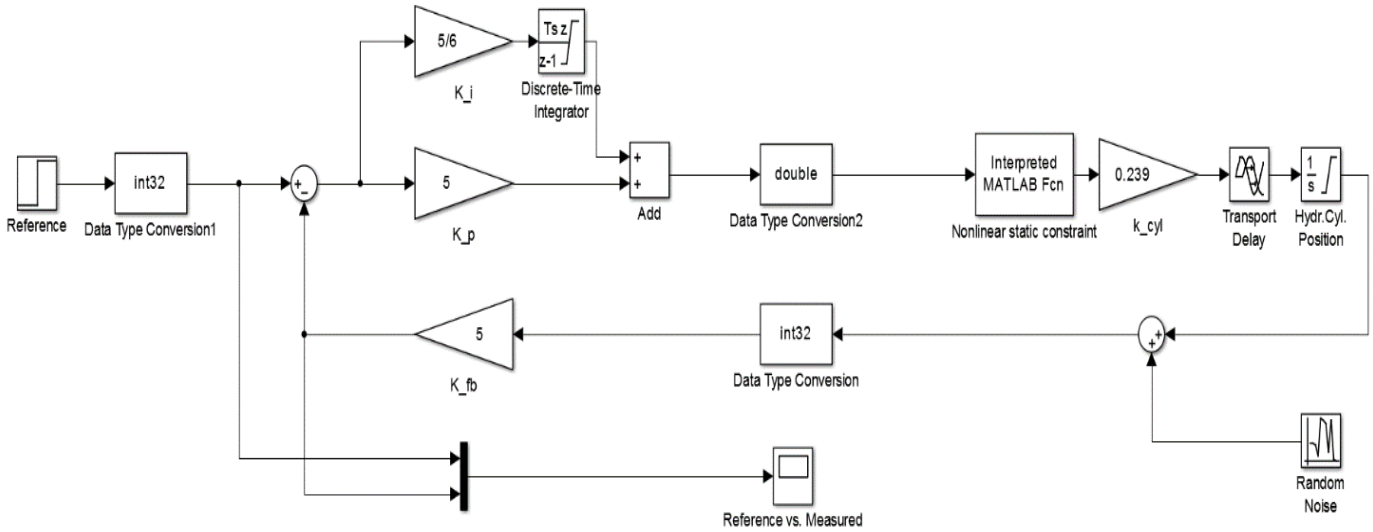

Figure 6. *Simulink model of the closed-loop digital control system*

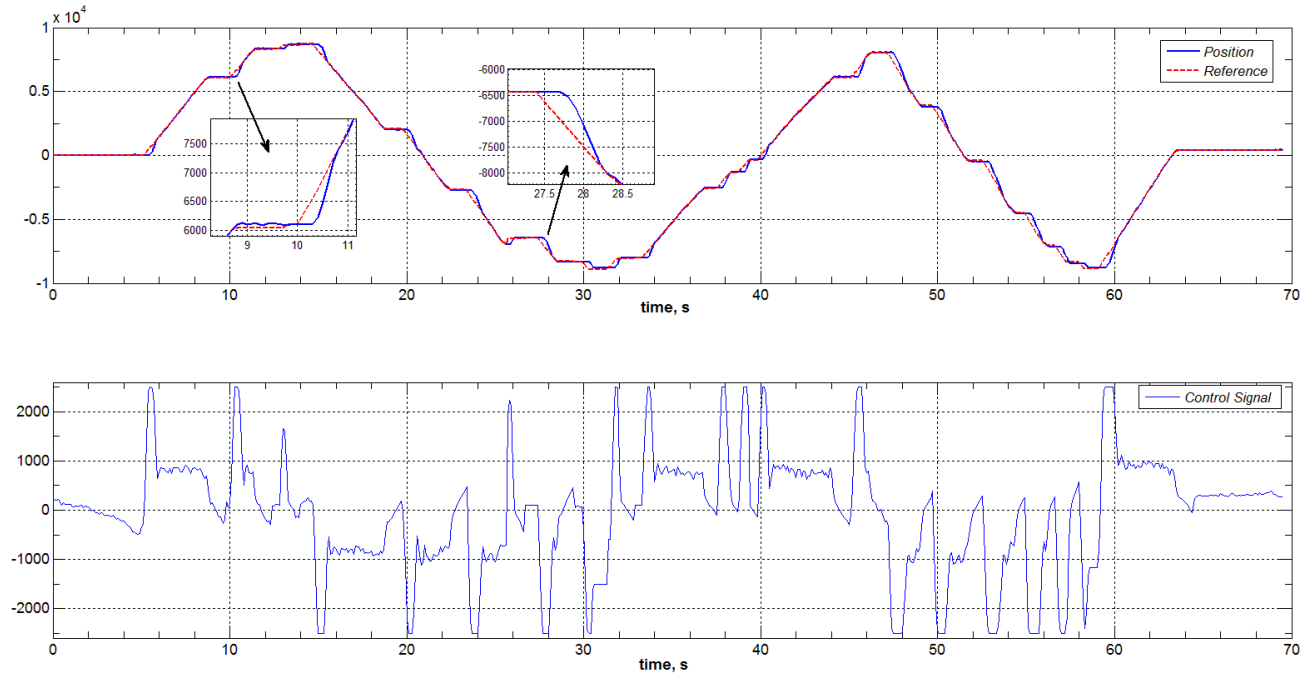

Figure 7. *Experimental results – tracking of operator command*

The analysis of experimental results shows:

- We observe zero error in steady state for constant and linearly increasing reference. Transient response is aperiodic without overshot.
- Settling time is smaller than 1 sec, which is comparable to human reactions.
- Control signal is close to its maximal value for the transient period, which indicates fastest output reaction.
- The performance measures are invariant in both movement directions. SNR of control signals is high which demonstrates the accuracy of the position measurement instrument. Its accuracy is distributed as quality to the whole closed-loop.
- We've estimated that position error is 0,1 mm, which is higher than human optical resolution (0,1-0,3 mm).

IV. Conclusion

Presented implementation of digital control test bench system for EHSU and presented experimental results lead us to the following important conclusions:

1. It is developed an experimental test bench for examination of electro-hydraulic steering devices, which is capable of two modes of control: techanical – through steering wheel and digital - through electronic joystick.

2. Closed-loop control system shows invariant performance for large class of operator commands, which can be observed from experimental records.

3. Collected experimental data can be used for system identification to infer more accurate models which can be basis for performance improvement.

Reference

[1] Mitov, Al., Il.Angelov, N.Stanchev, *Stand for electrohydraulic steering units type OSPE 200*, International Scientific Conference „RU & SU“ 2014, Ruse, 2014.

[2] CAN in PLUS+1 Guide, Fundamentals of PLUS+1 Guide Electronics, Training course, Almhult, Sweden, 2015.

[3] OSPE Steering Valve, Technical Information, 11068682, Rev CD, Sep 2012, Sauer-Danfoss, 2012.

[4] Plus+1 Controllers MC012-020 and 022, Data Sheet, 11077167, Rev DA, Sep 2013, Sauer-Danfoss, 2013.

[5] JS6000 Joystick Base, Data Sheet, 520L0722, Rev HA, Jan 2010, Sauer-Danfoss, 2010.

[6] Gateway Interface Communicator CG150 CAN/USB, Data Sheet, 520L0945, Rev CA, Jan 2014, Sauer-Danfoss, 2014.

ISSN 1314-7773

Nutrilab
food labelling

Journal of **FOOD** and **PACKAGING** Science, Technique and Technologies

НАО БЪЛГАРИЯ

National Academy of Packaging-Bulgaria